TRW8-31375 AMPS-FR

A28727

CR-144259

AMPS PARTICLE ACCELERATOR DEFINITION STUDY

Final Report

Contract NAS 8-31375

June 30, 1975

Prepared for

George C. Marshall Space Flight Center
Marshall Space Flight Center, Alabama

TRW
SYSTEMS GROUP

J. M. Sellen, Jr.
Systems Group Research Staff
One Space Park
Redondo Beach, California 90278

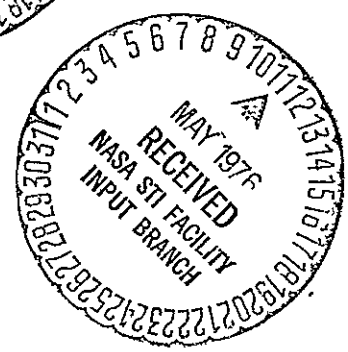

TABLE OF CONTENTS

LIST OF FIGURES

LIST OF TABLES

1.0 INTRODUCTION

The Particle Accelerator System of the AMPS (Atmospheric, Magnetospheric, and Plasmas in Space) payload is a series of charged particle accelerators to be flown with the Space Transportation System Shuttle on Spacelab missions. In the configuration to be presented in this report, the total particle accelerator system consists of an energetic electron beam, an energetic ion accelerator, and both low voltage and high voltage plasma acceleration devices. Figure 1 illustrates the Orbiter with such a particle accelerator system.

This definition study will not attempt detailed system design. Instead, emphasis will be given to the development of a system concept, which will then be examined qualitatively for its assembly and operation. To develop this system concept, a series of design criteria will be stated. The study will then examine considered mission modes and will attempt to derive systems requirements in these modes for the electron accelerator. From these mission requirements and the design criteria, the study will develop a logic for the system configuration, and will present a "unified" particle accelerator package. The energy storage and transfer elements consistent with this configuration logic will be examined, and the study will conclude, as noted above, with a description of specific aspects of the electron accelerator fabrication and operation.

2.0 SYSTEM DESIGN CRITERIA

Table 1 lists the system design criteria which will be used in this definition study, and a brief discussion of these stated criteria will be given here.

Criterion 1 recognizes the Shuttle/Orbiter system as a unique configuration and possibility in terms of space flight and sets, as a necessary goal, that missions be "tailored" to fully exploit these capabilities. This design criterion, however, weighs against missions and systems for which other launch vehicles are more appropriate and cost effective.

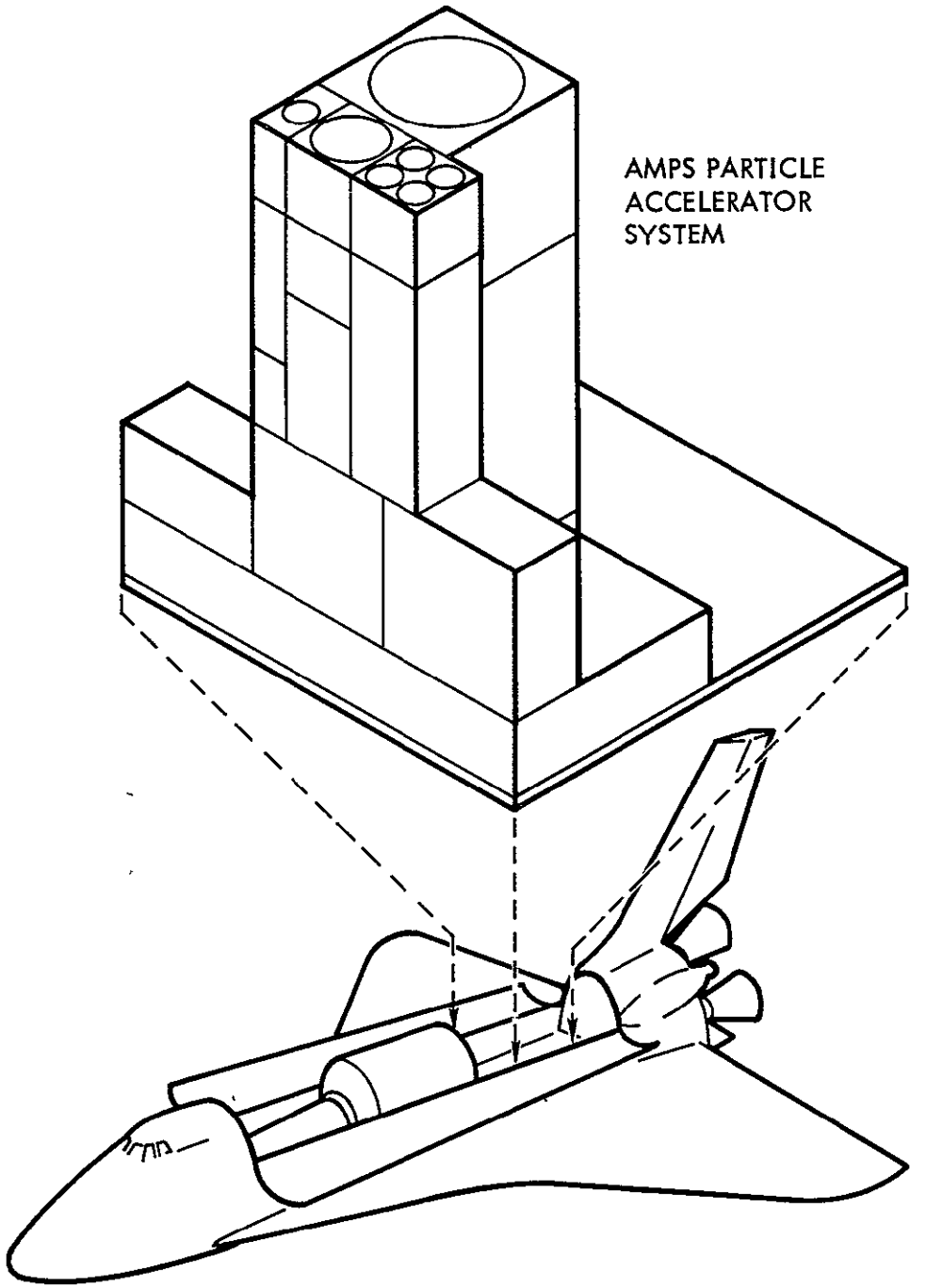

Figure 1. Space Shuttle Orbiter with Spacelab Module and AMPS Pallet Mounted Particle Accelerator System.

PARTICLE ACCELERATOR SYSTEM DESIGN CRITERIA

The AMPS Particle Accelerator System design must:

1) Recognize constraints and limitations in the Orbiter flight and exploit unique advantages in the Shuttle/Orbiter system,

2) Permit the execution of a broad spectrum of mission modes, including various species of accelerated particles, beam power levels, and total particle energy releases,

3) Allow for common usage by the various particle accelerators of the major mass and volume elements of the payload,

4) Be consistent with multi-purpose, multi-species, missions without extensive retrofit or recurring costs,

5) Possess initial systems versions capable of modular expansion into ultimate system growth modes,

6) Provide, in initial systems versions, for both useful science goals and technology verification goals, consistent with desired system growth modes.

Table 1. Particle Accelerator System Design Criteria.

Criterion 2 recognizes the long term role of AMPS. If this facility is to provide, adequately, for new and exciting scientific results which broadly advance the understanding of atmospheric, ionospheric, and magnetospheric coupling, then system capabilities must match this wide requirements range.

Criteria 3 and 4, follow from both cost considerations and mission planning considerations. If system "commonality" is not exercised, the science objectives for each flight must be consistently restricted to a limited set of all possible objectives, and any variations away from this narrower set of science goals will be penalized by extensive retrofitting costs.

Criteria 5 and 6 express other applications of this "commonality" concept. In Criterion 5, the modular expansion capability allows a commonality between initial and growth mode systems. Growth modes follow necessarily from the long range AMPS mission. The attainment of these growth versions will not proceed, however, if system redesign and reinitiation costs overburden available resources. A modular growth capability requirement, in turn, establishes implicit technology goals for early missions, and, Criterion 6 advances a demand for the satisfaction of combined science and technology goals.

3.0 MISSION CONSIDERATIONS IN THE AMPS PARTICLE ACCELERATOR SYSTEM DESIGN

3.1 Orbiter Opportunities and Limitations

Table 2 lists opportunities and limitations for a particle accelerator facility flown on the Shuttle Orbiter.

The characterization of a given parameter as an "opportunity" or a "limitation" is necessarily qualitative. For example, manned participation in the experiment (listed as an opportunity) can be a vital and helpful element if the experiment is properly configured. If, on the other hand, the experiment becomes overly complicated or time consuming, or, possibly, there is a delay following launch before the crew functions at desired capability, then manned participation may become a limitation to the experiment.

OPPORTUNITIES

- Facility Weight
- Facility Volume
- Total Energy Budget Per Mission
- Energy Release Rate
- Facility Recovery and Re-Use
- Broad Range of Associated Instrumentation
- Manned Participation

LIMITATIONS

- Mission Duration
- Orbit Altitude and Inclination
- Orbiter Movement During and Following Particle Release
- Contaminants (Both Material and Electromagnetic)

Table 2. Opportunities and Limitations for the AMPS Particle Accelerator Facility.

Other parameters listed in Table 2 may shift from the opportunity to the limitation category under experiment growth. For example, payload capability is large with the Orbiter (payloads into the 30 kilopound region may be considered for launch and return missions), and would permit a massive energy storage unit for the particle accelerator facility. Sufficient growth in the accelerator package, however, could eventually require energy storage units even more massive than allowed by the Orbiter, thus qualifying payload capability as a limitation. This situation is not to be avoided if the following is considered as a meaningful design approach.

(1) That developed scientific effectiveness of the AMPS mission will depend heavily on the proper "impedance match" between the particle accelerator facility and the Orbiter opportunities, and, that,

(2) for such an impedance match and for continued growth in the accelerator and in the delivered science results, ultimately, most of the listed "opportunities" in the Orbiter will become "limitations", thus fully exploiting Orbiter capabilities.

The principal opportunities in the Orbiter for a particle accelerator system is large payload weight (>30 kilopounds, as noted), large payload volume ($>10^2$ cubic meters), large total energy budget per mission ($\sim$1 megawatt-hour for all experiments, and, perhaps, 200 to 300 kilowatt-hours for particle accelerator experiments), high energy release rate ($>10^8$ watts, as will be discussed further), facility recovery and re-use (thus allowing significant cost savings plus meaningful technology goals for each mission), a broad range of associated instrumentation (in particle, wave, and quantum detectors), and manned participation.

The Orbiter limitations do impose a significant guiding factor on mission planning. A principal limitation is in mission duration, considered initially at 7 days, with possible later extension to 30 days. Experiments dedicated to observation of specific naturally occurring phenomena are not well matched to the Orbiter capability, if the mean time for a possible observation of such natural occurrences is comparable

to or larger than mission duration. Considering all factors, mean time for occurrence and observation of natural phenomena, if these experiments are included in the mission plan, should be, at least, two orders of magnitude below mission duration to allow multiplicity of observation and to allow for impact against the mission of competing experiments, or localized ground or Orbiter technical considerations (viewing ability from ground based stations, for example, and possible necessary, and difficult, Orbiter reconfiguration or reorientation).

Another area of limitation is Orbiter altitude and inclination. Naturally occurring phenomena over the polar regions or for very high L-shells, will not be observable with lower inclination orbits, and occurrences at altitudes other than the Orbiter altitude (assumed initially at 400 kilometer, circular orbit) are only observable at a distance (no direct, in situ, measurements). These orbital altitude and inclination limitations impact not only on observations of naturally occurring phenomena, but also in the accessability of particular regions in space for which a perturbation experiment may be planned.

A third area of limitation in mission planning is Orbiter movement during and following particle release. If charged particles are being accelerated and released and are, following release, caused to remain on a given magnetic field line, then Orbiter motion will limit the intensity of perturbation since particles released at different times, would, thus, act to perturb different regions of space. An additional impacting factor brought about by Orbiter motion is in separation of the spacecraft from the observed event if a time lapse occurs. For example, in electron echo experiments the Orbiter has moved away from the echo at the time of its return, and remote detection (through a subsatellite) is required.

A final area of limitation for experiments on the Orbiter may be in contaminants. Two forms of contaminants are of concern here. The first is material transport and deposition and could effect, for instance, surfaces on optical instruments, particle detection surfaces (channeltrons, for example), Langmuir probe surfaces (with buildup of insulating layers), and electron emissive surfaces (in the electron accelerator). Electro-

magnetic interference is another form of "contamination", since its presence could impact on the operation of certain low-level signal devices (for example, in wave detection). At present, there is no firm assessment of the magnitudes of either material contamination or of electromagnetic contamination, so the labeling of this area as one of limitation is tentative.

Surveying both opportunities and limitation areas, a planning approach will be taken which minimizes impact from the limitations while exploiting opportunities. This will lead to a "combined purpose" mission, as described in the following sections.

3.2 Mission Modes

Two mission modes for the Orbiter/Particle Accelerator System will be identified here. The first of these is a "monitor" mission whose purpose is to observe and quantify naturally occuring phenomena in the Earth's atmosphere, ionosphere, and magnetosphere. The monitor mission is, largely speaking, an inherited role from "classical" space physics whose tools included long duration orbiting spacecraft and short duration rocket probe flights. A second mission mode is the "modification" mission whose purpose is to alter one or another of the properties of these three regions of space, and as a result of controlled alteration of these properties, to gain new and fundamental insights into the inter-regional and intra-regional coupling processes. This modification mission marks, essentially, a new era in space physics, although there is some relevant rocket flight experience. Since the modification mission is a developed role, it entails high possibilities of return with not yet certain probabilities. The monitoring mission, conversely, has more assured areas of success, with a more limited total research return, since these areas have already seen vigorous exploitation.

Experiments which may be carried out in the monitor mission and space parameters which may be varied in the modification mission are listed in Table 3. The experiments listed under the monitor mission are those performed with an electron accelerator. For the modification mission, specific method of modification is not given, although in later discussions emphasis will be directed toward electron guns and magnetoplasmadynamic (MPD) arcs.

MONITOR MISSION

- Electron Echo
- $\vec{E} \| \vec{B}$
- Large Scale $\vec{E}$, $\vec{B}$ Morphology

MODIFICATION MISSION

- n_e, n_i
- T_e, T_i
- $\vec{B}$, $\vec{E}$
- $\sigma_{\|}$, $\sigma_{\perp}$; $\nu_{\|}$, $\nu_{\perp}$
- Ion, neutral species
- Plasma Wave Spectra

(Low Power Level Electron Beam-Space Plasma Interaction is a Forerunner to the Modification Mission)

Table 3. Monitor and Modification Missions for the AMPS Particle Accelerator Facility.

The electron gun applications in the monitor mission include the electron echo experiment, measurements of the presence of electric fields which are parallel to the Earth's magnetic field, $\vec{B}$, and determinations of the large scale morphology of electric and magnetic fields in the ionosphere. The interaction of a low powered electron beam with the ambient space plasma, directed along conventional lines of pursuit for beam-plasma systems, could be considered as a monitor of the condition of the ambient plasma. However, by increasing the levels of modulation in the electron beam, increased levels of beam-plasma coupling appear, and the experiment evolves into a modification of the space plasma.

The parameters which may be altered in the modification mission include n_e and n_i, electron and ion number density, T_e and T_i, electron and ion temperature, $\vec{B}$ and $\vec{E}$, the magnetic and electric field in the space, $\nu_{\|}$ and $\nu_{\perp}$, the effective collision frequencies for particle motion in parallel and perpendicular directions to $\vec{B}$, and $\sigma_{\|}$ and $\sigma_{\perp}$, electrical conductivity for particle motion along and across $\vec{B}$, both ion and neutral species (through both injection and in situ reactions), and the spectra of plasma waves.

3.3 Mission Requirements

3.3.1 Monitor Mission

The monitor mission experiments listed in Table 3 presume distinctions between electron echo, $\vec{E}\|\vec{B}$, and large scale, $\vec{E},\vec{B}$ morphology interactions. Such distinctions are somewhat qualified. Each of the reactions may be said to be an exercise between an electron and the electric and magnetic fields in the ionosphere and magnetosphere, with the Lorentz equation expressing the functional relationship between $\vec{E}$ and $\vec{B}$ and the particle motion. An electron echo experiment, however, also depends on collective interactions between the electron beam and the ambient plasma. The $\vec{E}\|\vec{B}$ experiment focuses attention on a specific component of the electric field, with, moreover, an emphasis toward observations of naturally disturbed regions of the ionosphere and magnetosphere. The large scale morphology experiments relate to both parallel and perpendicular E field components, and, in some instances as to whether magnetic fields are open or closed.

Since these experiments differ, requirements for the experiments differ. Requirements for the experiments also vary depending upon methods of detection. The electron echo experiments of McEntire, Hendrickson, and Winkler and Winkler, Arnoldy and Hendrickson used electron beams at 80 milliamperes and 45 kilovolts for 16-64 millisecond durations and had observable return signals to on-board detectors. For an electron echo experiment on the Orbiter, however, motion of the source point leads to significant separation distances of the spacecraft from the echo return point, and appeals must be made to detection from either subsatellites, or, perhaps, by optical sensing of returning electrons through the excitation of the upper atmosphere. This latter possibility exists for specific release and reflection points with echo conditions required at one end of a field line while an absence of reflection is required when electrons return to the regions near their release.

Estimates of electron beam power required for the detection of optical emission from electron impact on the upper atmosphere vary depending upon the separation distance from the excited region to the observer, the size and sensitivity of the optical detection device, background light signals, size and total volume of the excited region, specific wavelengths for detection (as contrasted to total signal detection), and the degree to which details of the excited region are to be perceived (width, height, striations, height-luminosity). Beam power requirements which result from any series of parameters chosen above must then be examined against the several experiments for which optical detection is the means of determining electron response. For the monitor mission experiments, not only electron echo but also $\vec{E}||\vec{B}$ and large scale, $\vec{E},\vec{B}$ morphology include optical detection as one of the methods for carrying out the measurement. The upper end power requirements of all of these experiments, then, will be paced by required beam power for optical detection.

From earlier rocket flights of Hess, Trichel, Davis, Beggs, Craft, Stassinopoulous, and Maier, and of O'Neil, Lee, Huppi, and Stair, required beam power is clearly in excess of 5 kilowatts. In order to allow viewing with large aperture, high sensitivity detectors for separation distances up to 1000 kilometers, a realistic power requirement is

50 kilowatts. An important trade-off study, as mission planning continues and definitions firm, will be to evaluate a system "effectiveness" (including costs, allowable operation time against various background light levels, and total available time during the mission for above-threshold excitation and detection), as a function of electron beam power and optical system size and sensitivity. For present design purposes, 50 kilowatts will be used as this beam power requirement.

While the upper end power requirements are set by the means and method of optical detection, lower end power requirements are paced by the sensitivity of on-board detectors of remote subsatellites. From the earlier electron echo experiments, these lower end beam power limits would appear to be in the range of 1 kilowatt. Monitor mission experiments, thus, range in power requirement from 1 to 50 kilowatts, and the major question in system design will be whether this power range is accessible with a single (grid-controlled) electron accelerator or will require use of both a high power and a low power beam. The use of a single accelerator over not only a wide power range but also wide current and voltage ranges raises, in turn, questions of flow properties and required control drive voltages. Section 8, Electron Accelerator Design Considerations, will discuss these performance areas in more detail. For present purposes, it will be assumed that a single electron accelerator performs acceptably over this power range.

The existence of comparatively high power levels in the electron beam (50 kW) also raises the possibility of alterations of the ionosphere. For measurements of $\vec{E}||\vec{B}$ in regions of the ionosphere disturbed by naturally occurring events, the additional impact of the passage of high level energetic particle flows may even further disturb and alter the region under investigation. There may be, then, some level of beam condition at which an experiment in the monitoring mission becomes an experiment in modification. Since the experiment is of value in both of the mission modes, a transition from monitoring to modification is not only valuable in terms of providing a multiple purpose experiment but is also valuable, perhaps, in allowing a more precise evaluation of the natural causes of the phenomenon. The experimental problem, then, will be to identify the specific realm of the measurement

(monitor or modification) as beam power is raised, noting the transition as an indication of natural perturbation levels.

Two final areas of consideration for monitoring mission requirements are the current-voltage ranges of the electron accelerator (within the power envelope previously derived), and required burst duration. The current-voltage regime of the accelerator will be discussed, as previously noted, in Section 8, which will also examine angular divergence properties of the flow as flow perveance is varied. The remaining concern, then, is burst duration.

Burst duration in the electron echo experiments ranged, as noted, from 16 to 64 milliseconds. Burst requirements for $\vec{E}||\vec{B}$ could be somewhat longer, since a search for disturbed ionospheric regions where $\vec{E}||\vec{B}$ may exist must, initially, be conducted over a broader size scale. Since Orbiter velocity is $\sim$8 kilometers per second, maximum velocity across $\vec{B}$ is set at this figure. A burst duration of 2 seconds would allow a search over a region whose extent would range from 16 kilometers to 8 kilometers, for angles between $\vec{B}$ and the Orbiter $\vec{v}$ ranging from 90° to 30°. Burst duration of 2 seconds would probably establish an upper end point for the monitor mission experiments, since large scale $\vec{E},\vec{B}$ morphology can be determined with beam bursts tailored more toward the electron echo experiment.

The power and burst duration range of the monitor experiments establish a region in a space (P,t), from which required power from the system power train, and required energy storage may be derived. This (P,t) diagram will be given in Section 3.4, Power-Time Regimes for Combined Mission Modes.

3.3.2 Modification Mission

3.3.2.1 General

Section 3.2 has noted that modification mission experiments introduce an essentially new era in space physics. As such, the possibilities of fundamentally new and exciting results are high, while probabilities remain undefined. The modification experiments necessarily involve pursuit of interactions beyond linear regimes, so that linearly-based theoretical considerations are of limited value. Additionally,

modification experiments may involve chemical reactions for which the rates of reaction are not known, and may, in point of fact, only be determinable in the unbounded geometry excitation experiments allowed with AMPS. For these several reasons, reaction thresholds are not precisely defined, and can only be treated in a qualitative manner in this study.

An additional major area of consideration is in reaction detectability. Section 3.3.1 has noted the many factors involved in signal detectability as this relates to required power in the monitor mission experiments. These factors apply equally to the modification mission.

In spite of both reaction rate (and direction) uncertainties and detectability uncertainties, some estimates of power requirements may be drawn for modification mission experiments. This study will consider four experimental areas, using general observations from naturally occurring phenomena plus estimates of characteristic times and distances, to indicate required energy release and release rate, or required particle number and release rate. An important conclusion from these generally derived requirement estimates will be that there is a consistent tendency for additional experimental return for additional input power, or energy, or charged particle number. It is the slope of the experimental return versus excitation level which leads to a conclusion of increasing effectiveness for the modification mission experiments for increased time and mission number, provided that particle accelerator system development is possible along lines of increased power, total energy release, and particle energy and species.

3.3.2.2 Auroral Simulation

Observation and measurements of auroral have been and continue to be a region of vital interest in space physics. An inherent problem in auroral studies, however, is imprecise knowledge of the source term in electron energy and energy distribution, electron flux density, period of initiation (and, necessarily, the extent of pre-conditioning of the upper atmosphere by those reactions initiated prior to the principal onset of electron deposition). The AMPS particle accelerator system can provide

a precisely known source term with a precisely defined onset, and, depending upon the choice of L-shell for electron release, with a deposition region whose initial properties are well defined.

A Class II + aurora (brightness in the 5577Å line at 50 kilo-Rayleighs and brightness at ∿35kR at 3914Å) is considered to require an electron energy flux of 2.2×10^{-6} watts per square centimeter (at average electron energy of $\sim 10^{+4}$ eV). A 50 kilowatt electron beam could provide excitation at this level over an area of 2.3×10^{10} square centimeters, an area roughly 1.5 kilometers on a side. The actual region of deposition for a 50 kilowatt electron beam is, of course, somewhat unknown in both lateral extent and depth of excitation, since primary electron motion across magnetic fields in the collisional slow-down is difficult to calculate. For present purposes a deposition depth of 10 kilometers will be used and a final area of 5 kilometers on a side will be assumed for an initially narrow beam. End point excitation levels for the assumed 50 kilowatt beam would still remain in the Class II level of aurora.

The lateral spread of the excitation across field lines and the Shuttle orbital velocity relative to the Earth's magnetic field will define a characteristic time of excitation. For 5 kilometers total lateral extent for a line beam of electrons and 5 kilometers per second Orbiter motion across $\vec{B}$ (assuming relative motion angles below 90°), leads to a characteristic time of ∿1 second, and prolongation of the beam burst through a 1 second interval would result in increasing levels of excitation in a given volume of the excited region. For burst durations above 1 second, other neighboring regions will begin periods of excitation and the total excited area will become more of a "streak" than a "point" in its appearance.

The characteristic time described above will be, of course, a function of electron primary energy. Increases in electron primary energy result in increased depths of penetration into the atmosphere, and a greater lateral extent of the excited region. Increases in the lateral extent of the region, lead, in turn, to increases in the period of time over which excitation in a given volume continues for a moving source. Thus, for increased acceleration energy and power, an assumed

10 kilometer lateral extent to the spread of an initial line beam, and for 5 kilometers per second Orbiter motion across $\vec{B}$, excitation would continue to buildup over a period of ∿2 seconds. It is important to point out that significant increases in allowable excitation time would result, thus, for polar orbiting AMPS since the Orbiter dwell time on a given tube of the magnetic field of the Earth is considerably longer ($\sin \theta_{rel}$ approaching zero).

The acceptance of Class II levels of excitation as a desirable simulation case leads to power requirements in the 50 kilowatt regime (the summary will list 30 to 300 kilowatts as an interesting power range for these experiments) with burst durations of the order of seconds. These excitation periods are sufficiently prolonged to allow an accurate assessment of both electron deposition patterns, and 5577Å oxygen emission. The 50 kilowatt, 2 second burst would result in final electron densities well in excess of 10^6 electrons per cubic centimeter in the region from 90 to 120 kilometers altitude, for those experiments aimed at charged particle density alterations in the E layer.

The considerations above lead to an estimate of experiment effectiveness as a function of beam power, as illustrated in Figure 2. As noted previously, threshold levels are very intimately linked to the detection system sensitivity, so that desirable minimum power can be reduced for increases in detection capability. For fixed detection capability, however, increases in beam lead to increased total experiment time above the noise backgrounds, and also to improved spatial and temporal resolution. The most important feature of the experiment return versus experiment power dependence is that it possesses a positive slope.

3.3.2.3 Species Growth (Air Chemistry)

Discussion in 3.3.2.2 considered the emission from O('S) at 5577Å, and concluded that burst durations of the order of seconds would be sufficient to determine buildup at this wavelength. Other emissions of concern under energetic electron deposition and which require buildup periods include NO and NO^+ chemiluminescence at 5.3μm, 4.3μm, CO_2 lines at 4.3, 9.4, 10.4, 13.6, and 15μm from vibraluminescence plus direct excitation from the electrons, and O, O^+, N, and N^+ emissions from impact

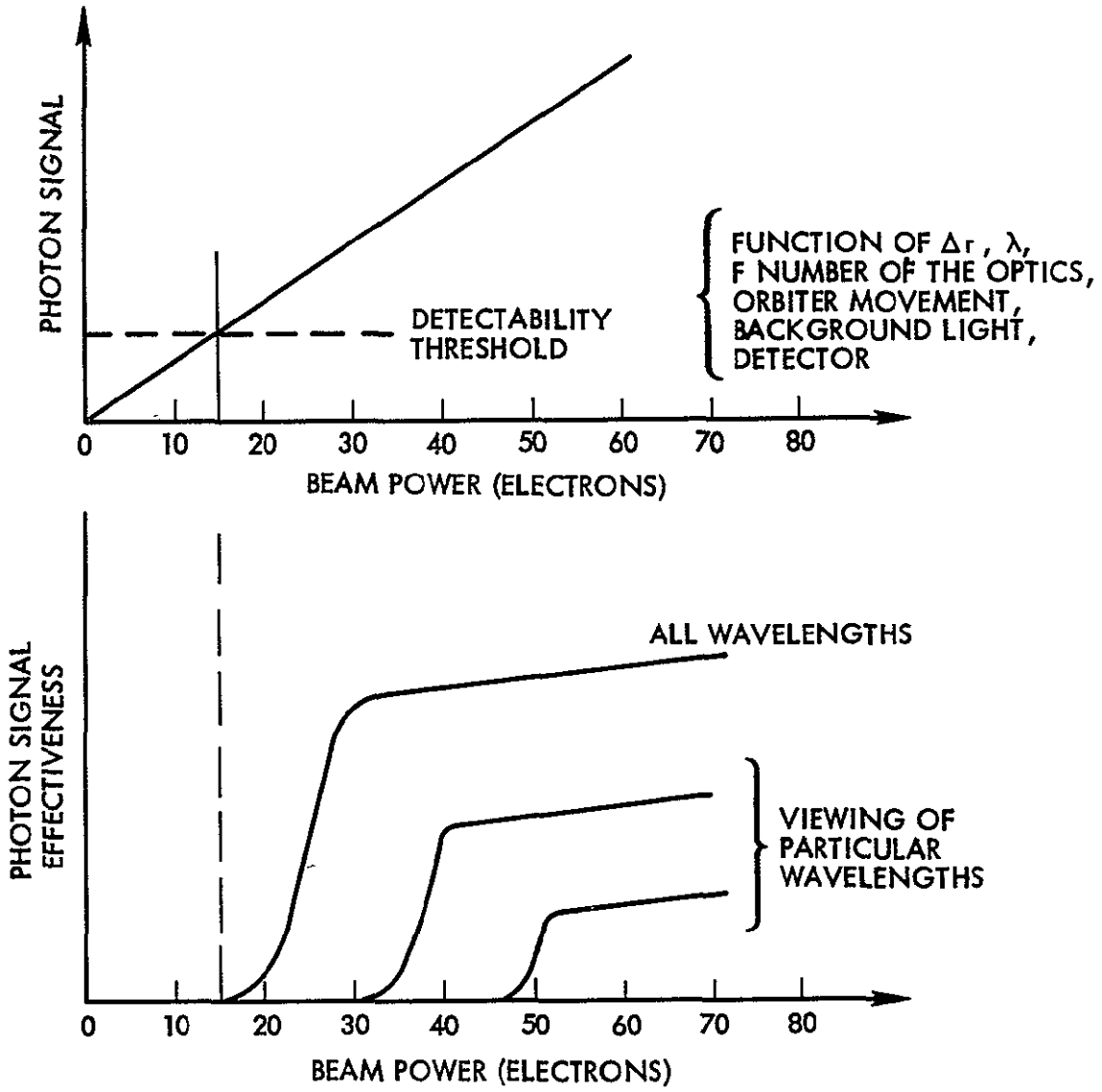

Figure 2. Experiment Effectiveness (Photon Signal Strength and Effectiveness) as a Function of Electron Beam Power for Prompt Emission from Atmospheric Excitation in Auroral Simulation.

derived air chemistry. Derivation of rates in some of the reactions involved in this air chemistry is beyond the capability of laboratory experiments because reactants diffuse to the walls and are lost before sufficient reacting time has elapsed. The unique ability of the AMPS species growth experiment to proceed in an "unbounded testing facility" can significantly advance understanding of these reactions and their rates with a principal question then being appropriate voltage and power levels.

Increases in the acceleration energy of the electrons leads to a greater depth of penetration into the atmosphere and a consequent increase in the dimensions of the reacting volume. For charged particles whose diffusion is principally along (rather than across) $\vec{B}$, an increased reaction time results from increased depth in the excited region. Since electron diffusion across $\vec{B}$ also occurs in the stopping process, the lateral size of the heated region also increases with increased beam voltage. Total dwell time of a reacting particle inside the excited region will depend not only on this depth and lateral extent (from electron slowdown diffusion) but also from the total burst duration. As noted in 3.3.2.2, increases in excitation proceed for burst durations comparable to the lateral spread of a point beam divided by Orbiter velocity relative to $\vec{B}$. For burst durations beyond this characteristic time, the excited region becomes elongated in the direction of Orbiter motion and will not result in significant further advances in exposure of species to reaction. A final dependence is upon beam current which may be expected, at fixed beam voltage, to be proportional to the number density of particles excited per unit time interval, by primary electron impact.

If species buildup in a reaction is proportional to the number densities of each of two reactants and escape to the boundaries determines an abundance level of reactants, then a final species density buildup would be expected to be roughly proportional to V^2I^2T where V is beam acceleration voltage, I is beam current, and T is burst duration. More complicated dependencies and higher power law dependence might be expected for species derived from a series of reactions.

Figure 3 indicates a qualitative dependence of signal return

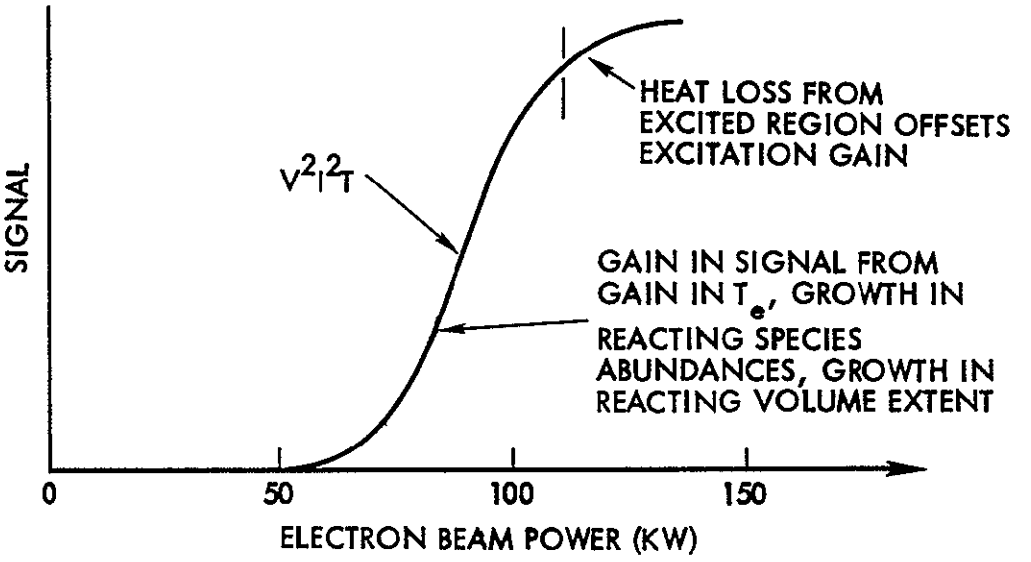

Figure 3. Experiment Effectiveness (Species Signal Strength) as a Function of Electron Beam Power for Species Growth (Air Chemistry Experiment).

versus beam power where signal return is assumed to be proportional to the density buildup in a species. The power law dependence indicated there is clearly above linear for some regime. Leveling off at higher power could occur if further power increases resulted in excitation of regions not intimately linked to the principal region of excitation of if increased heat conduction away from the region by energetic secondary and tertiary electrons were to occur. Again, as for the case of prompt emission signals, the most significant aspect of the dependence of signal return to beam power is the positive slope. Unlike prompt emission, however, this dependence is not simply linear, and could exhibit saturations, albeit at beam power levels significantly above the 50 kilowatt beam considered in Section 3.3.2.2. Useful power range for the species buildup will be listed in the summary for this section in the 50 to 500 kilowatt range.

3.3.2.4 Electron Temperature Alteration

Electron temperature alteration in an atmospheric region under energetic electron beam deposition has already been considered, implicitly, in Section 3.3.2.3, and emphasis in this section will be toward temperature elevations in F layer regions. The mechanisms for coupling electron beam energy to ambient electrons is more speculative here than for the atmospheric deposition case, but could proceed through resonant coupling between the space plasma and an electron beam whose current is modulated at either ω_{ce} or ω_{pe}.

The night-time F layer electron energy density has a maximum value of $\sim 3 \times 10^{-15}$ Joules per cubic centimeter, and the release of 10^5 Joules of energy, through the electron beam with resulting coupling into ionospheric electron temperature, could raise T_e by a factor of two over a total volume of 3×10^{19} cubic centimeters. This is a volume roughly 30 kilometers on a side.

The actual size and configuration of the elevated temperature region and the extent of electron temperature elevation will depend upon many factors. Modulation of the beam at ω_{pe} and its release along the B field line would probably result in a long cylindrical volume of excitation with elevated levels of both electron temperature and turbulent

electric fields. The combined effects of extended length along $\vec{B}$, a high turbulent E-field level, and comparatively reduced conductivity across $\vec{B}$ would be to reduce the rate of cooling in the affected region. If these cool-down times extend into the time realm above 1 second, then energy release rate in the electron beam at 100 kilowatt levels would be at a sufficient rate to bring the temperature elevation to almost maximum possible levels. If heat conduction drain-out of the excited region were to be at the 100 millisecond level, appropriately increased electron beam release power would be required to produce effective temperature elevation. Modulation of the beam at ω_{ce} would cause coupling through electron cyclotron resonance, and would probably result in enhanced cross field heat conduction, with a resulting excited volume more extended in the directions transverse to $\vec{B}$, and with a likely reduction in maximum temperature elevation throughout the volume because of the now more acessible heat transport process along $\vec{B}$.

Figure 4 illustrates possible temperature elevation as a function of electron beam power. The tendency for more rapid growth in ΔT_e as beam power proceeds past some lower level assumes an increased turbulent electric field with a resultant decline in heat conduction. The round-off region at higher beam powers anticipates additional heat transport developing through both enhanced loss per electron and increased (and now significant) cross field heat transport as a result of turbulent $\vec{E}$. Estimates of power requirements for major sized region alterations are at 50 to 100 kilowatts. Since the Orbiter has many particle spectrometers capable of measuring electron temperature elevation, and, since the excited region is now adjacent to the Orbiter (rather than at hundreds of kilometers as in the case of the excitation of the atmosphere) the power required for at least some level of observable effect is reduced. An estimate for observable effects at the Orbiter will be in the 10 kilowatt power region and above, with observable effects from ground based stations, using scatter communications, at the 50 kilowatt level.

3.3.2.5 Magnetic Field Disturbance and Plasma Density Alteration

Previous sections have been concerned with electron beam excitation of the ionosphere and atmosphere. This section will consider

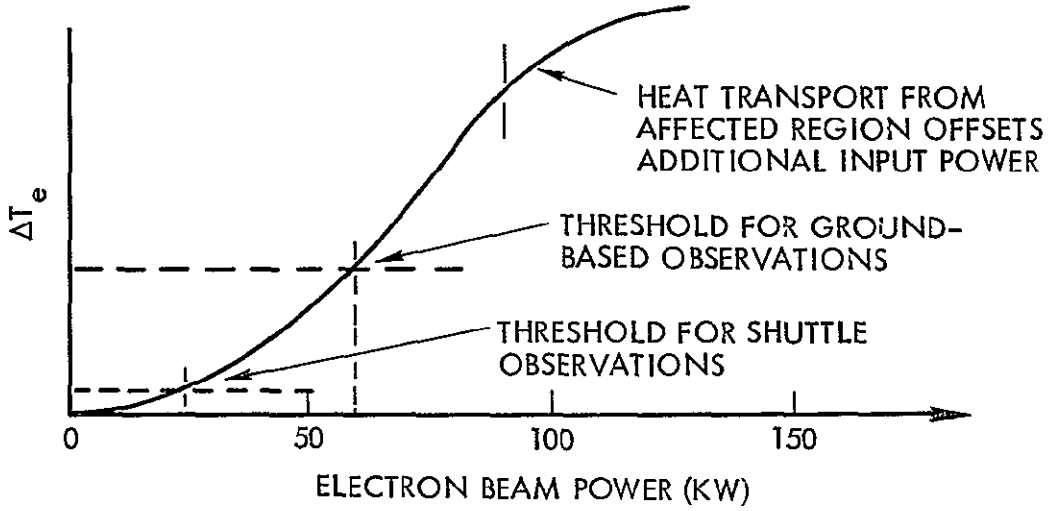

Figure 4. Electron Temperature Alteration as a Function of Electron Beam Power for Electron Beam - Ionospheric Heating Experiment.

ionospheric alteration using another form of particle release, the magnetoplasmadynamic (MPD) arc.

Magnetic energy density at the Orbiter altitude is approximately 2.5×10^{-10} Joules per cubic centimeter. The conversion and release of 10^5 Joules of electrical energy into an accelerated plasma would create a condition of $\beta = 1$ throughout a volume of 4×10^{14} cubic centimeters. If the resulting plasma shape after release, and following containment by the now displaced magnetic field, is spherical, the diameter of the sphere would be approximately one kilometer.

At present the level of diamagnetic behavior in the MPD arc plasma is not known. For present purposes, it will be assumed that field line exclusion occurs at least during the time for the plasma front to move across the 1 kilometer sphere diameter. For a plasma front velocity of 2×10^6 centimeters per second, the transit time across 10^5 centimeters is approximately 50 milliseconds. Conversion of 10^5 Joules into plasma over a 50 millisecond period places MPD arc power at 2 megawatts, well within arc capability ($\sim$20 megawatts for current MPD arc design).

The energy required to create and accelerate an ion-electron pair in an MPD arc is approximately 600 eV, and the conversion of 10^5 Joules would yield a plasma release of 10^{21} ion-electron pairs. This plasma, if containment in a volume of 4×10^{14} cubic centimeters is realized, would have a contained density at $\sim 2.5 \times 10^6$ ions and electrons per cubic centimeter, thus realizing a density increase over previous F layer density of from 2.5 to 25 (assuming $10^5/cm^3$ as night-time density and $10^6/cm^3$ as day-time density). The plasma release (and assumed, temporary containment) represents, thus, a major modification of magnetic field and plasma density patterns.

There are no firm estimates at present of the period required for the magnetic field to re-enter the plasma cloud or for the cloud to diffuse into the now-shocked ambient plasma, and the modification mission experiment here would be the diagnosis of the cloud containment and break-up and the resulting wave emission spectrum.

Power requirements on the basis of energy release per transit time across the containment region yield an arc power requirement of 2.5

megawatts for a 10^5 Joule release. If the energy release is raised to 10^6 Joules, spherical volume diameter of $\beta = 1$ plasma increases to $\sim$2.1 kilometers, and required power to achieve the release per transit time is $\sim$10 megawatts. The requirements summary for this experiment will list 2 to 10 megawatts as the range for MPD arc modifications of the ionospheric plasma.

3.4 Power-Time Regimes for Combined Mission Modes

Figure 5 illustrates mission requirements in beam power and burst duration for an electron gun in both monitoring and modification missions, and for an MPD arc in the modification mission.

The electron gun modification mission experiments are characterized by generally elevated power requirements. An exception is the low power level, low modulation level beam plasma experiment which is listed here under "modification" since it provides a logical forerunner to the high power, high modulation beam-plasma coupling experiments for ionospheric electron heating. Since the initial flight experiment in beam-plasma coupling will probably proceed more conveniently with a steady state beam, burst duration requirements for this experiment extend to the 1 hour point. As a modification experiment at high power levels, these burst durations will obviously be required to be shortened, and Figure 5 indicates .1-1 second for the high powered bursts.

Monitoring mission power requirements range to 50 kilowatts when optical detection of the beam-excited atmosphere is required. The lower bound of this power requirement is set by detection sensitivity for detectors in a subsatellite.

The highest power requirements occur for the MPD arc, and principal considerations in the magnetic field and plasma density alteration experiments is to transfer energy and plasma into the space plasma and magnetic field in periods less than the period for magnetic field re-entry into the ejected plasma burst. As noted in 3.3.2.5, this power capability exists in present day MPD arcs.

Although there are variances in the ranges in beam power and burst duration for the electron gun monitoring and modification missions, there are also significant regions of overlap. For optimized mission

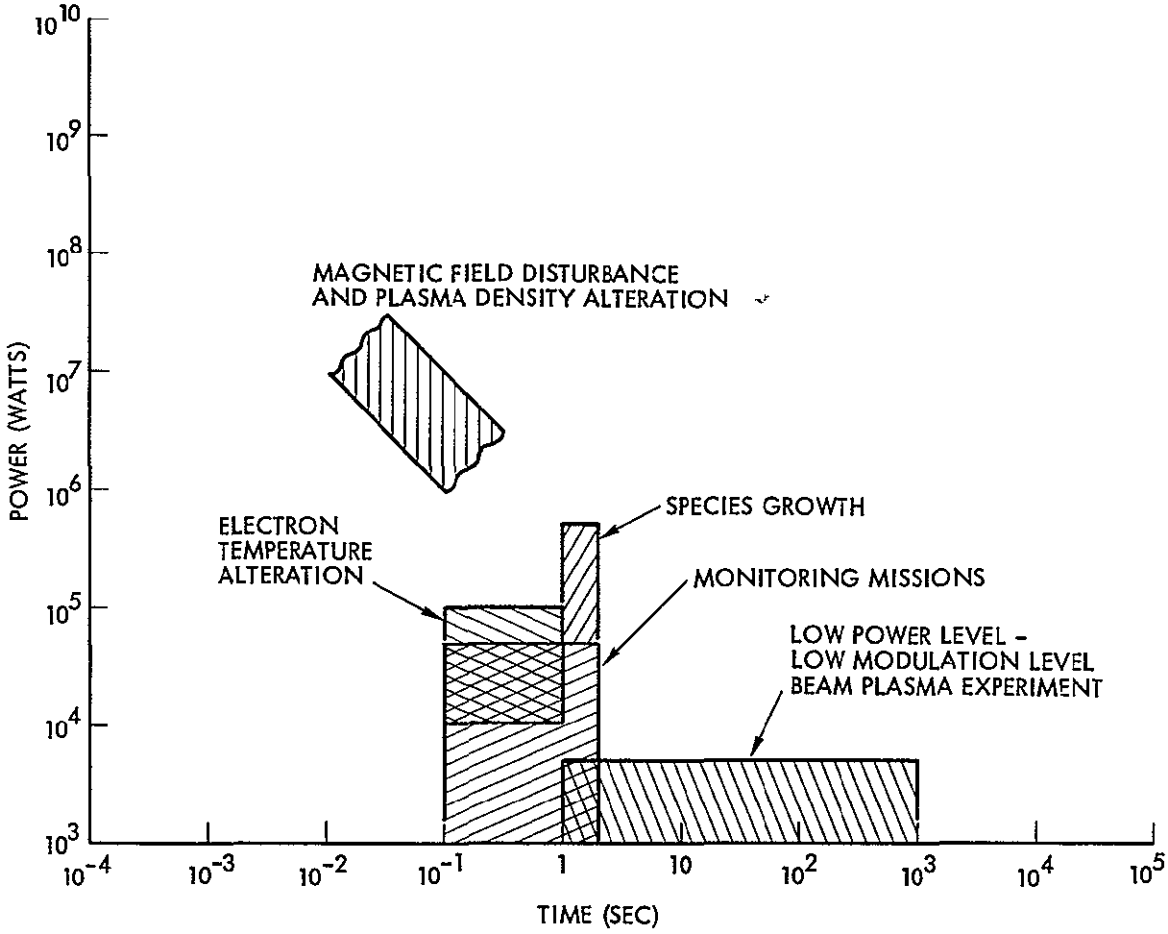

Figure 5. Mission Requirements for Beam Power and Burst Duration in Monitoring and Modification Missions.

effectiveness, the design of the particle accelerator system should permit the pursuit of both of these missions. If the particle accelerator system also permits the performance of the MPD arc experiments, then still greater scientific return may be anticipated. These factors are discussed further in Section 3.5, which follows.

3.5 Effectiveness in Single and Combined Mission Modes

Effectiveness in scientific missions is not defined easily. The parameters along which success may be evaluated vary widely, and, even for narrowed ranges of these parameters, are still subject, necessarily, to personal interpretation. In this study, effectiveness will be considered in the most qualitative terms. The principal features considered to be important are, (1), that the results of experiments provide new and major advances in the understanding of atmospheric, ionospheric, magnetospheric coupling, and, (2), in view of the unique opportunities afforded with the Orbiter/AMPS, experiments proceed into realms which are not attainable from either the laboratory or from alternative methods of space flight.

Figure 6 illustrates a qualitative and personal view of effectivenss of Orbiter/AMPS as a function of time for both monitoring and modification missions, where time is presumed to proceed through the decade of the 1980's. Mission-to-mission comparison of effectiveness is not undertaken here, and principal emphasis is upon the time dependence of mission effectiveness.

The effectiveness of the missions which monitor naturally occurring phenomena is shown as a series of declining lines with restoration through either additional diagnostic capability (manueverable subsatellites), extended orbital altitude and inclination (particularly in the transition to polar orbiting spacecraft and the consequent opening up of high L-shell examination), and additional mission duration (thus permitting observation of statistically less frequent events). In the periods between these additional diagnostic or orbital features, effectiveness is shown in decline as an inevitable result of the exploitation and completion in understanding of the base of natural phenomena under examination (including, perhaps, the abandonment of particular experimental searches in view of limited duration of the

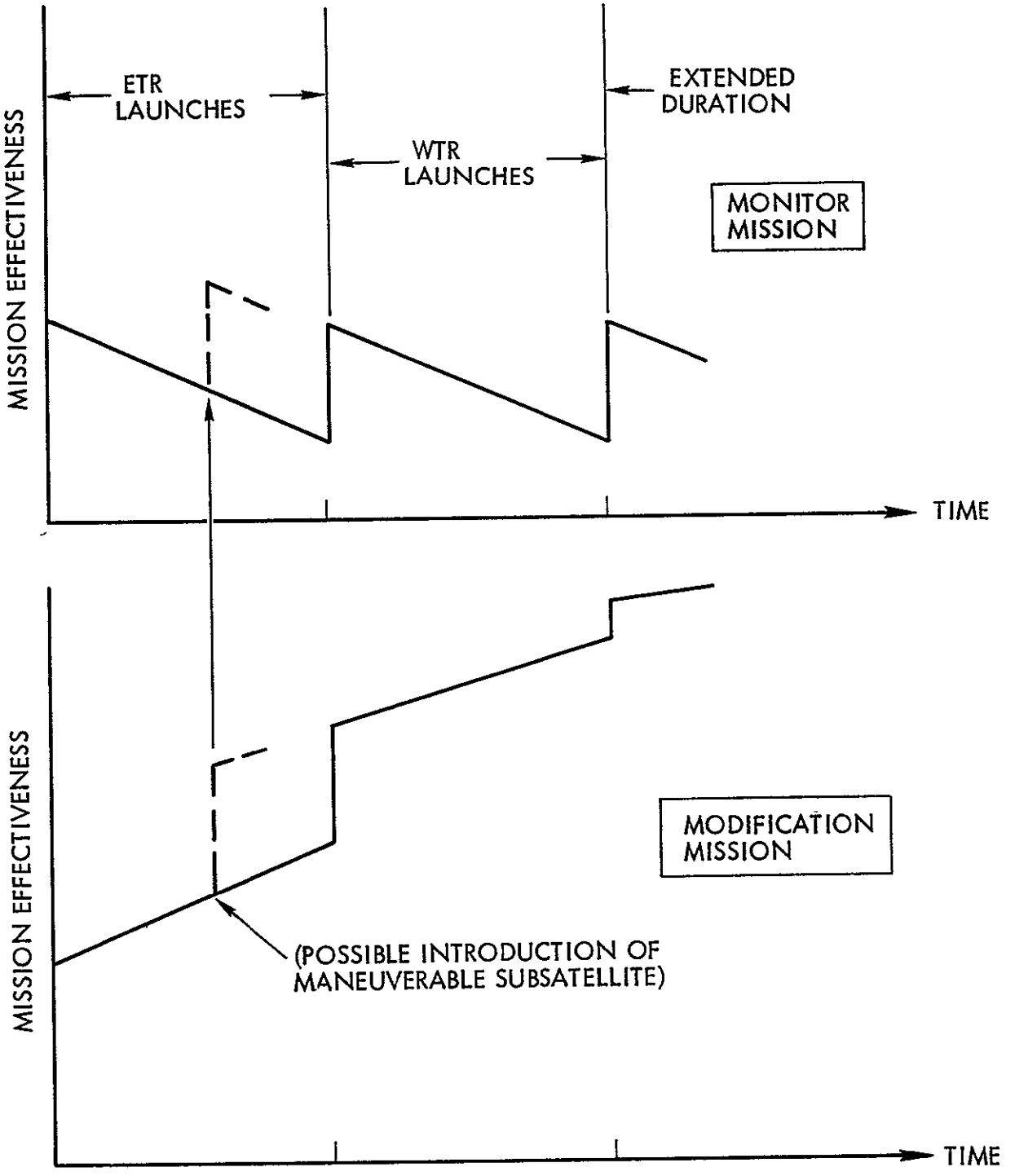

Figure 6. Mission Effectiveness as a Function of Time for Monitoring and Modification Missions (AMPS System Growth in Species and Power Assumed).

mission and the possibility of only infrequent observations in this period).

Effectiveness in the modification missions moves through upward adjustments for the same factors (additional diagnostic capability, orbital inclination, and mission duration) as for the monitoring mission. In the periods between these extra diagnostic or orbital capabilities, moreover, there are periods of increasing effectiveness. This increased effectiveness is considered to follow from allowable growth modes in the modification mission. Section 3.3.2 has examined experiment return as a function of beam power and total energy release and established that the slopes of signal return and experiment effectiveness are positive for additional power. Other growth modes not specifically detailed to this point of the study but nevertheless visible are in additional species in release including the ion accelerators and high voltage plasma guns.

The Orbiter/AMPS has, as noted, specific areas of advantages which make development of the particle accelerator system along the power and species axes possible, so that the considered developed effectiveness in the modification mission is consistent with overall system capability and with the specific possible system capability in the accelerator payload.

An important decision in mission planning would be required if the choice of mission excluded one or the other of the two considered modes. If this were to be the case, then a choice would have to be made between present certainties and limitations in the monitor mission against the extensive but as yet undetermined possibilities of the modification mission. From Section 3.4, however, it is evident that a common ground exists in, at least, the beam power - burst duration requirements of the two modes, and the most logical line of system design is to derive a system capable of exercizing roles in both of the indicated missions. An additional and necessary capability is expansion into the higher power, additional species release realm of the modification mission growth modes. The aim of this study will be to define a system with these several levels of commonality.

4. SYSTEMS CONSIDERATIONS IN AMPS PARTICLE ACCELERATOR DESIGN

4.1 Requirement for Energy Storage

Energy storage for the operation of the particle accelerator system is, ultimately, in the chemical energy of the stored hydrogen and oxygen for fuel cell operation. This fuel cell system is nominally rated at 7 kilowatts continuous operation with burst power to the 12 kilowatt level for durations as long as 100 seconds. This high power operation period may only be scheduled once in an overall span of three hours, and, even under this limitation, imposes further operation criteria on Orbiter orientation for maximum heat rejection by the radiators.

While fuel cell operation at 7 kilowatts is allowable, in principle, on a continuous basis, allocation of power must be made to a series of AMPS users, and available power to the particle accelerator system cannot be expected, on a realistic basis, to exceed 50% of this fuel cell output, and this level of allocation to the accelerator may require power-down conditions on many other AMPS systems.

The possibility of power at several kW on a steady state basis must be compared to the power-time requirements for the missions modes in Figure 5. The only experiment consistent with this steady state - several kilowatt fuel cell output is the low power level electron beam - space plasma interaction experiment, and even this experiment exceeds fuel cell capability when viewed as a forerunner for high powered ionospheric heating applications.

The combined mission power requirements and the fuel cell power limitation lead to a firm requirement for additional means of energy storage and transfer into the particle accelerator system. Several possible means of storage are:

(1) electrical, in which the energy is in $E^2/2\varepsilon$ of the storage material, as in capacitors,

(2) chemical-electrical, as in batteries,

(3) rotational kinetic energy, as in flywheels, and

(4) magnetic, in which energy is in $B^2/2\mu$ of the storage volume, as in superconducting coils.

Discussion in this Section (4) will be concerned principally with methods 1 and 2 above. Section 6, and the study Appendices will examine aspects of flywheel energy storage. Storage in superconducting coils is not considered sufficiently developed for application to this system need and will not be treated further in the study.

One additional possibility not listed above and which will be considered in this section only is that of an "add-on" fuel cell. In the add-on cell design, additional hydrogen or oxygen tanks are not placed on the Orbiter, and the add-on cell uses the tankage of the fuel cell dedicated to the AMPS payload. Surveying the power-time requirements of the mission modes in Figure 5, power to the 100 kilowatt level at 1 second burst duration would permit an exploitation of several of the proposed experiments. The add-on fuel cell could be purposely tailored to this very high power short duration burst condition. There are two possible disadvantages to such an add-on cell, however, and both stem from inefficiencies in the fuel cell. The first disadvantage is, that, because of fuel cell inefficiency (particularly at very high burst power conditions), the total energy budget for AMPS particle accelerator operation is reduced, with loss of energy translating directly into loss of either experiment duration or repetition, or, ultimately, the experiment itself. The second aspect of fuel cell inefficiency at high burst power is thermal loading on the Orbiter if the burst is prolonged beyond certain limits. The situation may be summed basically by noting that the combined effects of (small) fuel cell working voltages and fuel cell internal impedances (even under optimum configurations) do not permit efficient high power (10^5 watts and greater) operation, combined with high power density (since weight restrictions must still be considered in AMPS designs).

4.2 Voltage Level Considerations for Electrical Energy Storage

4.2.1 Single and Dual Tier Power Processing Configurations

The output bus of the fuel cell is at 28 volts dc, and some coupling must be performed to transfer current at this voltage into the storage unit prior to its eventual transfer to the particle accelerator.

Figure 7 illustrates two possible systems configurations to accomplish this transfer. The first of these involves a single tier of power processing from the fuel cell into the storage unit with direct coupling into a particle accelerator. The requirements for the power processor for this configuration are comparatively simple and no high power level processing is required. The second configuration entails a dual tier power processing with the first stage transfer energy from the fuel cell to the storage unit while the second stage transfers energy from this storage unit to the particle accelerator. Again, requirements for the first stage processor are not extensive. The second stage processor, however, must provide high levels of power to the accelerator(s), and, since variation of beam acceleration voltage will be required, a voltage variation capability must be present in the second stage unit.

4.2.2 Capacitor Bank Energy Storage

The stored energy in a capacitor bank is given by $CV^2/2$ where, for C in farads and V in volts, energy storage is in Joules. Current day capacitive energy storage is at ∿100 Joules per pound, and, since many of the beam power-burst duration requirements are of the order of 100 kiloJoules, a capacitor bank to provide energy storage would weigh in the order of 1000 pounds, well within the payload allotment of a particle accelerator system on AMPS.

If the capacitor bank is used in a single tiered power processing configuration, then the voltage capability of the bank must be at the highest voltage intended for use by the particle accelerator. Any reduction of bank voltage to permit a lower beam acceleration voltage than the designed peak value, will result in loss of energy storage capacity. Since variation of beam output voltage by at least an order of magnitude may be expected to occur for the full range of experiments on AMPS, variation in storage bank energy would vary by two orders of magnitude from peak to minimum voltage, and significant impact would be imposed on the allowed power-duration product for the lower voltage beams. The only possibility to avoid this "V^2" penalty would be to provide a range of series-parallel stacks of the capacitors, so that increased C is provided at lower V. The switch gear to perform this reconfiguration

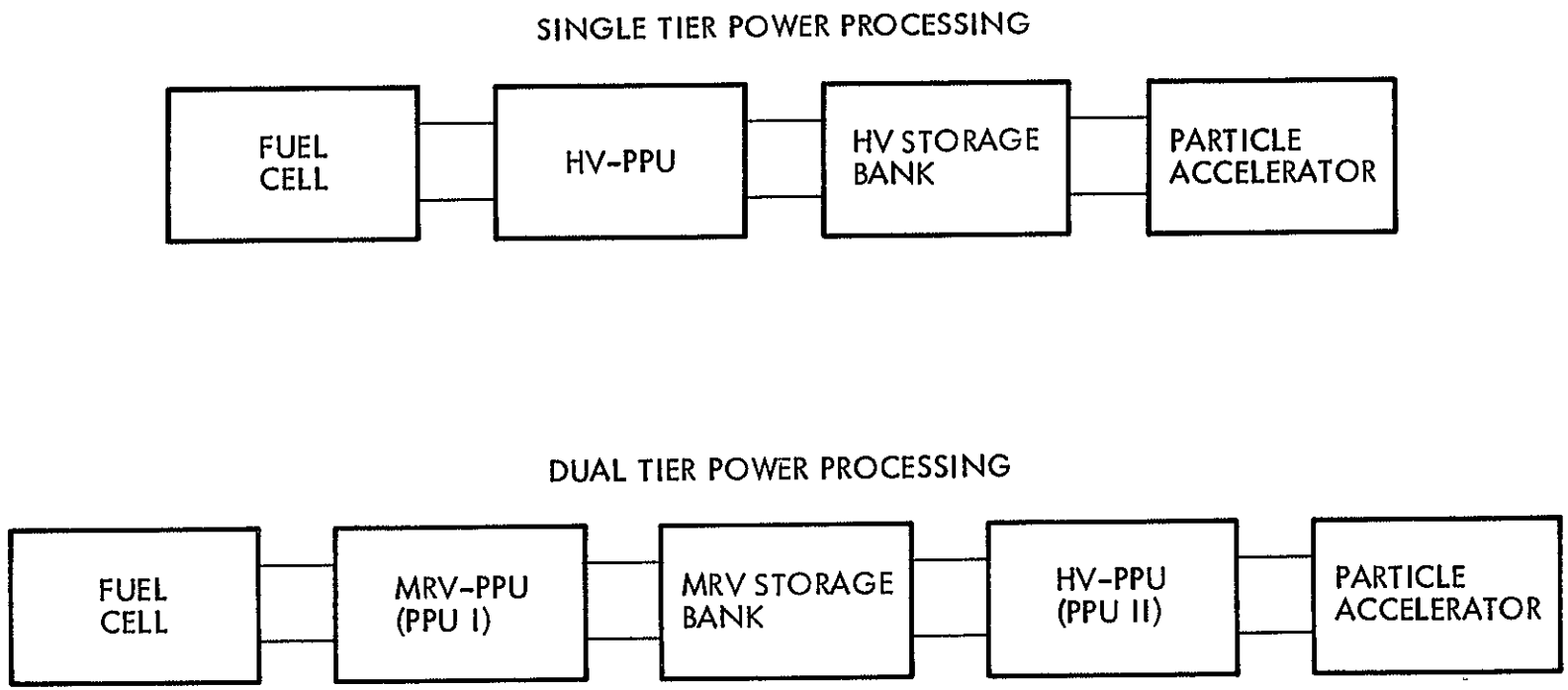

Figure 7. Particle Accelerator System Configurations for Single Tier and Dual Tier Power Processing.

would be forbidding even if peak voltages were only kilovolts. Since peak voltages in initial AMPS missions may reach to 50 kilovolts, the expected costs and design effort for the switchgear appear to be outside of acceptable limits.

Another consequence of single tiered power processing and capacitor storage is that any significant level of energy withdrawal from the capacitors results in an acceleration voltage decline. Since many of the experiments may require beam voltage to remain essentially flat throughout the burst, no practical method of operation exists except to oversize the capacitor bank by great margins and to proceed to small fractional energy transfer per burst (hence small ΔV).

Both of the possibilities discussed above must be carried out in the hazard context of high voltage storage and possible breakdown. Reconfiguration through switchgear and/or oversizing the bank add to the natural level of hazard and make the single tier processing to storage unit appear quite unattractive (see Table 4).

The use of the dual tiered system with a capacitor bank has several attractive features. The first of these is that voltage variation at the particle accelerator is now controlled by the power processor. This unit can provide both pulsed and modulated beam voltage. It can also keep the beam voltage flat during the burst at output voltages varying over a wide range for energy extraction from the capacitor bank up to $\sim$75% of stored energy, since the processor design permits input voltage variation by a factor of two for constant output voltage.

The voltage of the storage unit capacitors for the two tiered processing systems need not be at the high voltages corresponding to particle accelerator voltage. It should not, on the other hand, be at voltages like those of the fuel cell, since high power transfer with the processor then entails very high level currents and possible electromagnetic conduction and radiation interference noise. The desirable range of storage unit voltage would appear to be somewhere intermediate between the fuel cell voltage and particle acceleration voltages. For practical purposes this voltage level will be $\sim$500 volts which is consistent with the voltage rating of high energy density storage in electro-

SINGLE TIER POWER PROCESSING	DUAL TIER POWER PROCESSING
Low level requirements on single stage processor to high voltage storage.	Low level requirements on first stage processor to midrange voltage storage.
No second stage processor required.	Second stage processor required with comparatively high level requirements.
Storage unit to accelerator isolation element required.	Second stage processor provides isolation from storage unit to accelerator.
No voltage modulation capability.	Broad range of voltage modulation capability.
Maximum energy storage only at maximum acceleration voltage.	Energy storage at maximum irrespective of acceleration voltage.
Voltage decline for any significant level of energy transfer to accelerator.	No voltage decline at accelerator for up to 75% energy transfer from storage unit.
High level of hazard in energy storage.	Reduced level of hazard in energy storage.

Table 4. Performance Comparison of Single Tier and Dual Tier Power Processing Configurations with Capacitor Bank Energy Storage Unit.

lytic capacitors and is consistent with the present developed state of solid state switching units in power processor inputs. This storage condition will be termed a "mid range" voltage. A desirable feature in its usage is that voltage breakdown hazards are greatly reduced.

4.2.3 Battery Bank Energy Storage

The storage and processor configurations in Figure 7 can be applied, in principle, to battery bank units. In practice, at least one of the configurations is not practical. Single tiered processing into a battery which is then directly coupled to the particle accelerator would require a high voltage cell stack. The reliability in operation for a cell string with the very large number of required series units could not be expected to be high. The battery unit, moreover, would not be capable of operation over any range of voltage, but would provide instead, a single beam voltage condition. The hazard assessment of the high voltage battery is also forbidding, since a high power, high voltage battery pack would possess very high values of stored energy.

The use of a battery pack in the dual tiered system is not beyond consideration, and Section 6 will consider a battery pack, at "mid range" voltage, in this configuration. Here the voltage variation capability is provided by the second power over processing unit. Operation of this processor for a battery input is somewhat simpler than for the capacitor bank since battery output voltage will remain much more narrowly ranged than the capacitors, even for fairly significant depths of discharge from the cells.

4.3 Common Usage Considerations for Electrical Energy Storage

The energy storage unit of the particle accelerator system is expected to be a significant fraction of allotted system weight. As such it is highly desirable that this unit provide storage for the operation of as many of the particle accelerators as possible. Since AMPS also contains high powered systems for transmitter operations, an extra return would result if the energy storage bank can be used for these wave generating experiments. It will be seen in the later sections that the capacitor bank can be used for the electron accelerator, the ion accelerator, the MPD arc, and a high powered antenna driving processor.

The battery pack unit will be shown to be useful for electron and ion accelerators and the wave generating processor. The battery pack cannot, however, be used by the MPD arc, and neither the battery pack nor the midrange voltage capacitor bank can be used with the high voltage plasma guns, which require their own, specifically tailored, capacitor storage units.

4.4 Characteristic Transfer Times in Energy Storage and Associated Storage Risk

A "characteristic transfer time" can be assigned to an electrical storage unit and is defined here as the minimum period for efficient energy transfer from the unit to the power processor or to any given output load. An emphasis is placed here upon efficient transfer, since inefficient transfer, as discussed previously, results in truncation or elimination of experiments.

If the characteristic time for energy withdrawal and transfer is T_c, and the required power at an accelerator is P_b, then the energy stroage unit must have a total stored energy at the beginning of the beam burst of at least $P_b T_c$. The energy must also have stored energy of at least $P_b T_b$ where T_b is burst duration for a beam pulse.

Since total energy ω in the unit must be larger than both $P_b T_c$ and $P_b T_b$, energy storage considerations are paced by characteristic withdrawal times rather than integrated beam energy considerations if T_c is much greater than the general range of T_b.

For batteries it may be estimated that efficient drainage generally requires in excess of 10^3 seconds and, for some cell designs, in excess of 10^4 seconds. For an assumed T_c at 10^3 seconds and for beam power at 100 kilowatts, energy storage at the 100 megaJoule level is required. This very high level of required energy storage for efficient high powered transfer, raises serious questions concerning hazard, since any failure mode involving inability to cutoff the particle accelerator beam or any breakdown from the high voltage side of the battery to spacecraft ground will result in significant energy inputs to the Orbiter and consequent thermal loading. Figure 8 illustrates these possible energy storage requirements.

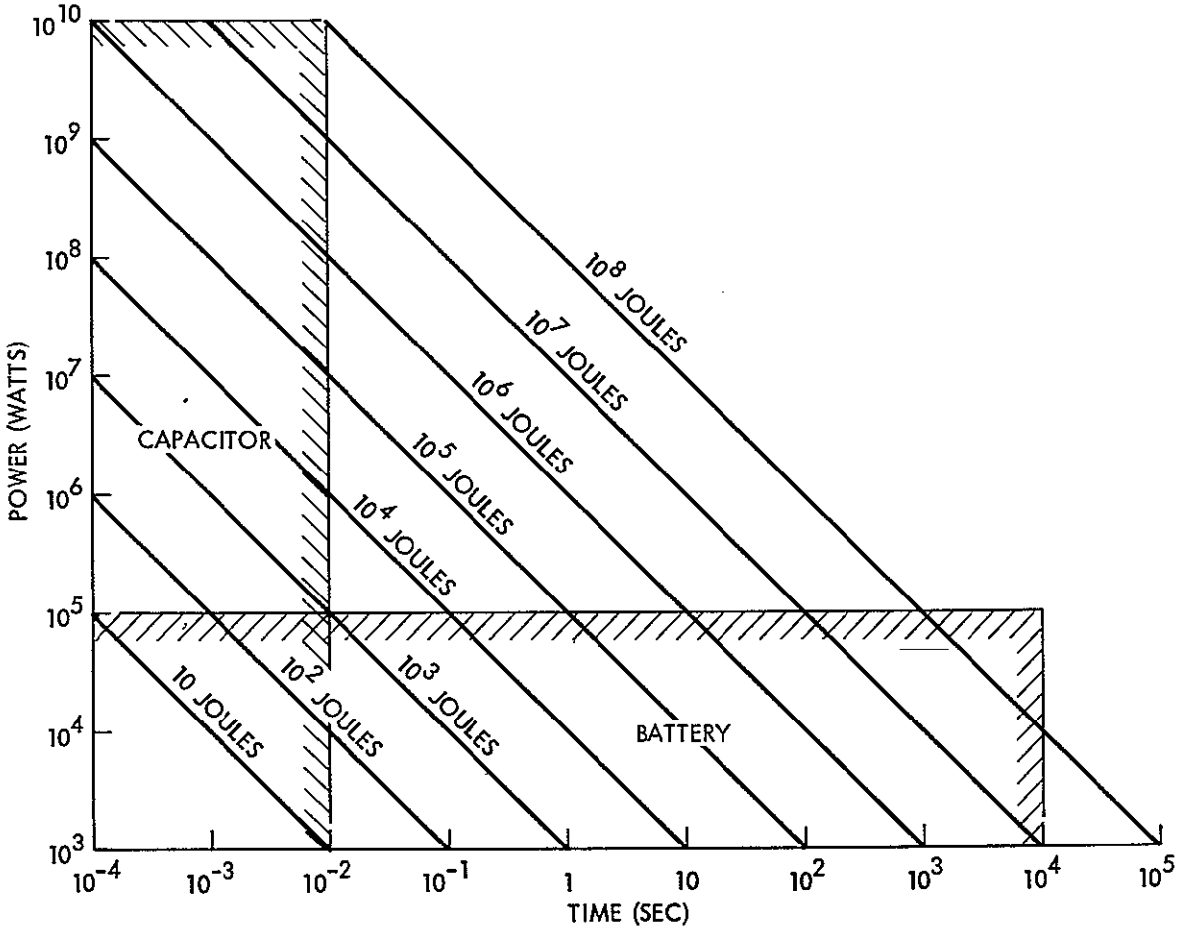

Figure 8. Energy Storage Requirements as a Function of Beam Power, P_b, and the Characteristic Time, T_c, for Efficient Energy Transfer. ($T_c \sim 10^{-2}$ seconds for Capacitors and $T_c \sim 10^3 - 10^4$ seconds for Batteries).

Unlike batteries, capacitors have very short characteristic times for efficient energy transfer. For present electrolytic capacitors T_c is of the order of 10^{-2} seconds, and the $P_b T_c$ product at 100 kilowatts is $\sim 10^3$ Joules, significantly less than required for a beam burst of 100 kilowatts at, for example, 1 second. In this case energy storage requirements are those established by the $P_b T_b$ product which, for the 100 kilowatt-1 second condition specified, is 100 kiloJoules. This is three orders of magnitude less than the energy storage requirement for batteries (and an assumed battery characteristic withdrawal time of 10^3 seconds). This shift by orders of magnitude in the energy storage requirement between capacitors and batteries imposes significant variance levels in the hazards associated with energy storage.

A final consideration for energy storage by capacitors is that characteristic transfer times of 10^{-2} seconds are sufficiently short so that energy storage still remains at $P_b T_b$ for the MPD arc cases. In Figure 5, MPD arc burst durations are in the 20 to 200 millisecond time regime. The hazard analysis for energy storage by capacitors will remain unchanged even for extension into the megawatt beam power range. For batteries, every extension of beam power extends the energy storage requirement and increases the storage hazard.

5. PROPOSED TOTAL PARTICLE (AND PLASMA) ACCELERATION SYSTEM FOR AMPS

An accelerator system which provides both energetic electron and ion beams, and both low voltage and high voltage plasma streams is illustrated in Figure 9. The system has the required common usage of power processing and energy storage units discussed earlier in Sections 2, 3, and 4, and as will be developed in this section, has conditions of modularity which admit development into a series of system growth modes.

The energy storage unit illustrated in Subsystem B of Figure 9 is a capacitor bank of .8 Farads capacitance with 500 volts rating. Section 6 will discuss battery and flywheel storage alternatives, and, while capacitors are advanced here as a preferred means of energy storage other means of storage may be required under other mission constraints and requirements.

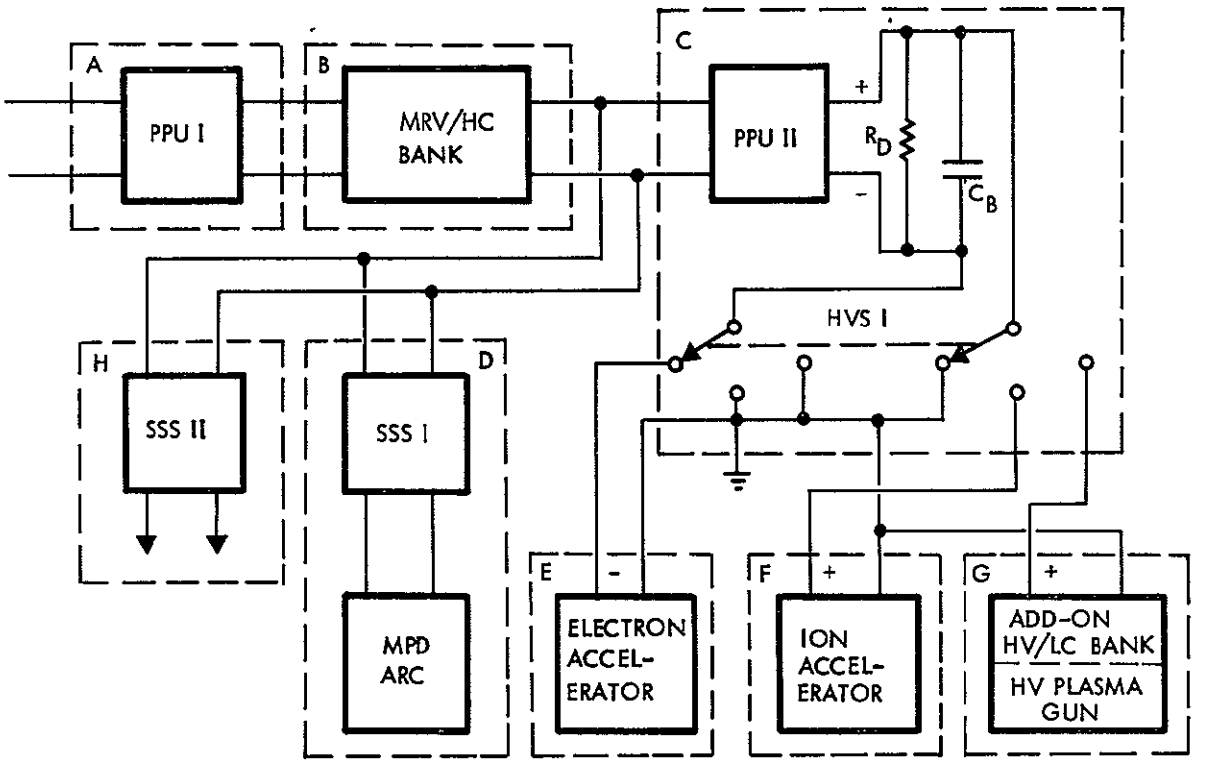

SUBSYSTEM	ELEMENTS
A	POWER PROCESSING UNIT (PPU) I (28V/400A//500V/23A)
B	MIDRANGE VOLTAGE/HIGH CAPACITANCE (MRV/HC) BANK (500V/.8F)
C	PPU II (500V/400A//30,000V/10A), DRAINAGE RESISTOR (R_D), BUFFER CAPACITOR (C_B), HIGH VOLTAGE SWITCH (HVS) I
D	SOLID STATE SWITCH (SSS I), MAGNETOPLASMADYNAMIC (MPD) ARC (500V/20,000A)
E	ELECTRON ACCELERATOR (30,000V/7A)
F	ION ACCELERATOR (20,000V/10A)
G	ADD-ON HIGH VOLTAGE/LOW CAPACITANCE (HV/LC) BANK, HIGH VOLTAGE (HV) PLASMA GUN
H	SSS II, TIE-OUT TO ADD-ON HIGH POWER AMPS SYSTEMS APPLICATIONS

Figure 9. Proposed AMPS Particle and Plasma Acceleration System.

The particle accelerator system in Figure 9 allows the second tier of processed power to be applied to either an electron accelerator or an ion accelerator or a high voltage capacitor bank storage unit for the High Voltage Plasma Accelerator. The capacitor bank storage unit also is capable of driving the MPD arc, through the solid state switch SSS I, or other AMPS high powered loads (such as the wave generators) through SSS II. Estimated weights and volumes of the subsystems are given in Table 5. Total weight and volume estimates for various accelerator systems and combinations of systems are also given in Table 5, and are illustrated in Figure 10. The important feature of these weight-volume estimates is that only small fractional variations occur for up-rating from a single accelerator system in an initial mission to a multiple accelerator system in an advanced mission. This capability will greatly facilitate mission planning, since extensive retrofit is not required, and will provide for much more cost effectiveness in carrying out the various experiments.

Break-outs of subsystem sub-elements are given in Tables 6, 7, 8, and 9 for the MPD arc, the electron accelerator the ion accelerator, and the High Voltage Plasma Gun. These tables describe subsystem elements, weights and volumes. An assembly of these various subsystem elements into a total accelerator payload for a half-pallet mount on AMPS is illustrated in Figures 11, 12, and 13. While the stacking arrangements shown there are considered to have merit in terms of conservation of pallet space and convenience in inter-connection, no attempt has been made at overall stacking optimization and other configurations can be generated. One firm requirement in the accelerator placement is that the output of the accelerators should be as far elevated as possible along the Orbiter Z axis, to reduce energetic particle deposition effects in Orbiter bay liners and Orbiter radiator thermal coating materials.

A final aspect of system design is possible growth modes (other than mere subsystem addition). Table 10 lists possible growth modes for each of the particle accelerators in the total accelerator system. For these growth modes to be realized without system re-initiation, modularity in the energy storage and processing elements must be present and in a conveniently exploitable form. These features, and other aspects

SYSTEM	WEIGHT (POUNDS/KILOGRAMS)	VOLUME/CUBIC METERS
A (PPU I)	100/45	0.25
B (LV/HC Bank)	1200/540	2.0
C (PPU II, R_D, C_B, HVSI)	250/110	0.5
D (SSSI, MPD ARC)	100/45	0.25
E (E-ACCEL)	100/45	2.5
F (I-ACCEL)	250/110	0.5
G (HV/LC BANK, HV P-ACCEL)	250/110	0.7

****

EXPERIMENT	SYSTEMS	WEIGHT (LB/KG)	VOLUME (M^3)
Electron Acceleration	A,B,C,E	1650/740	5.25
Ion Acceleration	A,B,C,F	1800/805	3.25
Low Voltage Plasma Acceleration (MPD Arc)	A,B,D	1400/630	2.5
High Voltage Plasma Acceleration (HV P-Gun)	A,B,C,G	1800/805	3.45
E-Gun+I-Gun	A,B,C,E,F	1900/850	5.75
E-Gun+I-Gun+MPD ARC	A,B,C,D,E,F	2000/895	6.0
E-Gun+I-Gun+MPD Arc + HV P-Gun	A,B,C,D,E,F,G	2250/1005	6.7

Table 5. Estimated Weights and Volumes for Elements of the AMPS Particle Accelerator Facility.

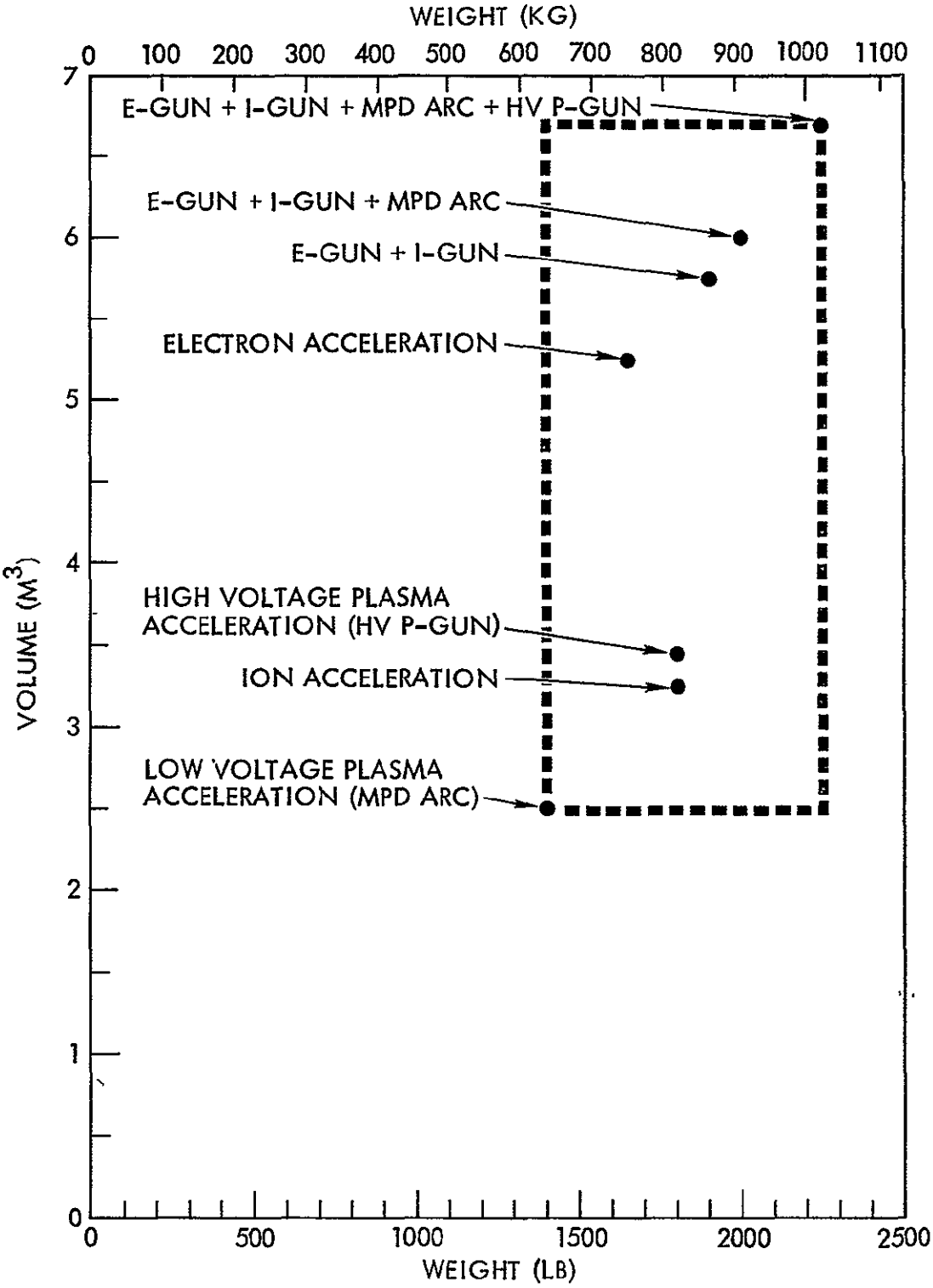

Figure 10. Estimated Weights and Volumes for Various Accelerator Combinations in the AMPS Particle Accelerator Facility.

SUBSYSTEM	DESIGNATION	ELEMENTS
D1	SSS I	Solid State Switch
D2	Gas Storage	Gas storage tanks, plenum chamber, gas pop-valve, gas pressure regulation valve.
D3	MPD Arc	MPD Arc Cathode, anode and supporting structure.
D4	Pulse Program	Bank voltage (V_{accel}), Δt burst, gas pressure set.

****

SUBSYSTEM	WEIGHT (LB/KG)	VOLUME (M^3)
D1	20/9.0	.05
D2	20/9.0	.12
D3	50/23	.06
D4	10/4.5	.02
D	100/45	0.25

Table 6. Magnetoplasmadynamic (MPD) Arc Subsystem Elements and Estimated Weights and Volumes.

SUBSYSTEM	DESIGNATION	ELEMENTS
E1	Electron Source	Cathode, control grid, accelerator electrode, cathode heater, control grid voltage.
E2	Output lens	Diverging lens, expansion region, converging lens, lens drive voltages.
E3	Magnetic Deflection	x-z deflection coils, y-z deflection coils, coil drive voltages.
E4	Pulse program	V_{accel}, V(t), I_{accel}, I(t), Δt burst, pitch angle (α), $\alpha(t)$, $\Delta\alpha$, beam diameter.

****

SUBSYSTEM	WEIGHT (LB/KG)	VOLUME (M^3)
E1	10/4.5	0.1
E2	50/23	1.7
E3	30/13	.6
E4	10/4.5	.1
E	100/45	2.5

Table 7. Electron Accelerator Subsystem Elements and Estimated Weights and Volumes.

SUBSYSTEM	DESIGNATION	ELEMENTS
F1	Bombardment Discharge supplies.	Electron bombardment discharge anode. Supply, electron bombardment discharge current supply, beam neutralizer heater and keeper supplies.
F2	Gas storage.	Gas storage tanks, gas pop-valves, electron bombardment pressure regulator valve, beam neutralizer pressure regulator valve.
F3	Ion Source.	Electron bombardment discharge ion source.
F4	Pulse program.	Discharge voltage, discharge current, gas pressure set, neutralizer heater, neutralizer keeper, V_{accel}, I_{accel}, Δt burst.

****

SUBSYSTEM	WEIGHT (LB/KG)	VOLUME (M^3)
F1	170/75	.24
F2	20/9	.12
F3	50/22	.12
F4	10/45	.02
F	250/110	.5

Table 8. Ion Accelerator Subsystem Elements and Estimated Weights and Volumes.

SUBSYSTEM	DESIGNATION	ELEMENTS
G1	Add-on bank	High voltage/low capacitance storage bank.
G2	Gas storage	Gas storage tanks, gas pop valve, plenum chamber, gas pressure regulation valve.
G3	JV Plasma gun	High voltage plasma gun anode, cathode, and supporting structure.
G4	Pulse program	Bank voltage (V_{accel}), Δt burst, gas pressure set.

****

SUBSYSTEM	WEIGHT (LB/KG)	VOLUME (M^3)
G1	200/87	.50
G2	20/9	.12
G3	20/9	.06
G4	10/5	.02
G	250/110	.70

Table 9. High Voltage Plasma Gun Subsystem Elements and Estimated Weights and Volumes.

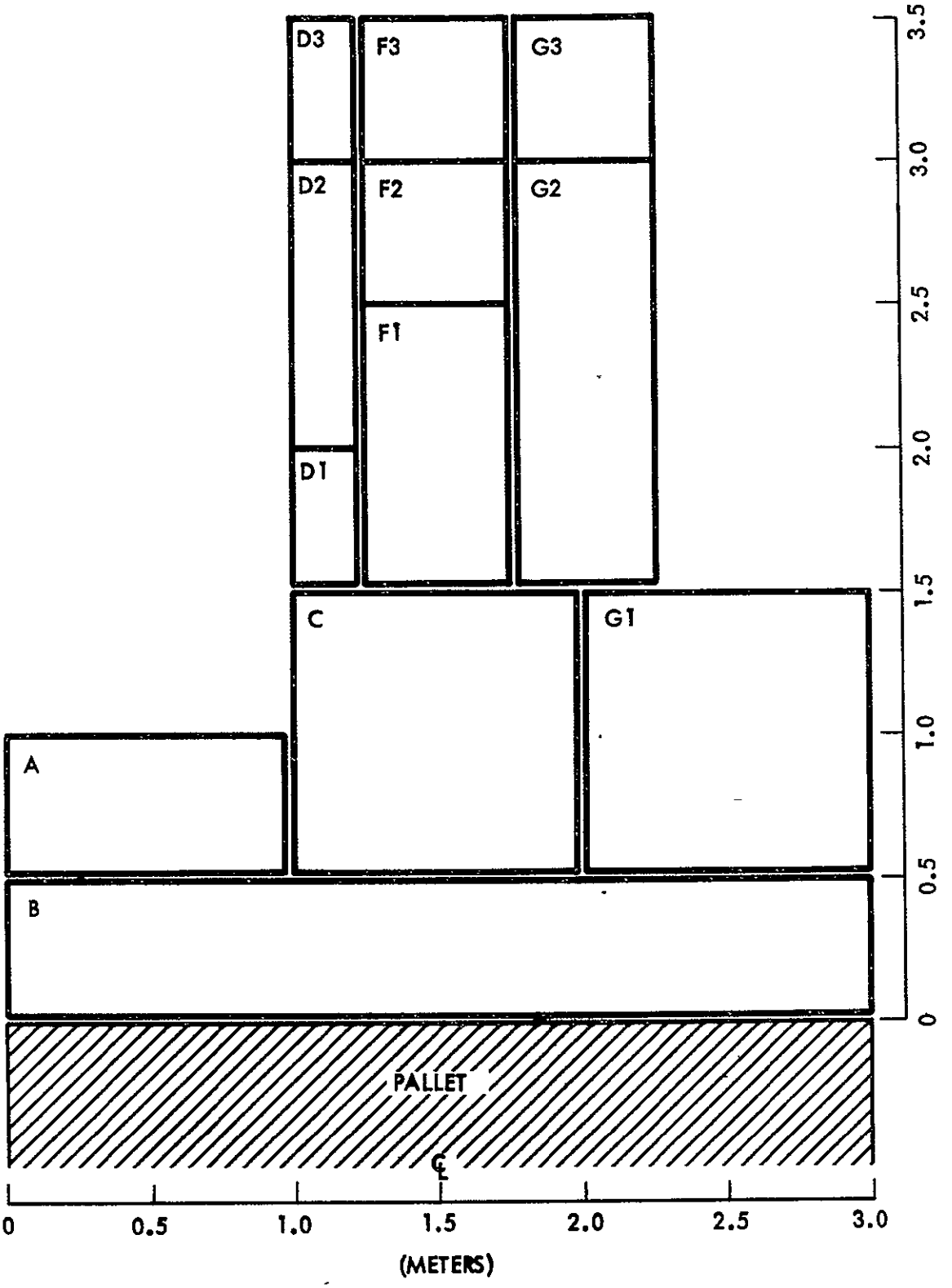

Figure 11. Pallet Mounted AMPS Particle Accelerator System (X-Axis View Looking Aft).

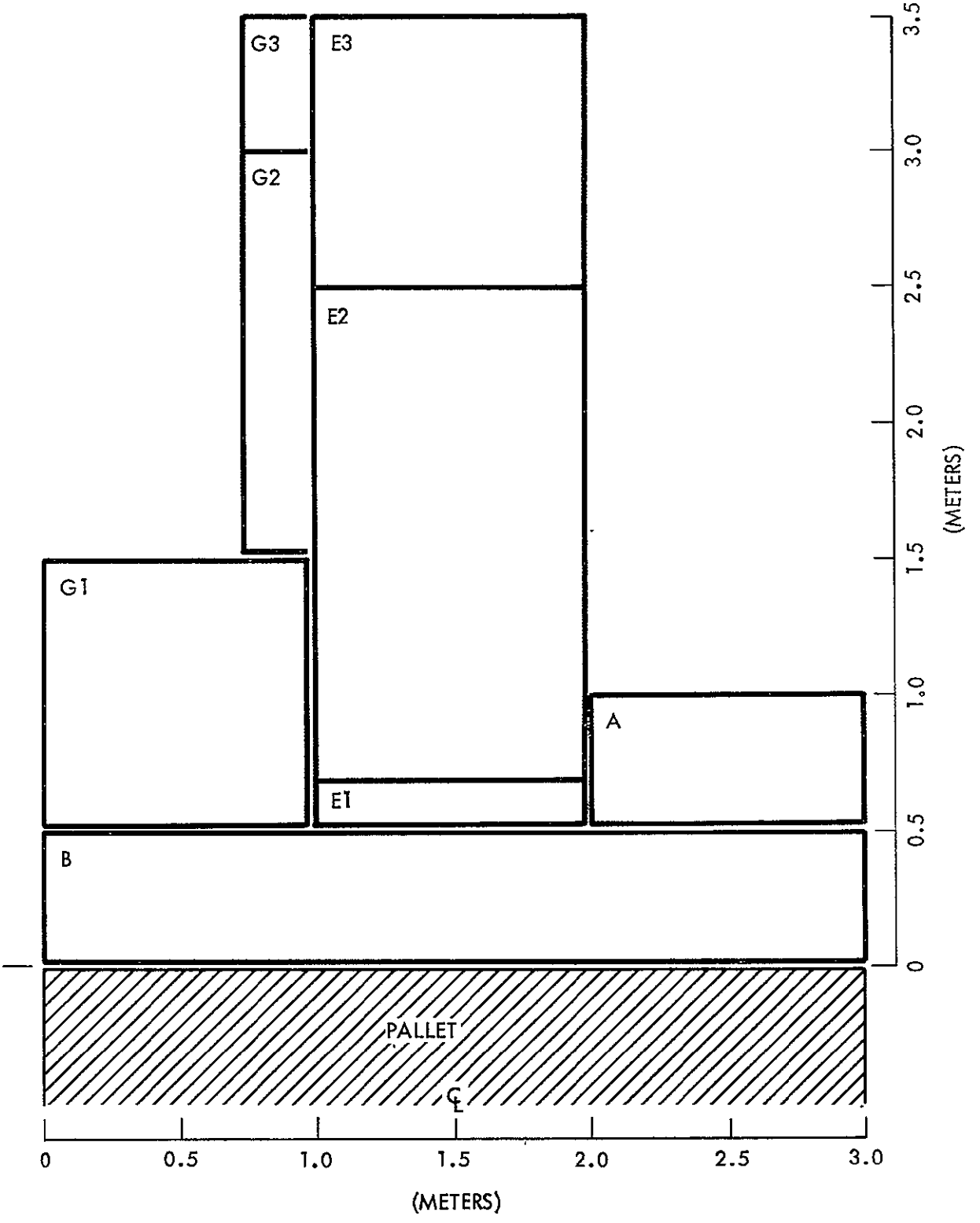

Figure 12. Pallet Mounted AMPS Particle Accelerator System (X-Axis View Looking Forward).

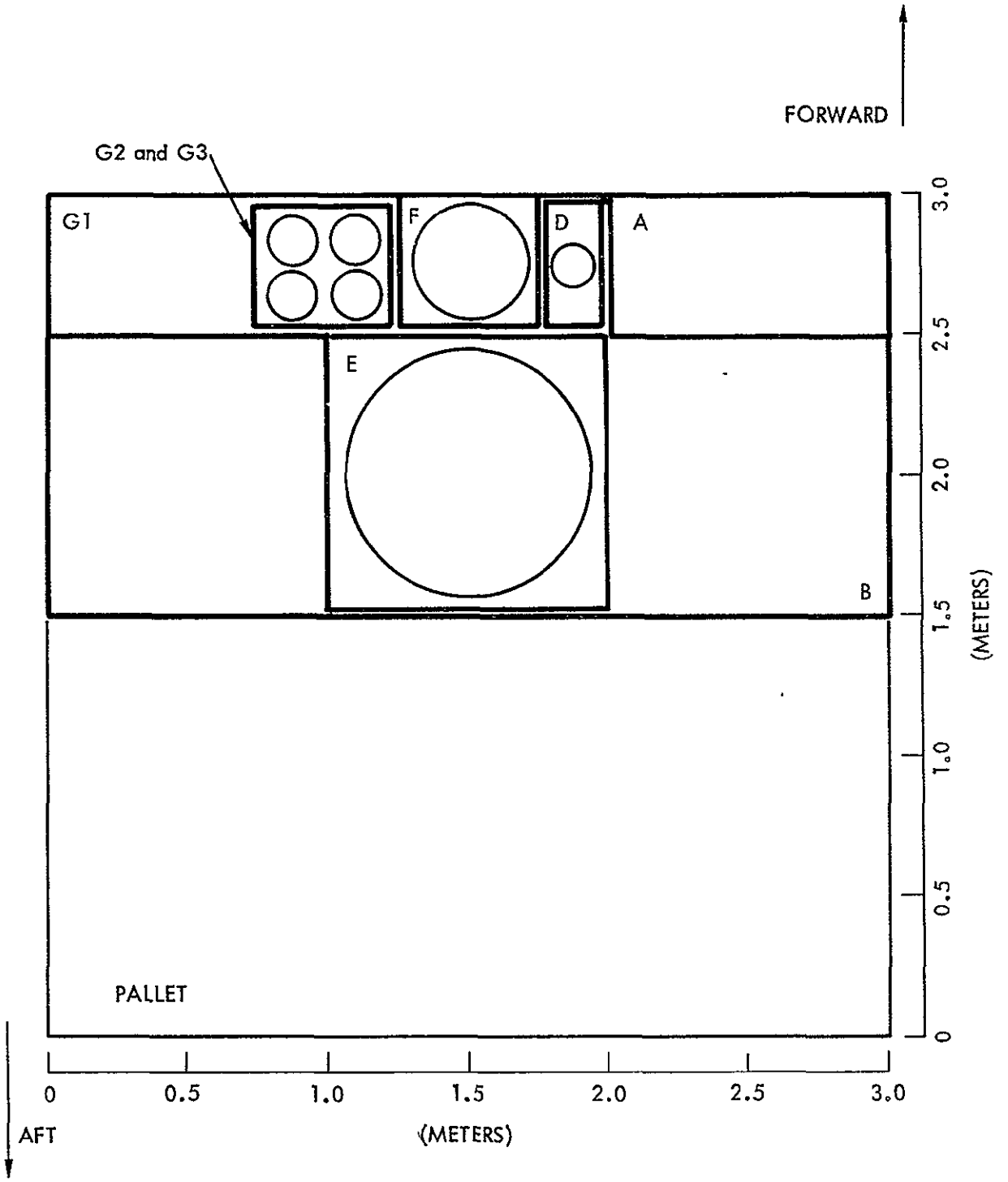

Figure 13. Pallet Mounted AMPS Particle Accelerator System (Z-Axis View Looking Down).

SUBSYSTEM	DESIGNATION	GROWTH MODES
A	PPU I	None contemplated.
B	LV/HC Bank	Increased capacitance/ energy storage.
C	PPU II	Increased output voltage. Increased output current. Increased total energy release per burst.
D	MPD ARC	Additional gas species. Increased energy release per burst.
E	Electron Accelerator	Increased acceleration voltage increased beam current, increased energy release per burst.
F	Ion Accelerator	Increased acceleration voltage, increased beam current, increased energy release per burst, additional gas species.
G	HV Plasma Gun	Increased capacitance/ energy storage in HV bank Increased energy release per burst. Additional gas species.

Table 10. Growth Modes for AMPS Particle Accelerator Subsystems.

of the energy storage and transfer systems will be discussed further in Sections 6 and 7.

6. ENERGY STORAGE ELEMENTS IN THE AMPS PARTICLE ACCELERATOR SYSTEM

6.1 General

Section 4 has discussed systems considerations and the required energy storage unit which follow from a requirement for beam power in excess of that available in a direct "latch-down" (fuel cell-to-power processor-to-particle accelerator) power configuration. Both capacitors and batteries have been identified as possible methods of energy storage and Sections 6.2 and 6.3 will review considerations for their use. Section 6.4 will discuss, briefly, factors relating to the use of energy storage wheels (super flywheels), with the bulk of the discussion on this approach contained in the Appendices.

6.2 Midrange Voltage Electrolytic Capacitor Bank

6.2.1 Energy Density

Two energy density figures will be derived for an electrolytic capacitor bank storage unit. The first of these is in energy per weight, which allows bank weight to be calculated for a required level of energy storage. The second energy density figure is in energy per volume, which allows bank volume to be calculated.

The capacitor chosen for examination is an aluminum electrolytic with a nominal rating of 1500 microfarads capacitance, a working voltage of 450 volts (with voltage surge capability to 500 volts), and a per unit weight of 750 grams. In actuality, the measured capacitance of a series of these units is consistently at ∿2000 μfarads for a delivered capacitance of 1212 μfarads per pound (2670 μfarads per kilogram).

A bank of capacitors at 1000 pounds (454 kilograms) would consist of 606 units of this type with a total capacitance of 1.2 farads The capacitance figure is larger than the 0.8 farads stated in the proposed system description in Section 5, as a result of a larger actual capacitance than the figure assumed earlier for a 1000 pound bank. For this 1.2 farads and for an applied voltage of 470 volts (20 volts above nominal rating but 30 volts lower than rated surge voltage), the total stored

energy is 133 kiloJoules for a stored energy density of 133 Joules per pound. The drain-out of energy to the half-voltage point (permitted under present allowed power processor input voltage) would provide an energy transfer of 100 kiloJoules at an energy transfer density of 100 Joules per pound.

The capacitor selected for test is 3 inches in diameter and 6 inches long (7.5 centimeter diameter, 15.2 cm length) for a total volume of 690 cubic centimeters per unit. The total volume of the 1000 pound bank (606 capacitors) is 0.42 cubic meters, which is significantly less than the 2.0 cubic meter figure given in the proposed system (Section 5). It should be noted, however, that a series of "packing" considerations will be present and have not yet been calculated. The required placing of the capacitors into the appropriate containers and required spaces for protective diodes and cabling will probably result in a total bank volume in excess of 1 cubic meter, but probably less than the earlier 2 cubic meter estimate. For the capacitors alone and for 470 volts applied and 2000 μfarad per capacitor, the energy storage (volume) density is 320 kiloJoules per cubic meter. For 75% transfer upon burst, transferred energy storage density is 240 kiloJoules per cubic meter.

The presently used figure of 75% energy transfer during a given burst does not mean a loss of 25% of stored energy. The capacitors do possess leakage and will, if left for sufficiently long periods of time, drain back to zero voltage. If the storage unit is being repeatedly charged and discharged, however, virtually the entirety of energy remaining in the bank at the burst conclusion is available for the succeeding burst. Factors which contribute to energy loss in the capacitors during and following the burst are discussed in the following section, which demonstrates high electrical efficiency in the storage and transfer.

6.2.2 Power Density

Power density will be derived on a power per weight basis only (without reference to power per volume, since volumetric considerations as seen from Section 6.2.1, indicate storage well within an acceptable volume).

The power density of a storage unit for a given AMPS experiment will depend upon specific features of the load. From previous considerations of total energy budget per mission, high electrical efficiency is required, and total system requirements will be for high power density at high efficiency .

Energy loss during current drain from the capacitor will result from internal impedance of the unit. The capacitor selected for study and testing has an equivalent series resistance of 0.15Ω, and, since the total 1000 pound bank consists of ∿600 units in parallel, equivalent series resistance of the capacitor combination is $2.5 \times 10^{-4}\Omega$.

For a capacitor C, at voltage V, and for total power withdrawal P, it follows that

$$CV \frac{dV}{dt} = -P \tag{1}$$

and

$$V^2 = V_o^2 - \frac{2Pt}{C} \tag{2}$$

where $V = V_o$ at $t = 0$ and power has been withdrawn continuously at P in the time interval from 0 to t (this is the mode of operation for the power "ladling" techniques used in present day processors). Since power is also given by

$$P = \frac{V^2}{(R_L + R_{int})} \tag{3}$$

where R_L = load resistance and R_{int} is internal resistance of the capacitor bank, and, electrical efficiency, expressed as a fraction, is given by

$$\varepsilon = 1 - \frac{R_L}{R_L + R_{int}} \tag{4}$$

it follows that

$$\varepsilon \doteq 1 - \frac{R_{int}\, PC}{CV_o^2 - 2Pt} \tag{5}$$

provided that $R_{int} << R_L$, a condition which will be generally valid except at very high rates of energy withdrawal.

The average electrical efficiency for a burst of duration T and constant power withdrawal P is given by

$$\langle\varepsilon\rangle = \int_o^{(PT)/P} dt \left(1 - \frac{R_{int}P}{CV_o^2 - 2Pt}\right) \Bigg/ \int_o^{(PT)/P} dt \tag{6}$$

$$\langle\varepsilon\rangle = 1 - \frac{R_{int}C}{2T} \ln\left(\frac{CV_o^2}{CV_o^2 - 2PT}\right) \tag{7}$$

The logarithm term has numerator and denominator proportional to initial and final energy storage which for current design has a maximum value of 4 (75% withdrawal for final V at half of initial V_o).

For $R_{int} = 2.5 \times 10^{-4}\Omega$ and C = 1.2 farads, $R_{int}C$ = .3 milliseconds, and electrical efficiency in transfer will remain high for any T greater than 1 millisecond. As noted in the earlier discussion of characteristic energy transfer times, the electrolytic bank allows very and efficient transfer.

Using Equation (7) above, the power delivered to a load may be calculated as a function of burst duration. Figure 14 illustrates this allowable P-t for both a 1000 pound bank and a 10,000 pound bank. As may be evidenced the P-t product is essentially fixed (100% efficiency in transfer) for T > .5 milliseconds (P < 100 megawatts for the 1000 pound bank). The 10,000 pound bank would allow efficient energy transfer to the 1 gigawatt (1000 megawatt) level.

The derivation of Equation (7) and the P-t curves for capacitors in Figure 14 have neglected inductive effects in the capacitors. In the time regime above 0.1 second this neglect is probably justified. For

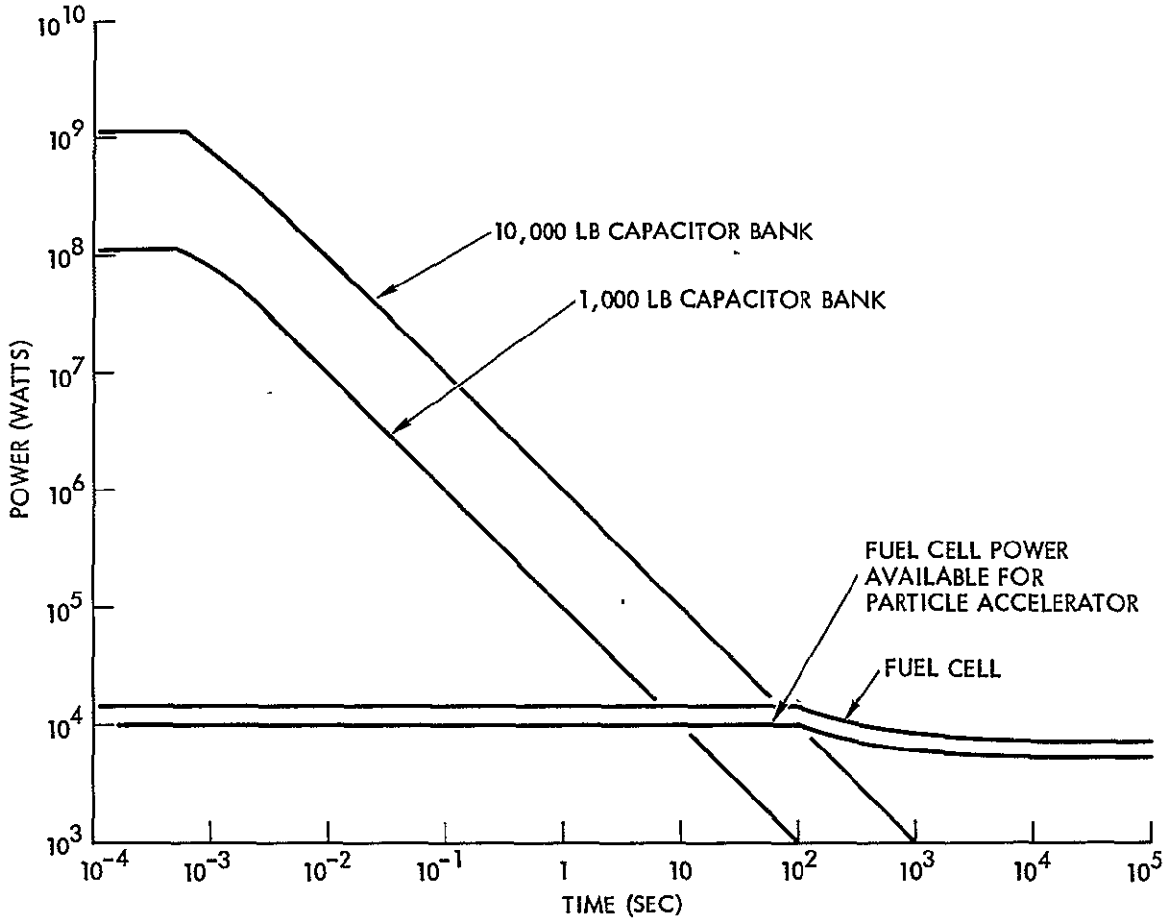

Figure 14. Allowable Power as a Function of Burst Duration for Capacitor Bank Storage Unit and Fuel Cell.

very short burst very high power operation, such as required for the MPD arc, these inductive effects are of importance. It is also desirable, moreover, for the MPD arc applications of the bank to specifically "tune" the bank with in-series inductors so that the bank behaves as a pulse forming network. Section 6.2.3 which follows will discuss a bank construction allowing for later introduction of such inductors. For initial applications in lower power bursts, such as the electron accelerator, these inductor entry points would be occupied by units of comparatively low resistance but with sufficient inductance to prevent current surges beyond a given design limit in the event of a high voltage short to ground, this being a failure mode of concern because of EMC implications.

An important and final aspect of the high electrical efficiency of the capacitor energy transfer is that heat injection requirements from the bank to the Orbiter are lessened. In order to optimize the bank performance, a thermal loop to the radiators will be requested and will be required to hold the bank within a given temperature range (as yet to be specified). Thermal loading on this loop will be that derived from conduction between the bank and the Orbiter structures and will not, as noted, be significiantly altered by bank operation.

6.2.3 Failure Modes

Three possible failure modes will be considered. The first of these is an open circuit failure between the capacitor and the input and output cabling. This failure is not considered to be either statistically significant (possibility of occurence) or operationally significant (change of system performance if the failure occurs) and will not be discussed further. The remaining two failure modes are short circuits either internal to the capacitor or between the high voltage bus of the capacitor bank and spacecraft ground.

Short circuits internal to the capacitor and for voltage applied can be self clearing if capacitance does not exceed a certain limit. For present electrolytic capacitors and this midrange voltage of 500V capacitors at the 2000 μfarad level are self healing for shorts from one side of the capacitor to the other. Since the total bank is several hundred such capacitors, an isolation is required between capacitors. Figure 15 illustrates the required diode in-diode out arrangement to provide this isolation. Figure 15 also illustrates an in-line fuse which will act to

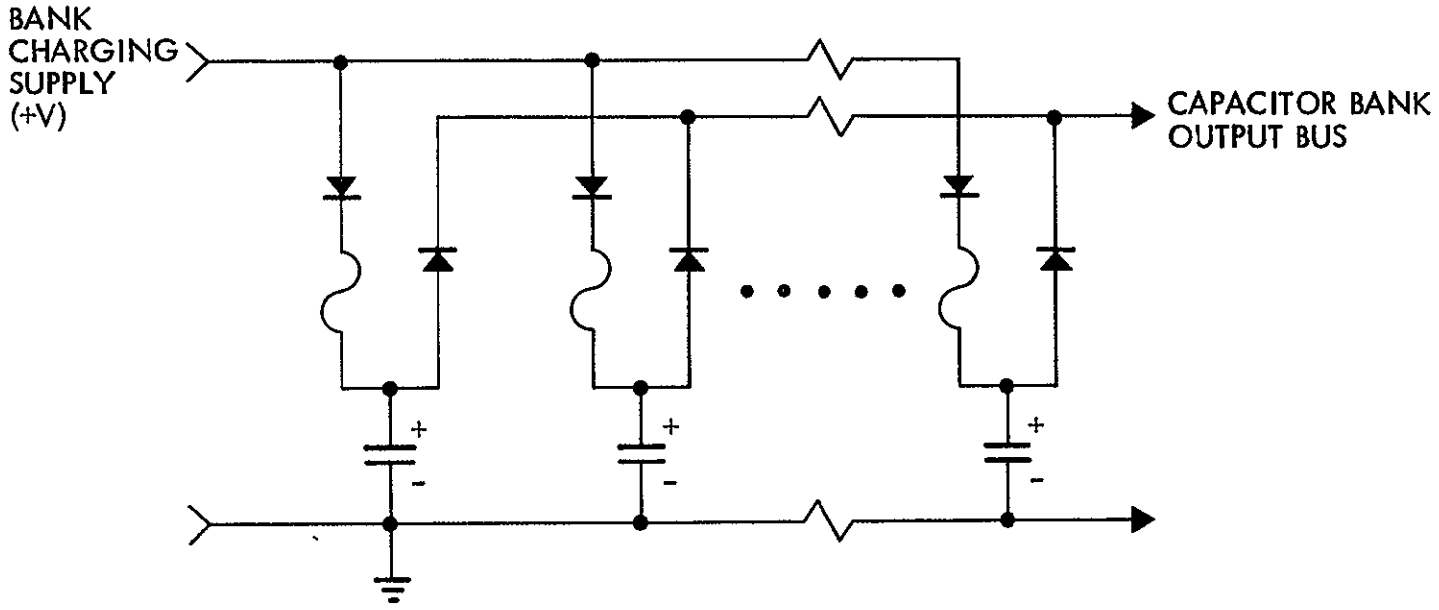

Figure 15. Diode In - Diode Out Charge Discharge Isolation for Capacitors in Energy Storage Unit.

remove a failed (shorted) capacitor from the charging line so that unimpeded bank recharge may proceed in the presence of a failed unit.

Breakdown under electric stress can be self-healing, as noted, provided the capacitor is below a certain capacitance. Shorting could also occur, in principle, as a result of vibration during the Orbiter launch. Since the units selected for test have not been previously tested for vibration, a three-axis shake test was carried out, using the vibration spectrum in Volume XIV. Capacitance was measured before and afterward and no measurable difference was observed, with the unit storing energy after the test to the same level and performance as before. While these tests were not exhaustive, they are encouraging:

The third failure mode of concern is shorting of the HV bus to the ground bus. A very low impedance short could, in principle, allow a very high discharge current whose conducted and radiated electromagnetic interference would inpact on the operation of the remainder of the Orbiter. To limit this possible surge current, it is proposed that inductors be installed as illustrated in Figure 16. The selection of L and the allowable resistance will be set by allowable surge current, expected power withdrawal for electron gun operation, and desired bank transfer efficiency. If system and bank use is later extended to the MPD arc, the inductors indicated in Figure 16 would then be tailored to match required L,C values for the MDD arc operating into a pulse forming line.

Another aspect of the capacitor bank wiring design in Figure 16, is to eliminate use of the Orbiter frame for any possible breakdown current. These practices are standard, for example, in the ion engine wiring on electrically propelled spacecraft.

Two important overall aspects in any assessment of capacitor bank failure modes are that (1) because of a low characteristic time, high power output capability does not require large values of energy storage (see Section 4.4), and storage of only 100 kiloJoules can provide power bursts to very high power levels, and, (2) it is not required that capacitors be charged either during ascent or descent, which are periods of high vibration.

A final consideration on hazards and failure modes associated with the bank is gas release from the capacitors if voltage polarity reversal occurs. While this condition becomes of concern for very high current

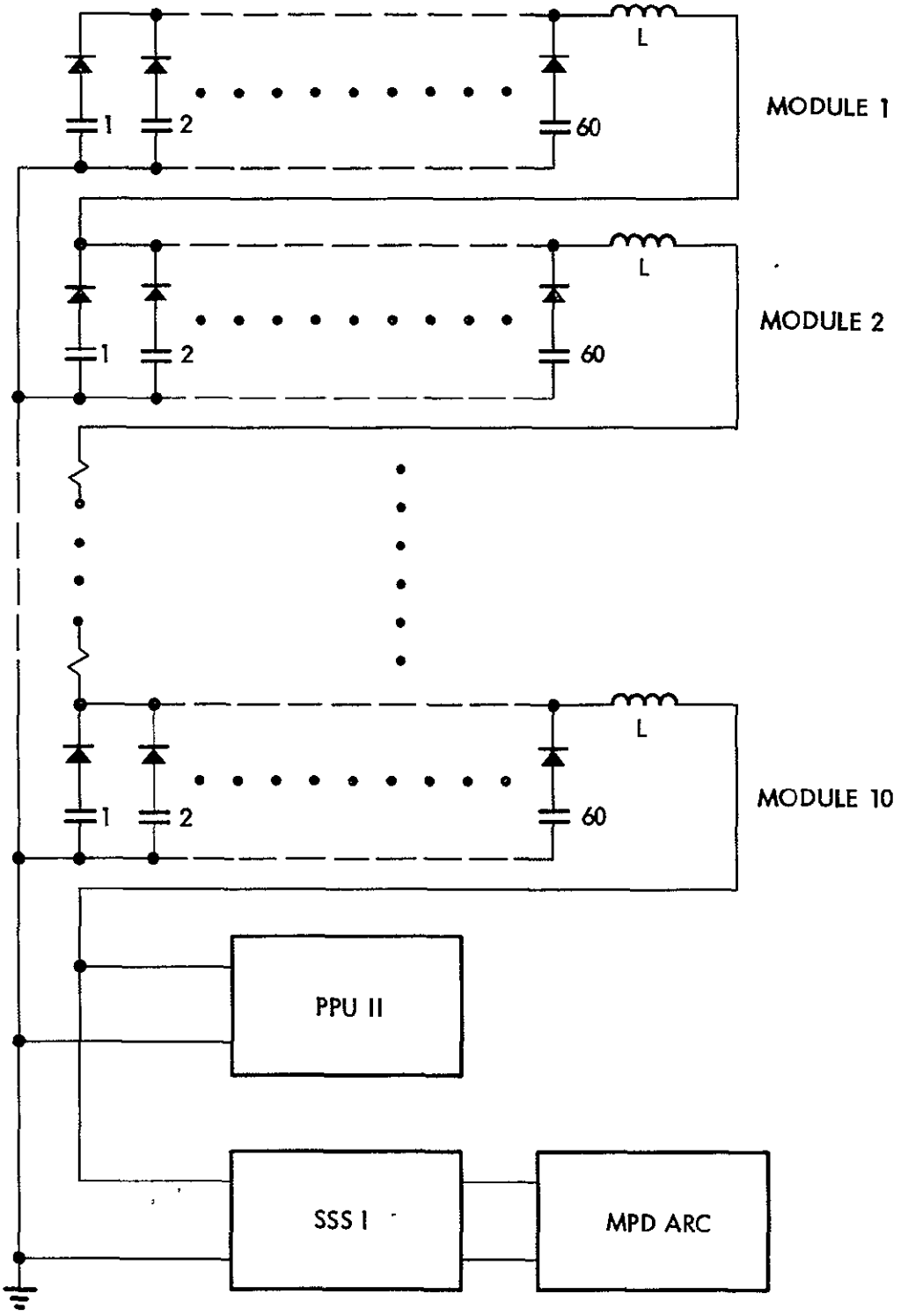

Figure 16. Inductors in Capacitor Bank Storage Unit (for Surge Current Limitation on HV Bus Short-to-Ground Failure Mode or for Shaping of Pulse Forming Line for MPD Arc (Different Inductors Required)).

operation (high level MPD arc) where circuit inductance may tend to continue current and ultimately, reverse capacitor polarity, the initial proposed bank use is with electron accelerators and will not tend to any possible polarity reversal. Since the capacitors are not hermetically sealed and electrolyte loss is not desired, the capacitor storage units (sub-elements of the total bank) should be sealed. A comparatively low pressure nitrogen fill is expected to be adequate. Pressure release vents will probably not be necessary. The principal concern for polarity reversal, then, relates to the capacitor deterioration which occurs, and circuit arrangement and operation to avoid such reversals should be provided and maintained.

6.2.4 Capacitor Bank Modularity

The most straightforward method of expansion of the capacitor bank is parallel addition of capacitors. While this provides additional energy storage capability and an additional power capability, the principal feature of the growth would appear to be in energy storage, since power capability for even a small bank exceeds electron gun power requirements.

Parallel addition of capacitors provide, as noted, increased energy while maintaining the bank output voltage range. This modularity matches precisely to the most convenient form of power processor modularity (see Section 7). Increase in bank output voltage by series additions of capacitors would require changes in power processor input and transformers. Increased voltages also may exceed permissible processor input levels for present day solid state switching units and would lead to increased hazards and breakdown modes. A final consideration on bank voltage is that the 500 volt figure presently considered is properly matched to MPD arc requirements. Use of higher voltage plasma guns is not an efficient method for the plasma density modification experiment. Use of high voltages may appear desirable for certain shock excitations of the ionosphere. For these high voltage plasma accelerators, however, a specifically tailored and separate bank will be required (see Figure 9).

The energy storage and transfer capability indicated in Figure 9 is ∿100 kiloJoules and Figure 14 has illustrated both 100 kiloJoules and 1 megaJoule storage and transfer. The smaller bank would use 600 capacitors and the larger bank would use approximately 6000. For the greatest convenience in system expansion, a bank sub-element should be designed which provides meaningful levels of capacitance but is still

suffciently small to permit innovative (and space saving) payload stacking arrangements.

6.3 Midrange Voltage Battery Bank

6.3.1 Energy Density

Energy density consideration for the battery bank involve a series of general factors which will be discussed prior to a more quantitative assessment of required battery performance.

The use of an energy storage system and the dual tier power processing arrangement in Figure 9 assumes a primary energy source (the fuel cell) and relegates the battery to storage and transfer roles. While this condition will continue to be assumed in this study it should be pointed out that missions may arise in which the add-on fuel cell system is either absent or, if present, is already dedicated to other requirements. For those missions, the battery bank becomes the primary energy source and battery selection, then, must be for primary batteries. Battery selection for such battery-driven missions may also be expected to focus on energy density as a principal requirement.

For AMPS and its fuel cell primary source and from the total expected energy throughput to the accelerators it follows that secondary batteries must be used in the battery bank. Assuming a mission throughput of 200 kilowatt-hours for the accelerators, and for a 1000 pound battery bank, throughput is at 200 watt-hours per pound which is significantly above storage capability.

Not only are secondary batteries required, their electrical efficiency in storage and transfer must be high, even for high level energy withdrawal rates, or as previously noted, experiments by the accelerators are truncated or eliminated. This requirement of high efficiency at very high power tends to move away from the principal lines of battery development. The major emphasis in battery development, it will be advanced, has been toward increased energy storage and increased reliability and cycle life under comparatively deep levels of discharge under comparatively low rates of energy withdrawal. In some instances as, for example in aircraft engine starting batteries or in batteries for electric automobiles, high power density requirements emerge as drivers, rather than high energy density, and, even in these examples, efficiency is not as high as is desirable.

The approach that will be taken in this study will be to stipulate an energy density. The level that will chosen will be deliberately set at a low value of 10 watt-hours per pound (36 kiloJoules per pound, 80 kiloJoules per kilogram). It will be shown later that this low energy density setting will not effect system performance at any level of significance. This low energy density requirement, however, will allow battery design to focus attention, instead, on reducing cell internal impedance to the lowest possible levels, and on improving cell reliability under conditions of high current-short duration bursts.

A study approach of stipulating cell performance is not a particularly desirable one. It follows, however, from a literature examination that exhibits wide variations between prediction and performance, particularly if requirements move outside the main stream of battery performance. If it should develop that batteries can be supplied which clearly exceed the stipulated performance and if costs for the battery system are not excessive and battery ability is sufficient, then the additional possibilities for the AMPS accelerator experiments can be reviewed and mission plans revised to exploit these capabilities.

6.3.2 Power Density

To evaluate power density a unit cell will be stipulated with a cell voltage of 2 volts and a cell interval impedance of 10^{-3} Ω. The battery pack required to power the processor would consist of series string of 250 such cells, with an open circuit voltage of 500 volts. The maximum power of such a battery would be for a load resistance equal to total string internal impledence (250 x .001 Ω = .250 Ω). For combined cell and load impedance of 0.5 Ω, battery current is 1000 amperes, string output voltage is 250 volts (250 volts lost internally), and power input to the processor would be 250 kilowatts. As noted earlier, variation of processor input voltage within a factor of 2 is premissible for constant power throughput. For an assumed battery weight of 1000 pounds this would represent delivered power at 250 watts per pound at an electrical efficiency of 50%. The cell weight allowed for this 1000 pound battery (250 cells) is 4 pounds. No allowance is made here for auxilliary circuitry.

Figure 17 illustrates the allowable power as a function of burst duration for this 1000 pound stipulated battery. Also shown there are

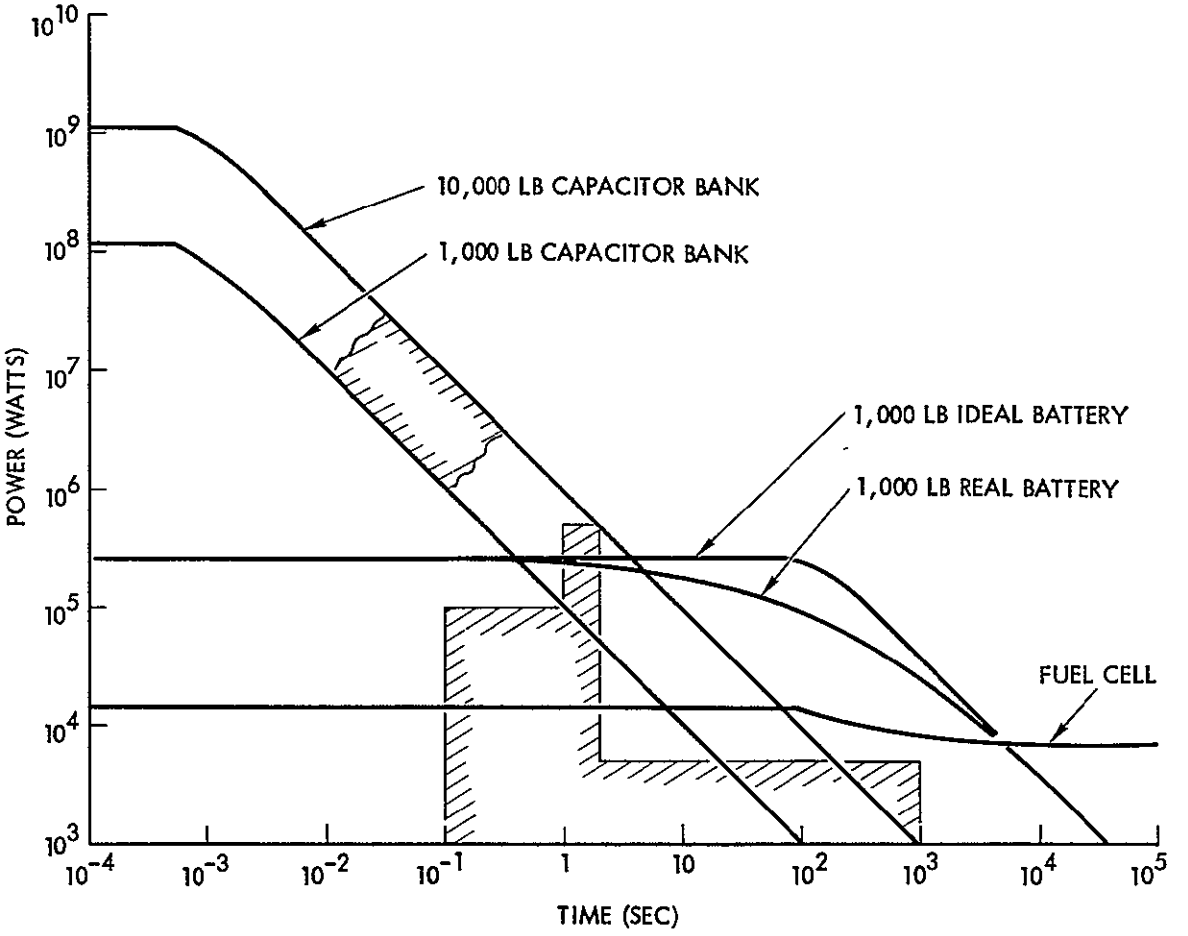

Figure 17. Allowable Power as a Function of Burst Duration for Batteries, Fuel Cells, and Capacitor Bank and Power-Burst Duration Requirements for Monitor and Modification Missions.

P-t lines for the capacitor bank (see Figure 14) and for the fuel cell in a direct latch-down to the accelerators. Figure 17 also lists P-t requirements described earlier (Figure 5) for various experiments in the combined mission mode.

Ths most crucial aspect of stipulated cell performance is the internal impedance of 10^{-3} Ω. The cell is expected to maintain this impedance at current levels of 1000 amperes. From the weight requirement of 4 pounds and 1000 amperes, current density in the cell could range to approximately 1 ampere per square centimeter. Maintaining low cell internal impedance may be difficult under these current density conditions. It should be emphasized, moreover, that current flow at the 1000 ampere level is at 50% efficiency, so that internal dissipation is 250 kilowatts into the battery, and, since there are 250 cells, is at 1 kilowatt per cell. The heating of the cell may, in turn, initiate destabilization of cell properties, noting here that increased internal impedance for a given cell results in increased cell dissipation. Since cells are in series in the battery pack, resistance growth in one cell may grow rapidly if it proceeds beyond certain, as yet unspecified, limits. These destabilizing possibilities contribute to concern for open circuit (or high resistance) failure modes (see Section 6.3.3).

Figure 18 illustrates electrical efficiency as a function of power into the processor for both the assumed battery and a capacitor bank of equal weight. The loss of electrical efficiency at high burst power for the battery has already been emphasized as it affects total mission experiment capability. Another important aspect of this inefficiency is the ultimate thermal loading on the Orbiter. The AMPS particle accelerator experiments are high powered experiments and particularly so for the modification mission. What is desired is to convert electrical energy into released particle energy which deposits into space. Every source of inefficiency, in processors or storage units or accelerators, contributes to the power dissipation in the Orbiter whose radiators necessarily are limited in heat rejection capability. Thus, even if inefficiency could be tolerated from a mission experiment requirement, it is not desirable from a system thermal loading standpoint.

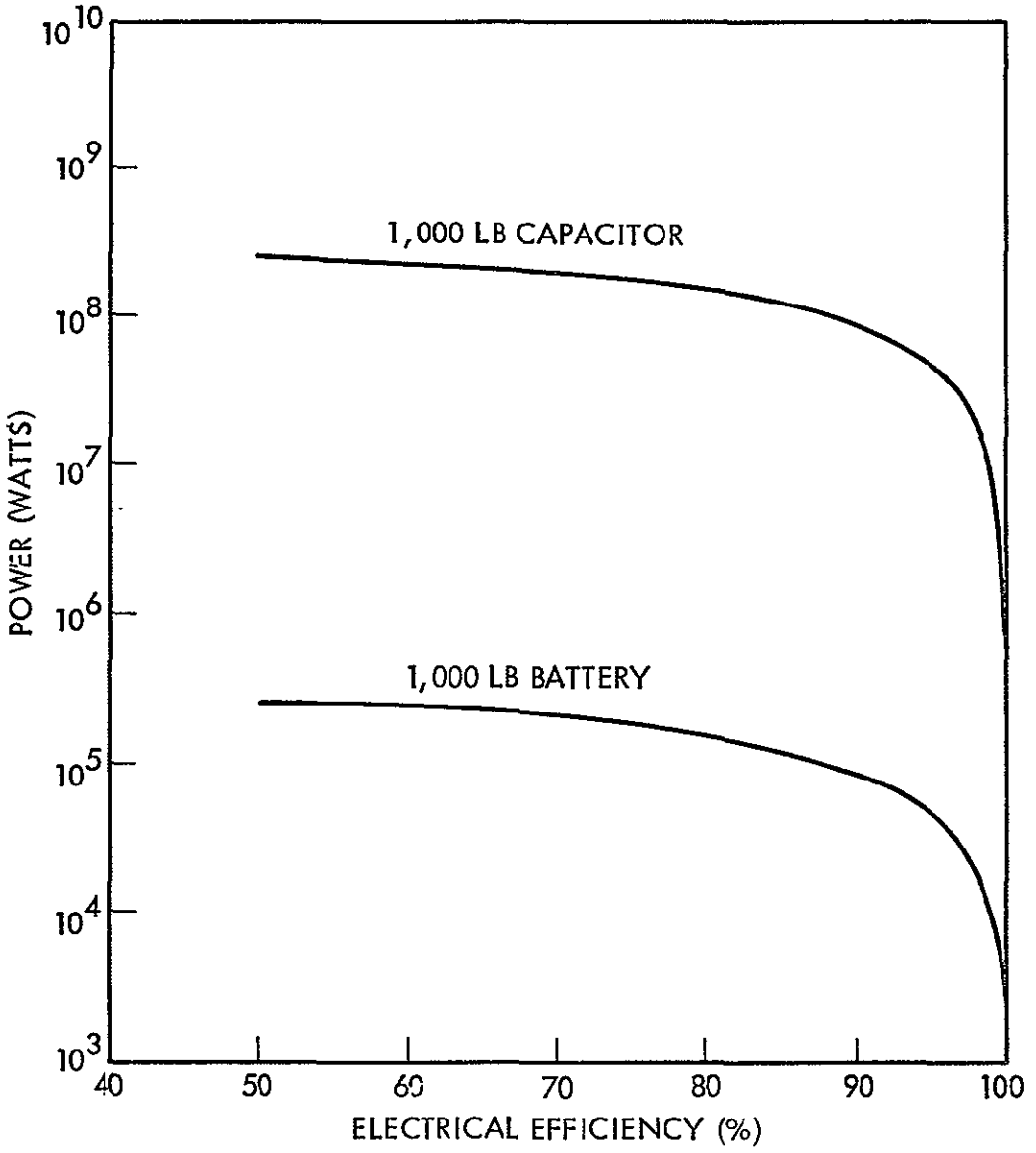

Figure 18. Electrical Efficiency in Transfer as a Function of Transfer Power for Capacitor Bank and (Stipulated) Battery Bank.

Our final aspect of cell internal impedance (and the impact which this parameter has one battery efficiency and power density) is cell method of construction. Two possible approaches in construction are the conventional prismatic cell and the more recently developed bipolar cell. Reliable cell performance at very high powers may not be possible with prismatic cells for 1 milliohm internal impedance when all other factors, including fragility of plates and separators under Shuttle launch, and required weight per cell are taken into consideration. In this case an appeal might be made toward a bipolar cell design. It is not considered to have been demonstrated, however, that construction and operation of such cells is fully understood, particularly in gas release during charge and discharge periods, separator behavior, shelf life, and in-series destablization failure modes.

6.3.3 Failure Modes

The basic failure modes for the battery are identical to those considered earlier for the capacitor bank (see Section 6.2.3). These modes are both open and short circuit failure of a unit, in this case a cell, and shorting from the high voltage bus to spacecraft ground.

This open circuit failure, which was of little statistical or operational significance for the capacitor bank, must be considered as a major area of concern for the battery bank, since a series stack of cells is utilized. Because of the basic series (rather than parallel) configuration, ever "partial" failures of increases in cell sensitivity impact significantly on battery performance, and an open circuit precludes all accelerator system operation except the direct latch-down mode (fuel cell-to-power processor-to accelerator).

Cell resistance can destabilize upward over a series of repeated current surges in either charge or discharge modes and elaborate control circuitry is required for certain types of cells because of thermal runnaway under charge conditions. The weight and cost of such control circuitry has not been included in battery discussions which considered only cell weight, but, in any ultimate design, these factors may be expected to significantly increase the system complexity. Even if the system employs such charge-up controls, the high burst currents on discharge may cause destabilization of individual cells which, because of the series stack, impact on total system performance.

Some relief from these "series-configuration enhanced" failure modes might be obtained by series-parallel cell stacks, but controls for this arrangement are even more complicated and cell-to-cell matching must be very precise to avoid adverse reactions by cells in the parallel portion of a series-parallel stack. An accurate assessment of failure modes in such series-parallel stacks and for the somewhat unique AMPS operational conditions may be expected to be difficult and costly.

The short-circuit of a cell is not a failure mode which eliminates further total system operaton, but the affected cell is lost for storage and transfer purposes. The consequences of a short circuit are somewhat different for batteries when compared to capacitors, however, since loss a battery results primarily in a power loss capability which the loss of a capacitor results in an energy storage loss. It will be advanced here that loss of power capability will probably be a more significant loss than energy storage capability. Section 6.3.4, which treats Modularity Considerations, will discuss further implications connected with battery packs and the power limitations in their use.

The third failure mode of concern is the shorting of the high voltage bus to ground. While this failure mode was of only limited hazard to continued operation of the remainder of the Orbiter when it occurs in a capacitor bank, this failure mode is of particular concern if it occurs in the battery pack. The reason for this additional level of concern is that the battery has such large quantities of stored energy (see discussion of characteristic times and energy storage requirements in Section 4.4) and their uncontrolled release can result in significant levels of thermal impact to the Orbiter.

A final aspect of battery failure distinct from capacitor failure is that the batteries will be in a charged state during launch and will probably be in a charged state during descent. These periods of high vibration are also, thus, periods of large energy storage. The reasoning toward this charged state during launch and descent is the following: (1) to undergo launch with uncharged cells and to then charge on orbit requires significant periods of time and levels of energy transfer after launch, and the launch of fully discharged cells may also open up other failure mode and destabilization possibilities; (2) the period of preparation for return and actual descent cannot be expected, in general,

to allow a gradual deep discharging of the battery. Premature and forced early re-entry would almost certainly preclude cell discharge.

6.3.4 Modularity Considerations

The basic modularity direction for the battery bank is for increased series stacking of batteries. This provides additional power and would allow continued use of a proven cell design, but would result in a voltage increase at the battery output which violates the modularity principle in the power processor (fixed V, increasing I). To match the processor modularity principal, a cell stack for increased power would require increased current capability which, in turn, would require either a series-parallel stack or the introduction of a new, higher current capacity cell. The series-parallel stack has, as noted, particular problems in reliability, and the introduction of a new cell also introduces new questions of reliability as well as increased costs.

The battery pack has been noted to possess an improper modularity for a presumed desired increase in system power (an allowed increase in system weight). Weight allowances do not always increase, however, and, with a still highly undefined system such as the present AMPS, premissible weight for the energy storage bank could decrease. For batteries such decrease impacts directly on the power capability of the system since this is the boundary most likely to be encountered in system operation. A decrease in allowed weight for the capacitor bank, however, impacts primarily in stored energy capability. As noted in previous sections, loss of power capability may be much more costly than loss of energy storage capability.

6.3.5 Battery Bank-Capacitor Bank Comparisons

Battery bank and capacitor bank energy storage units have been reviewed for energy density, power density, electrical efficiency, failure modes and modularity. Table 11 reviews principal features for these two systems approaches. While capacitor banks generally appear to possess an overall advantage, study emphasis should be continued for both battery and capacitor storage methods. Total burst energy release experiments at the megaJoule level and above will probably be more effectively performed by batteries, and, in the absence of an add-on fuel-cell, the battery acts as the primary energy source.

PARAMETER	CAPACITOR BANK	BATTERY BANK
Energy density	$>10^2$ Joules/pound	10^4 to 10^5 Joules/pound
Characteristic time for efficient energy transfer	10^{-2} seconds	10^3 to 10^4 seconds
Power density at greater than 80% efficiency in transfer	10^5 watts/pound	10^2 watts/pound
Short circuit failure mode consequence	Loss of energy storage capability	Loss of power capability
Open circuit failure mode consequence	Loss of energy storage capability	Loss of all circuit capability
Output bus short to ground consequence to Orbiter	Controlled, minor	Not controlled and may be severe
Modularity	Increased energy storage and increased power capability at fixed V and increasing I	Increased energy storage and increased power capability at fixed I and increasing V.

Table 11. Comparisons of Performance of Capacitor Bank and Battery Bank Energy Storage Units.

6.4 Energy Storage Wheels

Recent studies of energy storage in flywheels and super flywheels have revealed that these systems are comparable to batteries in watt-hours per pound. While storage in rotational motion does reach high energy density levels, the power density of a wheel and the required generator is much more difficult to define. A principal question is allowable rate of energy withdrawal. If, as it is believed, the characteristic time for energy withdrawal from wheels is comparable to that from batteries, power density from the wheel will be limited. In addition, generator weight must be considered which raises questions of power density in the generator. These considerations tend to indicate allowable P-t from wheels at less than allowable P-t from batteries.

Energy storage wheels also present systems problems if spacecraft reorientation is required since this introduces substantial questions on allowable bearing stress. There are, in addition, the torquing and gyroscopic effects on the spacecraft. These subjects are discussed in somewhat greater detail in the Appendices. The present sutdy will consider that, while wheel energy storage and transfer may present certain desirable properties for some systems where combined attitude control and power generation is desired, they are probably not the most attractive choice for AMPS, where frequent vehicle re-orientation may be expected to occur and where re-orientation induced stress on wheel bearing and wheel lock-up could introduce potentially terminal failure modes to the spacecraft.

7.0 POWER PROCESSING ELEMENTS FOR THE AMPS PARTICLE ACCELERATOR SYSTEM

7.1 General

Section 4.2.1 has discussed and Figure 7 has illustrated both single and dual tier power processing elements. From considerations given there a dual tier processing configuration has been adopted for the proposed system. Discussion in this section will continue this presumed two level arrangement. As noted in Section 4, requirements for the first stage of such power processing are not extensive, while much more extensive requirements exist in the second stage. A brief discussion of both forms of processor for the dual tier configuration will be given in this body of this report, with additional details in the Appendices.

7.2 Fuel Cell-to-Storage Bank Processor

The processing of power from the 28 volt fuel cell line to 500 volts (maximum) on the energy storage unit is carried out by PPUI of Figure 9. In the overall systems specifications given there, this unit has been specified at a 10 kilowatt processing level. While this 10 KW figure may be required ultimately, it has also been noted that power from the fuel cell to accelerator cannot on a realistic basis be expected to be at this level for initial AMPS operations. This follows from a general fuel cell steady state output at 7 KW, portions of which may be expected to be firmly allocated to ongoing Orbiter and AMPS needs. From this it would appear that 5KW represents the maximum possible throughput to the accelerator energy storage unit.

An important concept that has been stressed for all elements of the power train is modularity. Using modularity, initial system design and validation may take place at a lower level, with later add-on expansion to a final full sized accelerator unit. For meaningful modularity, subdivision should not occur by more than 1 order of magnitude. On this guideline, a unit of the first stage processor would be at least 500 watts. The first power processing unit, termed the "charger" in the Appendix has been sized at 3 such 500 watt units, for a total processing capability of 1.5 kilowatts, which is $\sim$ 30% of ultimate (large system) design requirement.

Estimates of PPUI weight are 12 kilograms for a 1.5 kilowatt unit with an estimated system efficiency of 85 percent. This power density of approximately 60 watts per pound is somewhat lower than the earlier estimate of 100 watts per pound in Table 5. It is assumed that a thermal control loop from the Orbiter is available for cooling the elements of the processor and has been utilized in the above indicated 85% efficiency. Increased watts per pound can be delivered if lower efficiency is allowable. Since unit weight is not particularly large, however, a more desirable alteration may be to increase electrical efficiency in a lower power density, higher weight unit.

The charger design will be somewhat altered by selection of a battery for the energy storage unit. Basically, however, this processing method is compatible to either batteries or capacitors.

7.3 Storage Bank-to-Accelerator Processor

The power processor from the storage bank to the accelerator is designated as PPU II in Figure 9. From the mission requirements discussed in Section 3 and illustrated in Figure 5, the power requirement in this unit could range to 500 kilowatts if certain modification mission experiments are to be performed. Using earlier discussed principles of modularity, and for a meaningful approach to an ultimate 500 kW capability, a subunit PPU II should be expected to perform at the 50 kilowatt level. From Figure 5 it may be seen that this power capability accomplishes all monitoring mission experiments and the opening phases of the modification experiments (the very high power MPD arc experiments do not require the processor and require only that storage be in capacitors).

The power level chosen for the basic PPU II module is 50 kilowatts, and, for 90% electrical efficiency, unit weight is estimated at 55 kilograms. In Table 5 a 200 kW unit has been estimated at 250 pounds (114 kilograms), so that the earlier 200 kW version is optimistic in its weight assignments. Increases in power density can be achieved by allowing reduced efficiency, and 50 kW can be delivered by a 35 kilogram unit (65 watts per pound) at 85% efficiency. Efficiency may be more critical than weight, however, and designs may shift to even heavier, higher efficiency configurations.

The processor design assumes that a thermal control loop is present. Using this loop in both PPU I and PPU II allows a steady state 1.5 kW "latch-down" operation. For very high power bursts, the thermal mass of the unit is used to prevent excess temperature rise. For the 55 kilogram unit, a 1 megaJoule throughput (50 kilowatts for 20 seconds) results in a 5° Centigrade temperature rise. These P-t capabilities are very favorable when reviewed against mission requirements in Figure 5. Since parallel operation of power modules allows increased energy throughput, a ten module 500 kilowatt processor could provide a 10 megaJoule energy processing without undue temperature rise. Such throughput lies completely outside of capacitor bank capability, and would represent a comparatively significant drain on batteries at the 1000 pound level.

The directions of modularity, for both PPU I and PPU II are for increased current at fixed voltage. This modularity matches to the capacitor bank, but is not matched, as noted, by a battery storage unit, where

preferred increases in power would be derived with fixed current and increasing voltage.

To this point in the study, attention has been directed into power levels and burst durations as the parameter space in which experiments, storage units, and power processors, must have a matched capability. As will be seen in Section 8, Electron Acceleration Design Considerations, other important parameters are beam current and acceleration voltage. The power processor described here and in the Appendix delivers 50 kilowatts for 2.5 amperes at 20 kilovolts. Delivery of power at other voltages and currents will certainly be required and redesign of the processor for an optimum match to accelerator needs will probably be required.

8.0 ELECTRON ACCELERATOR DESIGN CONSIDERATIONS

8.1 General

Figure 9 has illustrated a total accelerator system consisting of electron and ion guns, and both low and high voltage plasma guns. This study will examine only the electron accelerator portion of the total system. Study emphasis will continue to emphasize the more general design problems which will tend, ultimately, to select one or another version of an electron accelerator. Principal emphasis in such selection should be given, it is felt, to those designs with a capability to perform a broad range of experiments in both the monitoring and modification missions. System configuration in the energy storage and transfer elements has already been studied to satisfy such broad ranges of requirements, and continued emphasis on this principle in the electron accelerator design is required to yield high overall mission effectiveness.

An earlier examination of design considerations for a high current high power electron beam was carried out for the Plasma Physics and Environmental Perturbation Laboratory. For convenience and because of continued relevance, some of the findings under that earlier program are given in the Appendices to this study. Figure 19, which provides a block diagram of the elements of the electron beam system, is given here, and is drawn from that previous program. It is felt that this earlier configuration remains valid for present AMPS needs.

One final aspect to be noted is that systems consideration in this study have emphasized beam power and burst duration as principal parameters. While this remains valid, both acceleration voltage and current have ranges of requirements within the overall power requirement. These voltage and current specifications will enter into the design of PPU II, the processor linking the energy storage unit to the accelerator. PPU I and the energy storage unit will not be specifically concerned with accelerator voltage and current, but only on the product power and the required burst duration.

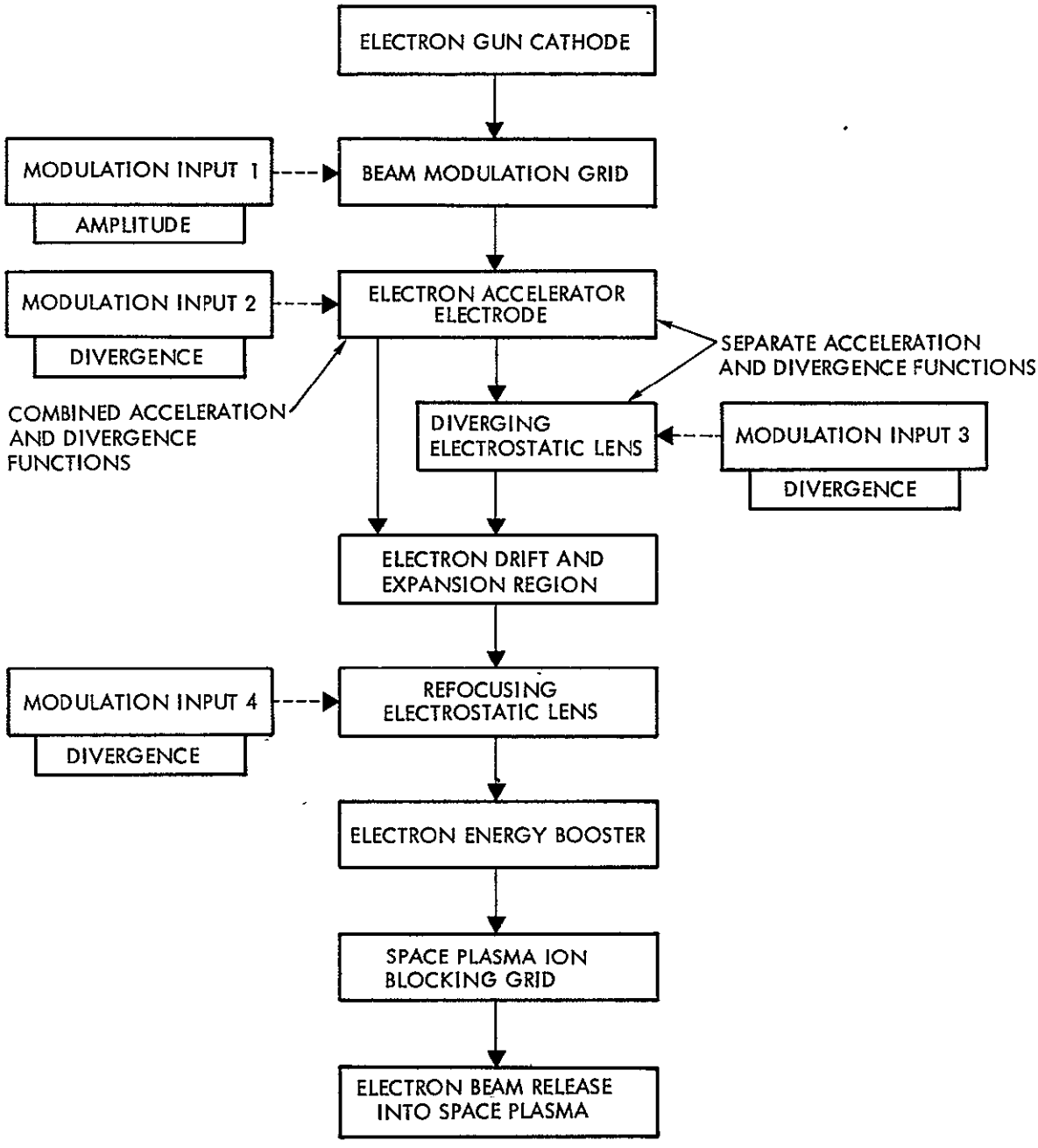

Figure 19. Block Diagram of Elements of Overall Electron Beam System.

8.2 Acceleration Voltage Requirements

8.2.1 Steady-State Operation

As noted earlier, high-powered electron beam operation clearly exceeds fuel cell limits, so that an energy storage system is required, and burst duration is necessarily limited. Even such bursts, however, may be described as "steady state" operations, if it is considered that voltage variance does not occur during the period of beam release. Section 8.2.2 will discuss possible operation in which acceleration voltage is deliberately varied during beam release. This section will consider that a voltage pulse occurs at the output of PPU II, but that electron flow is initiated after a steady state voltage output is obtained, and the electron flow is terminated prior to voltage pulse termination.

Acceleration voltage requirements will clearly range through at least one order of magnitude in variation. For an electron echo experiment, levels from 20 kilovolts to 40 kilovolts may be generally required. For measurements of $\vec{E} \parallel \vec{B}$, beam energy required may be of the order of a few kilovolts, since the total potential fluctuations in the naturally perturbed ionosphere and magnetosphere may only be of this magnitude. While beam injection at high pitch angles with respect to $\vec{B}$ has the effect of lowering the effective gun voltage, it would still appear reasonable to require beam voltage reductions at the PPU II output to the level of, say, 4 kilovolts.

Auroral simulation experiments may also be expected to require shift variations in beam voltage. A possible range here is from 4 kilovolts to 20 kilovolts. If modification and excitation of the atmosphere below 90 kilometers is desired, then beam energy will be required to exceed even the earlier noted 40 kilovolt point.

Variation of the output level at PPU II is fully within the capability of that design. The upper end is determined by the turns ratio on the transformer. The lower end point can extend to zero volts, effectively, since the circuit is under active control, and diminutions in the power ladling rate result in lowered output voltage.

The principal question in transformer turns-ratio selection and component selection is the upper voltage end point. In the power processor

analysis given in the Appendices, this end point was set at 20 kilovolts with a rated current, at that point, of 2.5 amperes. If higher voltages are desired, re-configuration is possible, along the line of constant peak power (for example, 1.25 amperes at 40 kilovolts). Variations of required peak voltage will not impact significantly on processor design, provided these requirements remain below approximately 50 kilovolts. For deep penetration and excitation of the atmosphere, where beam voltages of 100 to 200 kilovolts may be required, substantial system change will be demanded. Figure 19, in an attempt to allow possible growth modes to very high beam voltages without total re-configuration of the system, has indicated a separate energy boost stage. While this approach may be feasible and should be studied further, the voltage breakover requirements on all elements of the accelerator upstream of the energy boost stage must also match to these very high voltage levels, and extra, and perhaps prohibitive, initial systems costs could result from such requirements. For the present study, the very high voltage range requirement will not be satisfied by PPU II. As developed in the Appendices, its peak output voltage is at 20 kilovolts. If 40 kilovolts should emerge as an initial AMPS requirement, re-configuration to higher output at PPU II is possible and would be carried out.

8.2.2 Voltage-Modulated Operation

Because of its voltage control capabilities, output voltage of PPU II may be varied during beam release if this experimental performance is required. The peak voltage variation rate for upward increases in voltage will be determined by peak processor current onto the buffer capacitor, C_B in Figure 9, and the beam output current at the time of required voltage variation, and the magnitude of the bleeder resistor, R_D. For peak downward variations in voltage, the processor throughput is set to zero, and voltage decline is paced by beam current, buffer capacitance, and drainage resistance. Values have not yet been firmly assigned to C_B and R_D. If voltage modulation is desired for AMPS experiments, the requested (dV/dt) rates will establish requirements on these output stage resistance and capacitance elements.

8.3 Acceleration Current Requirements

8.3.1 Steady-State Operation

Steady-state operation is defined here as in 8.2.1. After the voltage pulse is applied, and after the accelerator control grid voltage is shifted from the OFF to the ON state, the beam current during the burst is defined as the steady state current. Section 8.3.2 will discuss accelerator operation where the control grid voltage is intentionally varied to create a time-varying output beam. It should be emphasized that the gun design of Figure 19 assumes a control grid. This element is required not only to provide deliberate modulations of the current but also to prevent inadvertent releases of electrons at other periods (for example, during and after voltage pulse applications). It should also be noted that the most convenient method for repetition of beam bursts may be to retain the output of PPU II at a given voltage and switch the beam ON and OFF with the control grid.

The minimum levels of beam current requirement may occur for electron echo experiments detected by remote satellites bearing their own particle counters. Detection of electron echo and $\vec{E} \parallel \vec{B}$ by beam excitation of the atmosphere requires large beam currents. Large beam currents are also required in auroral simulation, species growth, and temperature alteration experiments in the modification mission. Estimates of current requirements here range to 10 amperes; lower end current requirements are at the 100 milliampere level.

For a system with a control grid, satisfaction of the lower end current requirement is not difficult. System difficulty and configuration is paced by the high end requirement. For PPU II, this current capability has been set at 2.5 amperes which does not satisfy a 10-ampere requirement but is, nevertheless, a substantial release of electrons. The 2.5 ampere point and 20 kilovolts provides the processor peak power at 50 kilowatts. As noted in 8.2.1, voltage requirements may rise above the 20 kilovolt point and, if re-configuration occurs, peak current capability will diminish (since peak power is fixed). Ultimate system design must await, then, a review of experimental requirements to determine processor output voltage and current levels. For the present study and processor design, a choice of output voltage at 20 kilovolts (peak) and 2.5 amperes (peak)

has been made as the most plausible parameter configuration within the present broad list of AMPS requirements. It should also be noted that the processors are modular and that additional processors increase possible output current at peak voltages.

8.3.2 Current-Modulated Operation

Whereas voltage modulation has not emerged as a strong AMPS requirement (8.2.2), current modulation capability may be expected to be a strong requirement. The electron beam heating of the ionosphere could require modulation at ω_{ce} and ω_{pe} ($\sim$ 1 megahertz and $\sim$ 10 megahertz), and any number of experiments may desire clearly initiated and terminated beam pulses. It will be advanced here that system movement from beam OFF to beam ON at full amplitude should be possible within 0.1 microseconds, and modulation from zero to full amplitude should be possible for frequencies to and including ω_{pe}. This modulation capability should also be capable of control from low level (percentile) to full amplitude modulation.

8.4 Angular Divergence Requirements

8.4.1 Steady-State Operation

Angular divergence requirements for the electron beam may be expected to be comparatively strict for monitor mission experiments and comparatively relaxed for modification mission experiments. For electron echo and $\vec{E} \,||\, \vec{B}$ experiments, a Full Width Half Maximum of .1 radians appears to correspond to generally expressed experiment requirements. It may be possible to increase this allowed divergence by a factor of approximately 5 for auroral simulation experiments and by approximately 10 for the species growth experiment. This relaxation of requirements for the high current high power beams is helpful, since angular divergence effects from large levels of space charge in these beams will be present to some degree despite appeals to divergence and refocusing output stages on the electron accelerator (see Figure 19, discussion in 8.0, and the Appendices). For experiments utilizing electron beam-ambient plasma coupling, either at low or high powers, the allowed divergence may be expected to be somewhere between the narrow "electron echo" requirement and the broad "species growth"

allowance. A principal question in the ultimate selection of either a single, plural, or multiple gun approach will be the degree to which these various divergence requirements can be satisfied by the various systems. If a high perveance (high current at high voltages) gun can be designed to produce a narrowly diverging beam for control grid voltages near beam cutoff, then satisfaction of the divergence requirements can probably be accomplished with a single gun. The addition of divergence and refocusing stages will further improve satisfaction of the divergence requirement, but is a secondary consideration relative to the ability of the gun to emit narrow beams near cutoff.

8.4.2 Divergence Angle-Modulated Operation

Experiments requiring modulation of beam divergence (as a means of pitch angle width modulation) have not appeared at present. For the system in Figure 19, modulation of voltages in the divergence and refocusing lenses at the accelerator output can produce a divergence angle width modulation. Unless requirements for such modulation are stated, however, system capability would appear to be better served by attention to modulation of pitch angle itself, rather than pitch angle width.

8.5 Pitch Angle Requirements

8.5.1 Steady-State Operation

8.5.1.1 Pitch Angle Magnitude

Experiment requirements speak generally of electron release at pitch angles from 0° to 90° (along $\vec{B}$ to perpendicular to $\vec{B}$). While this angular range is naturally interesting, since it allows all possible orientation of electron velocity relative to $\vec{B}$, practical considerations will place limitations on θ. The practical considerations arise from the Orbiter surfaces and the consequences of energetic particle deposition into those surfaces. The deposition of energetic electrons into dielectric material can cause severe charge-up, with subsequent break-downs which affect material properties and may affect Orbiter operation from conducted and radiated electromagnetic interference. The power associated with

interception of the beam on spacecraft surfaces is of concern for both conducting and insulating surfaces. Other portions of the AMPS payload may have even more sensitive reactions to energetic beam interception. For all of these reasons, pitch angles at 90° cannot be considered feasible since release of the beam at these angles will almost certainly result in re-interception on the Orbiter and on payload elements.

In addition to circulation and interception directly attributable to electron cyclotron motion about $\vec{B}$, there are, very possibly, other processes which will scatter electrons from the beam onto nearby surfaces. Taking all processes together, a practical upper limit to allowable pitch angle may be more nearly described as 60°, and even this release condition must be examined relative to interception on the Orbiter tail surfaces. Section 8.6 will discuss the desired placement of the exit planes of the various accelerators in order to minimize interception effects.

8.5.1.2 Method of Generation of Pitch Angle

Three possible methods for the generation of a given pitch angle for electron release are: 1) motion of the Orbiter, 2) motion of a movable platform on which the accelerator is mounted, and 3) magnetic deflection coils at the electron gun output. It is anticipated that use of method (1), reorientation of the Orbiter to set up a given angle between the axis of the electron accelerator and $\vec{B}$, will be used, although it appears desirable to limit the use of this approach, inasmuch as is possible. The reasons for minimizing or not using Orbiter reorientation are: (1), to minimize propellant usage on the RCS system, thus prolonging possible maneuverability for other experiments and requirements, (2), to decouple the Orbiter position from required electron release direction to avoid possible Orbiter orientation conflicts arising from either other experiment requirements or from other operational requirements (for example, radiator positioning for maximum thermal release), and, (3), to minimize possible contaminant effects on the electron accelerator cathode by repeated required firings of the RCS.

The use of a movable (gimballed) platform for the electron accelerator has not been used in the system shown in Figure 9. The reasons against the use of the gimballed platform for the electron accelerator are: (1) costs, (2), additional volume requirements to avoid electron beam system encounters with other payload elements, and (3) enhanced possible beam interception problems since table motion must necessarily result in electron gun exit plane motion into regions more deeply placed in the Orbiter bay, and, (4), the overall size and weight of the electron accelerator (particularly if output divergence and refocusing stages are present).

The use of magnetic deflection coils (in conjunction with possible Orbiter reorientation) has been chosen as a means of pitch angle specifications. Since electrons are easily bent, even at 50 kilo-electron volts, the B-fields required for deflection are not large. The use of the deflection coils allows the gun exit plane to be placed as near as possible to the top of the Orbiter payload bay envelope. Using a remotely positioned three-axis magnetometer and crossed magnetic deflection coils at the output, pitch angle may be automatically set and maintained, or varied in a prescribed manner, with little or no demands on the Orbiter RCS system. The crossed output coils also allow the "2-D scan" of electron beam current density discussed in Section 9, Electron Beam Diagnosis.

Problems which must be examined for the use of the deflection coils are magnetic contamination effects on other experiments, and possible angular dispersion of the beam (or particular concern if a large exit diameter beam is utilized).

8.5.2 Pitch Angle Modulated Operation

The use of magnetic deflection coils at the electron output allows a time variance of the beam pitch angle. This parameter variation is expected to be of value for any experiment aimed at measurement of electron response as a function of beam pitch angle. Until experiment requirements emerge, however, for extent of pitch angle variation and rate of change in pitch angle, the required magnitudes of drive currents and voltages on the output deflection coils will not be determined.

8.6 Electron Accelerator Placement

8.6.1 Axial Direction

Axes of all of the particle accelerators are along the orbiter Z axis. In this orientation, the distance separating the beams from Orbiter surfaces is at a maximum. It is possible, in principle, to orient along the Y axes and have the beam emerge over the Orbiter bay doors, but the beam is then in close proximity with the wings. Release of beams along the X axis results in direct interception inside the bay (it is assumed here that the accelerator exit plane cannot be outside of the payload bay envelope)

8.6.2 Exit Plane Placement

The exit planes of all accelerators are placed as near as possible to a Z axis interception with the payload bay envelope. If orientation of the Orbiter Z is along $\vec{B}$, the principal deflection by the magnetic deflection coils is toward the Y axis. (Coils exist for deflection into both X-Z and Y-Z planes; the major deflection coil is the Y-Z. Both X-Z and Y-Z coils are used in the 2-D scan of the electron beam current density.)

8.7 Electron Beam Diameter

Requirements for specific electron beam diameters have not appeared at the present. For high current high space charge electron beams, a possible method to prevent beam blow-up from space charge forces it to diverge the beam until its density is less than the density of the space plasma. The techniques for divergence and refocusing are illustrated

in Figure 19 and discussed in the Appendices. This technique, if successful, would allow the generation and release into space of high perveance electron streams with comparatively narrow divergence cones. By modulating both the initial, diverging, lens, and the final, converging, lens, final beam diameter can be modulated. There is, as yet, no apparent experimental requirement for such spatial modulations, and, unless specific requirements arise, the drive voltages on the input and output electrostatic lenses need not have high frequency modulation capability.

8.8 Contaminant Effects

8.8.1 Contaminants Imposed on the Accelerator by the Orbiter

8.8.1.1 Material Contaminants

The cathode of the electron accelerator must, of necessity, use a low work function material for the electron emitting surfaces. For sealed electron tubes, both oxide coated surfaces and dispenser cathodes are utilized. For laboratory accelerators where active pumping of the system is employed, dispenser cathodes, which contain barium in a porous tungsten emitter and from which a continuous barium diffusion to the surface maintains a low work function emitting surface, are frequently used.

For the electron accelerator on AMPS, two aspects of material contamination of the cathode must be considered. The first of these is transport and deposition of non-charged material contaminants from the various payload elements and Orbiter systems (including various liquid and gaseous vents and the Reaction Control System) to the cathode surface. Some relief from these effects may be gained by a planned closedown of material venting during electron accelerator operation. A second avenue of relief, in principle, is supplied by the magnetic deflection coils which allow electron beam pitch angle specification with more limited use of the RCS system, thus minimizing thruster plume contaminant effects.

A second form of material contamination results from the formation of ions under electron beam impact of neutral molecules and the backward acceleration and impact of those ions on the cathode emitting surfaces. This back-bombardment can remove emitting material. However, it can also

sputter away contaminant layers affixed to the material, and, while ion back bombardment is not openly solicited, its effects are both harmful and beneficial.

In view of successful operation of dispenser cathodes in the presence of contaminant effects, an initial cathode material selection would appear to be such barium dispensing porous tungsten cathodes. It would also appear to be worthwhile, however, to consider alternative cathode materials in the event that cathode poisoning effects are more severe than anticipated.

Three possible alternative cathode approaches are: (1), cesiated porous tungsten, (2), "plasma" cathodes, and (3), pure refractory metal cathodes. The cesiated porous tungsten cathode would employ a cesium reservoir and heater which supplies cesium vapor to the rear side of a porous tungsten plug. Diffusion of cesium to the forward (emitting) face of the porous tungsten results in a low work function surface which can maintain electron emissivity under high levels of arriving contaminants. The system is complicated, however, in its requirement for the cesium reservoir and in the transport and diffusion through tungsten of the cesium.

"Plasma" cathodes are used as electron sources for the neutralization of ion beams in electric thrusters. They supply high levels of electron current, and, since the electron emitting materials are on interior walls of the hollow cathode, ion back bombardment effects are not present. Since access to the hollow cathode is through a very small hole, contamination by neutral deposition is also greatly reduced. A principal question of effectiveness derives from required shaping of the electron emitting surface in electron accelerators for laminar flow properties under acceleration. This shaping will probably be difficult for the discharge plasma which is the source of electrons for acceleration. In addition, a gas reservoir for the plasma discharge breakdown must be provided as well as an ancillary electrode and voltage (the "keeper").

The third alternative choice is the use of the refractory metals (tungsten, molybdenum, for example). These cathodes are essentially non-poisonable because of their very high operating temperature. The dis-

advantages in the use of the untreated refractory is the large required cathode heating power and the consequent thermal loading it imposes on other portions of the accelerator and, ultimately, on the Orbiter.

For present purposes, the use of dispenser cathodes appears acceptable. This selection should be reviewed when more accurate assessments of material contaminant effects are available.

8.8.1.2 Electromagnetic Contaminants

The use of magnetic coils to set, or vary, electron beam pitch angle has been described previously. Use of that approach relies on the ability to determine the Earth's magnetic field, $\vec{B}$, and a three-axis magnetometer is assumed to be a portion of the AMPS payload. For this magnetometer to function effectively, however, the contaminant magnetic fields from the Orbiter must be substantially below the level of the Earth's magnetic field. If large current circulation loops should exist on the Orbiter, contaminant fields will also exist and could significantly perturb magnetometer operation. Figures 20 and 21, drawn from a discussion of contaminant magnetic field effects in the Appendices, illustrate contaminant field levels for two sizes of loops. If such current flow patterns were to exist on the Orbiter, significant perturbation of the magnetometer would result. The fields from the larger loop could also affect the electron beam directly.

Discussion in the Appendices on possible avenues for contaminant field reduction indicate that sufficient reduction can be achieved without undue effort, provided that this effort is made. Continued attention should be given to current path routing. As assessments of contaminant fields improve in accuracy, their impact of magnetometer operation and electron accelerator operation should be reviewed to assure that the beam is not perturbed by these Orbiter (and payload) currents.

8.8.2 Contaminants Imposed on the Orbiter by the Electron Accelerator

8.8.2.1 Electrical Charge-Up

Two aspects of electrical charge-up are of concern. The first of these is total charge-up of the Orbiter as a result of the release of large

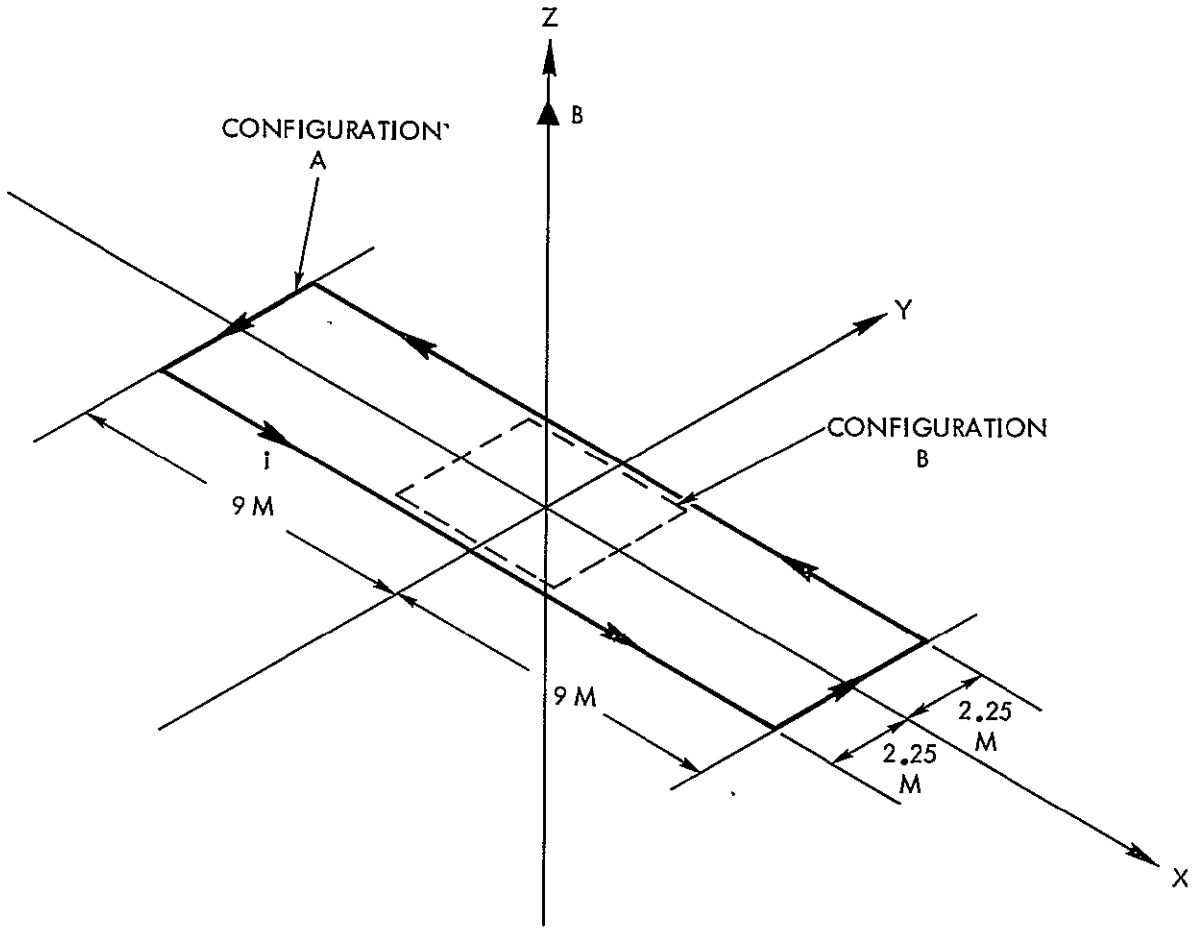

Figure 20. Current Flow Configuration and Axes

$$\left(B_z(x,y,z) = 400\ i \left[\frac{xy}{(x^2 + y^2 + z^2)^{1/2}} \left(\frac{1}{(y^2 + z^2)} + \frac{1}{(x^2 + z^2)}\right)\right]\right.$$

with B_z in $\gamma (= 10^{-5}$ gauss) for i in amperes, x, y, z in meters).

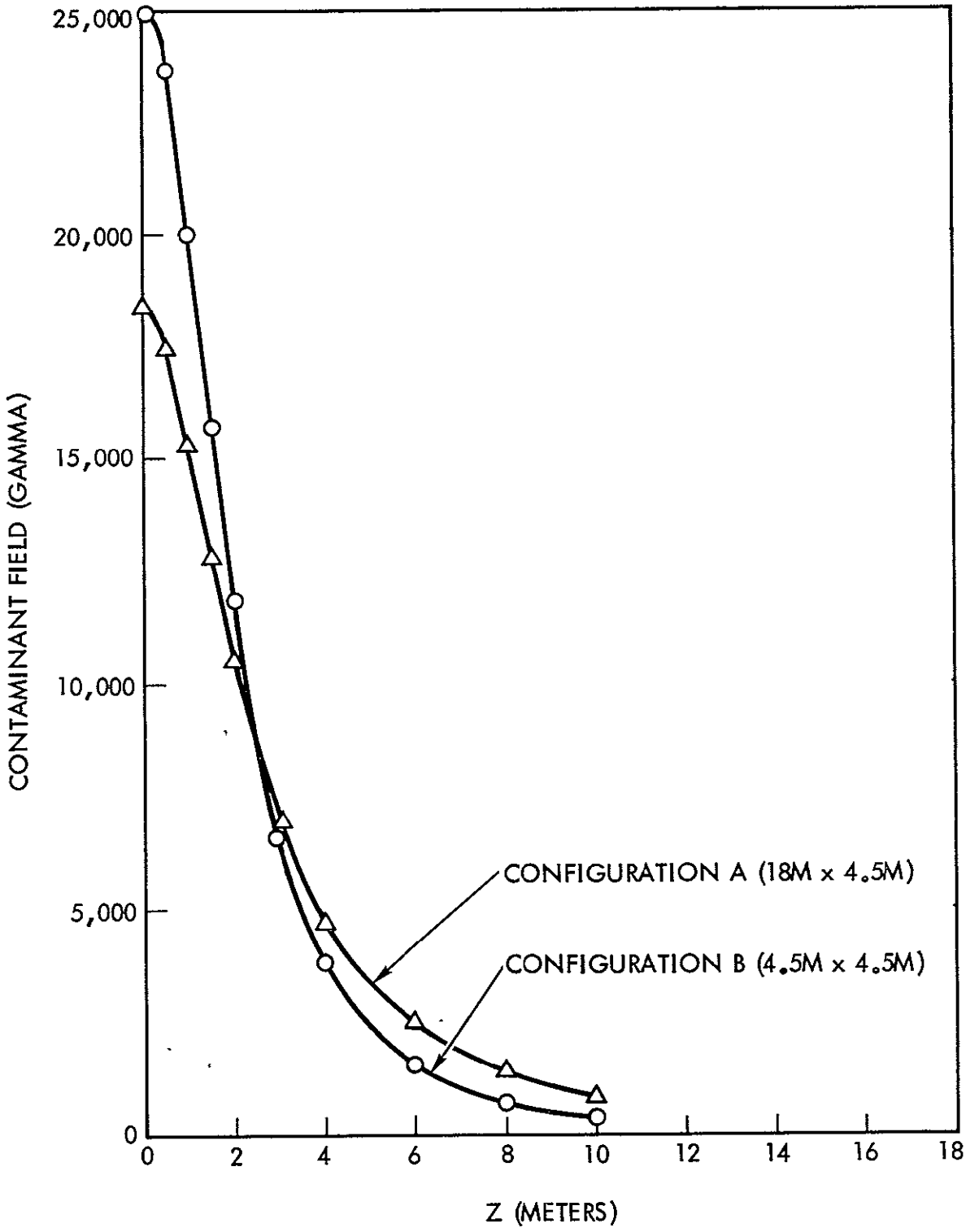

Figure 21. Contaminant Magnetic Field Along Z-Axis for 100 Ampere Current Flow in Illustrated Geometry as a Function of Z Separation.

currents of electrons. Section 10 will discuss this subject in more detail, but it will be noted here that one of the functions of the Gas Plume Release (see also Section 9) is to alleviate such total spacecraft charge-up effects. The effectiveness of this method, as well as others, in alleviating charge-up in space will probably be known accurately only after space experimentation, and an important in-flight experiment will be to evaluate orbiter electrical equilibration during high level electron beam release.

The second aspect of charge-up as a result of electron beam operation may be termed "local" charge-up, and results from energetic electron deposition in spacecraft insulating surfaces. These effects have been treated previously in terms of allowable electron beam pitch angle (Section 8.5) and in the placement of the axis and the exit plane of the accelerator (Section 8.6). Hopefully such placement will prevent localized areas of charge-up on insulating layers. In-flight visual monitoring and post-flight examination of such surfaces for evidence of charge-up should be a flight and ground support crew responsibility.

8.8.2.2 Conducted and Radiated Electromagnetic Interference

The accelerator system contains significant levels of stored energy in its midrange voltage unit, and, during beam bursts, in its buffer capacitor. The discussion of Failure Modes in Section 6 has emphasized methods (such as the inductors) for the limitation of current surges in the event of a short from the capacitor bank output line to ground. The wiring of the capacitor bank imput and output leads can also be such as to minimize conducted electromagnetic interference effects. These wiring approaches are also treated in the Appendices relative to the power processors (borrowing from techniques used earlier and successfully for ion thrusters on electrically propelled spacecraft).

A final area for consideration here is the possible beam radiation for large current electron beams at high levels of modulation. No specific assessment of such effects can be made at present, and it may be that in situ experiments will be required to evaluate the radiation from such beams and if they are of sufficient strength to interfere with Orbiter operations.

8.9 Single, Plural, and Multiple Gun Considerations

8.9.1 General

Sections 8.1 through 8.8 have reviewed various requirements for the electron accelerator and Section 3 has treated required beam power and burst duration for monitoring and modification missions. Table 12 summarizes these requirements. Surveying these performance areas, a major question in system design is whether a single electron gun can be used or whether a plural (several) or multiple (many) gun approach is required. This question must be viewed in several aspects. The first of these examines a single experiment, (for example, a high current, high power level excitation of the atmosphere,) and asks whether one, a few, or many guns of similar design must be used. A second aspect of even a single experiment, is whether more than one gun type may be required (for example, in a deliberate $\vec{E} \parallel \vec{B}$ excitation, a high power level perturbation beam and a low power level sensing beam might be required). The final aspect of the gun number requirement is whether the total group of experiments can be satisfied by a given gun type, whose multiplicity must, in a further examination, be determined. To understand some of these factors in more detail, the study will first examine perveance considerations, and limitations, in electron beams.

8.9.2 Perveance Considerations and Limitations

The perveance of an electron beam is defined as beam current divided by the beam voltage to the three-halves power. A one ampere beam of electrons with 10,000 volts acceleration potential has a perveance of 10^{-6} amperes per $(\text{volt})^{3/2}$. For units of convenience, a perveance of 10^{-6} is termed a "unit" perveance. "Unit" perveance is also an approximate upper bound to the amount of current for a given acceleration voltage which may be accelerated in a single cathode-accelerator electrode structure and have essentially parallel flow at the accelerator electrode plane. Even with such initial tailoring of the electric fields and the electron flow, the magnitude of space charge in unit perveance beams causes a rapid growth of radial divergence in the flow as electrons proceed away from the gun (see discussion in Appendices, with space charge

PARAMETER	MONITOR MISSION	MODIFICATION MISSION
Acceleration Voltage	4 kV to 40 kV	10 kV to 40 kV
Voltage Modulation	Not required	Not yet determined
Beam Current	.1 to 1 ampere	1 to 10 amperes
Current Modulation	Percentile level	Zero to full beam for $\omega \leq \omega_{pe}$
Power	1-50 kilowatts	30-300 kilowatts
Burst Duration	.1 to 10^3 seconds	.1 to 2 seconds
Angular Divergence	<.1 radian	<.3 radians
Divergence Angle Modulation	Not required	Not yet determined
Pitch Angle	0° to > 60°	0° to > 60°
Pitch Angle Modulation	Not yet determined	Not yet determined

Table 12. Performance Range Requirements of the Electron Gun for All Experiments in the Monitor Mission and the Modification Mission.

spreading beam contours for unit perveance flow and the possible correction methods of refocussing and release-into-plasma).

Since accelerated current in a space charge limited flow is proportional to perveance times the three halves power of the voltage, and since unit perveance is one ampere at 10,000 volts, this same gun will deliver 2.83 amperes at 20.000 volts, for a total beam power of $\sim$ 56.6 kilowatts. The 20 kilovolt, 2.5 ampere version of PPU II discussed in the earlier section on power processors is, thus, an approximate match to a unit perveance gun.

If 50 kilowatts of beam power is required, but at 1.25 amperes and 40,000 volts, the beam is $\sim$ .16 unit perveance. This is a comparatively low perveance gun. A high perveance gun with a control grid can, of course, yield a flow at overall low effective perveance. A unit perveance gun with control grid operating toward cut-off could be used for this lower perveance requirement. One additional factor, however, is angular divergence. For monitor mission experiments required beam angular width of half maximum may be expected to be $\sim$ .1 radians. Thus, as noted earlier, a high perveance gun may be used for low perveance applications provided that beam angular divergence is narrow for the high perveance gun operating toward cutoff. The converse situation is not allowable. Low perveance guns cannot generate high perveance flows.

From the above discussion, it would appear that a unit perveance gun can satisfy not only many of the modification mission experiments but also the bulk of the monitoring missions. For some of the modification experiments, however, not even unit perveance may be a high enough current flow at the required acceleration. As an example, consider a 50 kilowatt auroral simulation experiment configured to 10 amperes at 5 kilovolts (duplicating here a suspected energy range of auroral activity). The perveance in this flow is $\sim$ 30 unit perveances, well beyond the capability of a single gun. For this particular experiment, then, a clear requirement for a multiple gun approach emerges. For beam perveance at the unit to two unit level and below, a single gun approach is possible. It should be emphasized, however, that questions remain for very high current

release and possible Orbiter charge-up. If multi-ampere flows cannot be released without significant charge-up, then the multiple gun requirement experiment discussed above is not practicable, and such multi-gun approaches are not required.

8.9.3 Space Charge Considerations

Section 8.9.2 has discussed space charge divergence forces in unit perveance flows and noted that even an initially parallel exit flow rapdily diverges under these electric fields. One method for alleviation of some of these divergence effects is to subdivide a unit perveance flow into many smaller beams which are then physically separated from each other by distances large compared to initial diameter of the sub-beam. In this case, initial divergence in each sub-beam proceeds more nearly like that of a single low perveance beam with, however, some beam-to-beam forces. After the beams merge, of course, the relevant space charge blow-up now considers the perveance of all the merging sub-flows, for the effective beam diameter at the merge point. By the merge point, moreover, the group of sub-beams could be well immersed into the space plasma, with significant reductions of space charge force fields.

Several aspects of the multiple beam divergence and merge pattern, however, are not considered appealing. The determination of current density in such initially separate-ultimately merged flows is difficult to carry out, and, the beam-plasma interaction may become very complicated because of the large rates of change between beam density and ambient density in the region from the outlet plane of the guns to the merge point. The beam-to-beam and beam-to-space plasma interactions are, moreover, now complicated by every possible source of variations amongst the member beams, including current amplitude variations, divergence variations, and axial alignment variations.

A single high perveance beam is comparatively easy to diagnose, but, as noted, diverges under space charge forces. The possible solution to this desire for a single beam with essentially parallel flow and no rapid space charge driven divergences is the expansion and re-focussing of the electron beam with subsequent release into the space plasma.

8.9.4 Experiment Considerations

Section 8.9.1 has referred to an experiment in which a single high current high power beam acts to deliberately initiate, if possible, a region of $\vec{E} \parallel \vec{B}$, while a second, low power, probing beam examines the affected region. Such an experiment requires two clearly differing beam conditions and requires at least two guns. It need not require two different types of guns, since a high perveance gun near cutoff could act as the probing beam. Both guns could be run from the same high voltage output at PPU II provided that both beams have equal acceleration potentials. Differing acceleration potentials would clearly require at least two processors of the PPU II form.

From the discussion above and that in Section 8.9.2, the great bulk of all suggested electron beam experiments can be performed with a single gun of approximately unit perveance. If it should develop that very large currents may be released from the spacecraft without charge-up, the addition, in parallel, of other high perveance guns could deliver these very high perveance flows. The modularity principle here is to increase current at essentially a fixed voltage range. Technology verification goals which, once validated, allow expansion into various growth modes have been shown to exist for the power processors and the energy storage unit and also exist for the electron guns. The level for meaningful modularity would appear to be at approximately unit perveance in the electron accelerator.

8.9.5 Failure Modes and Recurring Costs

Failure modes for an electron gun include both open and short circuit possibilities for any lead. In addition, a variety of other aspects enter into, at least, partial failures. These include loss of emission from the cathode, loss of beam axial alignment, loss of beam divergence properties, and variation in grid modulation effectiveness on beam current. In a single electron gun, these factors comprise a significant number of elements to be protected against. For a multiple array of n electron guns, the number of possible failures is multiplied by at least n, and, depending upon levels of pessimism may be multiplied by

factors ranging from n^2 to n! Considering, as an example, an experiment in which pitch angle is modulated or varied, there are no significant complications with a single beam, but with multiple beams, variation in response of each beam to the magnetic deflection must be known, not only for pre-flight operation of the accelerator, but also during the flight with whatever in-flight systems alterations may be in process.

The use of a multiple gun array also raises significant questions of costs of both initial and recurring forms. Since part count is increased for multiple gun arrays, initial costs are increased, and since part replacement will probably extend into the cathode and the control grid, replacement part count is increased and recurring costs rise. These arguments would tend to favor, then, a single gun approach with possible expansion into a plural (few) gun approach if certain growth modes appear desirable. This would offer lowest initial costs, and, provided initial technology goals are achieved, would offer lowest recurring cost operation.

8.9.6 System Recommendation

The operational factors presented in this section lead to a recommended system of a single electron gun of approximately unit perveance. Table 13 summarizes recommended system properties for the electron accelerator. This accelerator is capable of performance of the experiments in both mission modes and provides a meaningful level of performance for modular expansion into AMPS growth modes.

PARAMETER	VALUE
Gun number	1
Perveance	∿ Unit perveance
Voltage capability	40 kilovolts
Current capability	3 Amperes at 20 keV
Cathode Type	Dispenser.
Control Grid Modulation capability	Zero to full beam at rates from $\omega = 0$ to $\omega = \omega_{pe}$
Output stages	Divergence plus refocusing
Pitch Angle Control	(Crossed Coil) magnetic deflection.

Table 13. Recommended System Parameters for the AMPS Electron Accelerator.

9.0 ELECTRON BEAM DIAGNOSIS

Elements of the Beam Diagnostics Group for the electron accelerator are summarized in Table 14 with weight and volume estimates in Table 15. Table 16 provides a summary of capabilities for the various levels of the Beam Diagnostics Group. Level I, which includes only the Gas Plume Release, permits a determination of either electron beam or ion beam total flow characteristics without the use of either a Remote Manipulator System or a deployable boom structure. In this diagnosis, a gas burst is released along the axis of the electron beam system (which is also near the ion beam axis) and the electron beam is then pulsed into operation. Figures 22 and 23 illustrate the gas plume placement relative to the electron beam. Excitation of the gas by the energetic electrons causes optical emission viewed either by eye, imaging systems, or photometers. This diagnosis permits a rapid "3-D" evaluation of the flow in the beam, from which beam location, line-up, and tailoring can proceed rapidly to the desired flow shape. This gas plume release, as noted, should be applicable for either energetic electron or ion beams. The high voltage and low voltage plasma guns emit luminous plumes as a natural consequence of their method of formation and excitation and will not require a "target gas" for optical evaluation of the flow.

As noted in the capabilities for the Gas Plume Release, a variety of experiments can be performed with this added feature. Included in those capabilities are: generation of ion-electron pairs to provide electron return currents to satisfy Orbiter current neutralization requirements during high current electron beam release, generation of high number, high density low energy plasma bursts as B-field line markers, and neutral and ion gas chemistry experiments for the non-bounded geometry which the Orbiter provides.

For general electron beam location, line-up, and tailoring, the Orbiter z-axis would be aligned with $\vec{B}$, the Earth's magnetic field. There are, however, experiments in which non-zero pitch angle electron beam injection may wish to have the gas plume optical "picture" of the flow.

AMPS PARTICLE ACCELERTOR SYSTEM BEAM DIAGNOSTICS GROUP

LEVEL	SUBSYSTEM	DESIGNATION	ELEMENTS
I	a	Gas Plume Release (GPR)	Storage Tank, Plenum Chamber, Gas Regulator valves, gas pop valves, gas release nozzles (4).
II	b	Faraday cup (FCP)	Multigridded boom mounted Faraday cup, cabling and connectors.
II	c	Retarding potential analyzer (RPA)	Multigridded boom mounted Retarding potential analyzer, cabling and connectors.
II	d	Cold probe (slow V_p) (SV_pP)	Boom mounted cold probe, cabling and connectors
III	e	$\dot{B}$ Probe ($\dot{B}P$)	Boom mounted probe for $\dot{B}$ measurement, cabling and connectors
III	f	E Probe (EP)	Boom mounted probe for E measurement, cabling and connectors
III	g	Fast V_p Probe (FV_pP)	Boom mounted probe for fast measurements of beam plasma potential, cabling and connectors

LEVEL	DEFINITION
I	Provides electron and ion beam diagnosis but does not require use of Remote Manipulator System (RMS)
II	Provides electron and ion beam diagnosis and does require deployment through either RMS system or diagnostic boom movement system. Does not complete diagnosis of parameters for interaction of electron and ion beams with ambient space plasma.
III	Requires deployment through either RMS system or diagnostic boom movement system. Intended to complete diagnosis of parameters in interactions of electron and ion beams with ambient space plasma.

Table 14. AMPS Particle Accelerator System Beam Diagnostics Group.

SYSTEM	WEIGHT (POUNDS/KILOGRAMS)	VOLUME/CUBIC METERS
a (GPR)	20/9	.12
b (FCP)	20/9	.005
c (RPA)	20/9	.003
d (SV_pP)	10/5	.001
e ($\dot{B}P$)	10/5	.001
f (EP)	10/5	.001
g (FV_pP)	10/5	.001
	100/45	.13

LEVEL	WEIGHT (POUNDS/KILOGRAMS	VOLUME/CUBIC METERS
I	20/9	.12
I + II	70/32	.13
I + II + III	100/45	.13

Table 15. Estimated Weights and Volumes for AMPS Particle Accelerator Beam Diagnostic Group.

The capabilities of the Gas Plume Release shall include the following: 1) Determination of electron and ion beam flux densities through optical excitation of released gas, 2) Ion-electron pair generation for ion release/electron return satisfaction of orbiter current neutralization during electron beam release, 3) Low energy high number plasma release onto B-field line, 4) Atom excitation in non-bounded configuration (ion chemistry experimentation).

The capabilities of the Level II Beam Diagnostics Group shall include: 1) The determination of the current densities in the electron and ion beams, 2) The determination of charged particle acceleration energies in the electron and ion beams, and 3) The determination of exhaust beam plasma potential.

The capabilities of the Level III Beam Diagnostics Group shall include: 1) The determination of the time rate of change in magnetic field in the electron beam-ambient space plasma system interaction, and 2) The determination of electric field and plasma potential in this system.

Table 16. Capabilities of Level I, II, and III Beam Diagnostics.

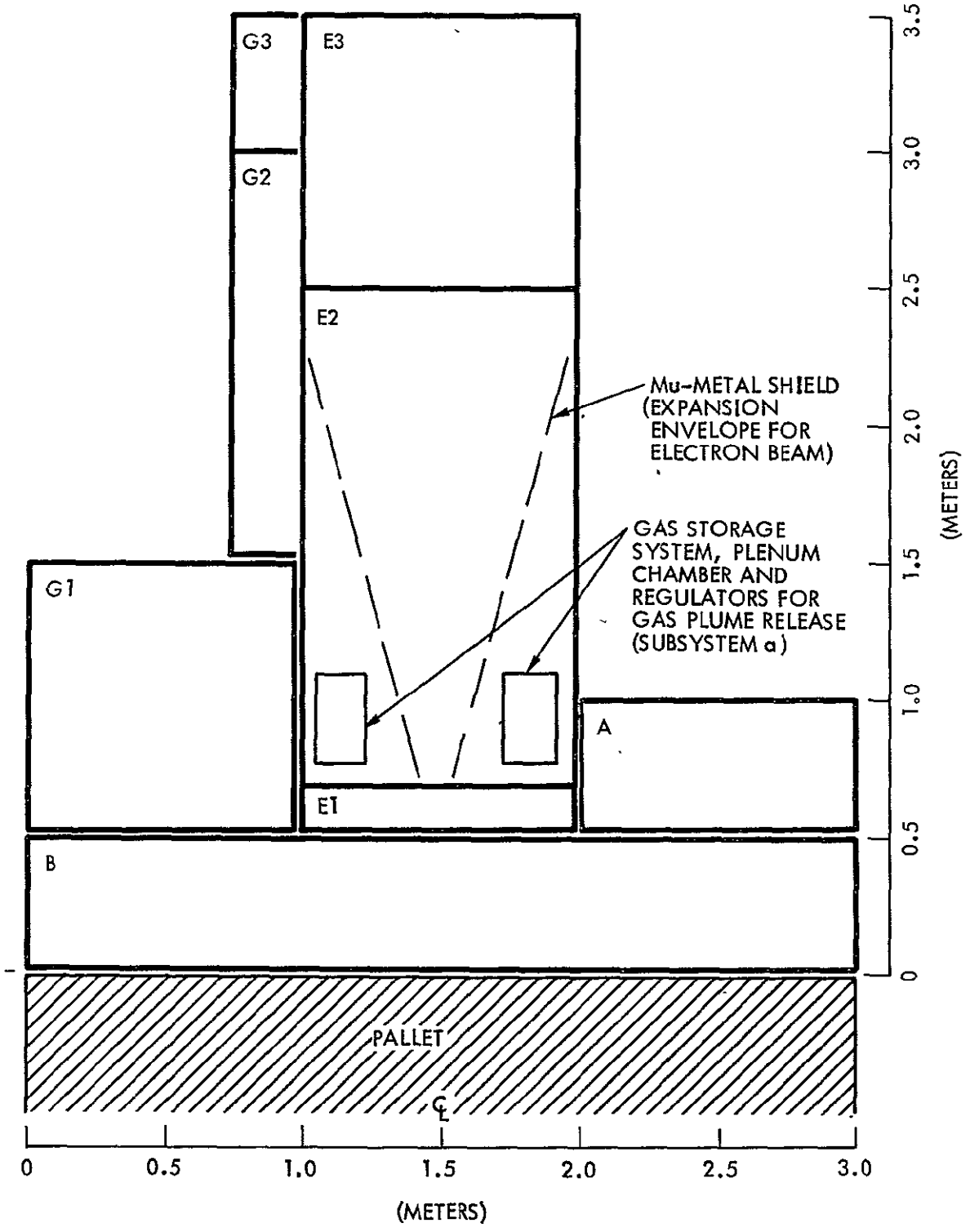

Figure 22. AMPS Particle Accelerator System (X-Axis View Looking Foward) with Gas Plume Release System Installed.

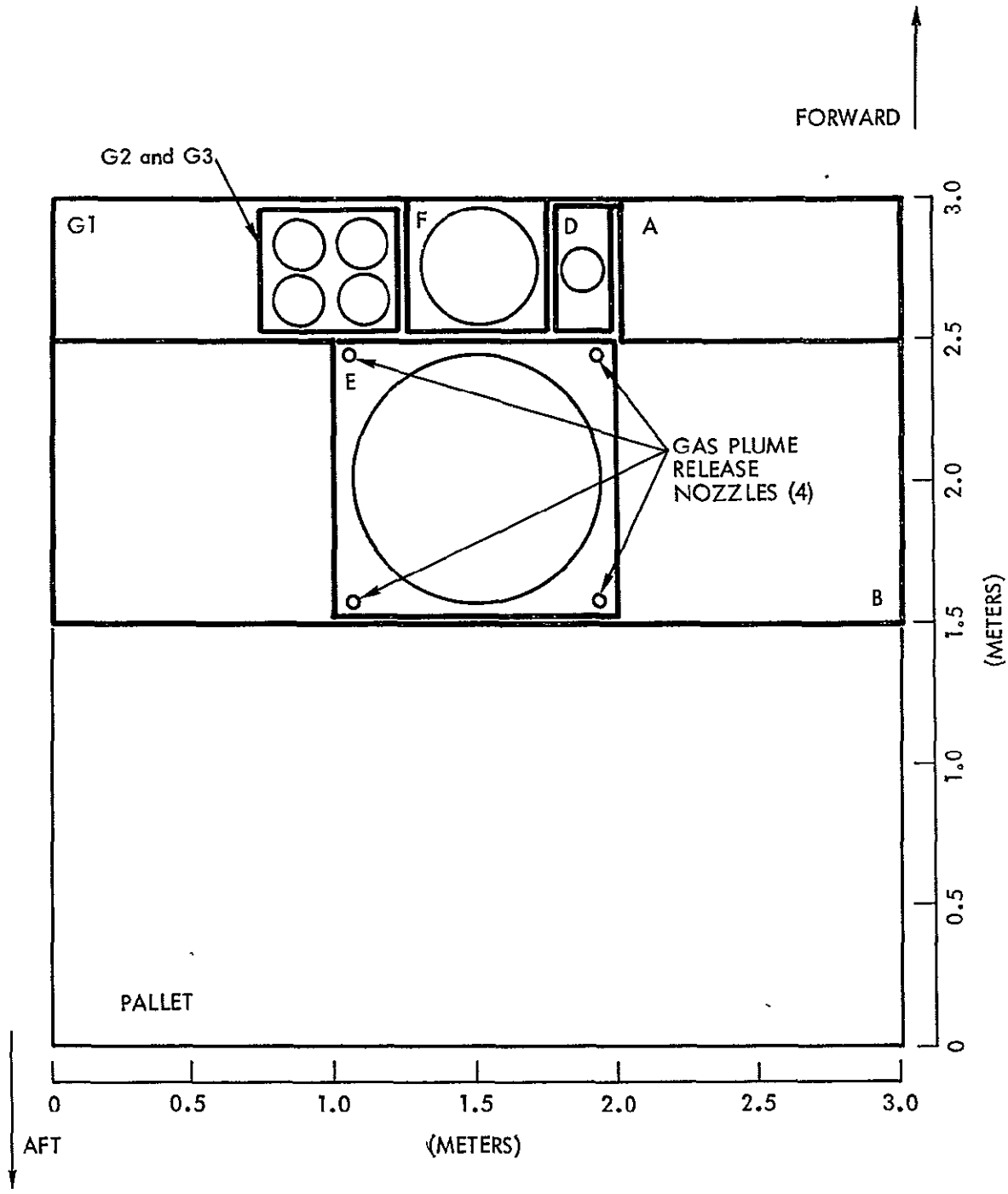

Figure 23. AMPS Particle Accelerator System (Z-Axis View Looking Downward) with Gas Plume Release System Installed.

Possible problems in the use of the gas plume release include plasma generation in the gas plume to that point where electron beam-gas plume generated plasma interactions dominate the total flow process.

While the Level I diagnosis is not a complete beam characterization, its simplicity, speed of operation, and lack of ancillary system requirements make it an attractive system candidate. Electron beam deposition experiments for artificially generated aurora could, for example, be adequately diagnosed by this process.

The Level II diagnostic group consists of three instruments: a Faraday Cup, a Retarding Potential Analyzer, and a probe for measurements of exhaust beam plasma potential. Level II (and also Level III) instruments require the use of either the Remote Manipulator System or a deployable boom. Level II (in combination with Level I) provide a complete characterization of the electron and ion beams (because of energy densities and possible current circulation processes, both high and low voltage plasma gun diagnosis will utilize other instruments).

The Faraday Cup scan of the electron beam can proceed either through a stationary beam with point-to-point movement of the Faraday Cup, or stationary positioning of the Faraday Cup and movement of the beam. The X-Z and Y-Z magnetic deflection coils (Subsystem E3) can provide a rapid 2-D scan of the beam so that total current density two-dimensional current flow patterns can be determined with a single beam burst of the electron accelerator. For movement of the probe, a much larger number of bursts will be required, consuming both time and available energies.

The Faraday Cup probe diameter has been placed at 10 centimeters. This selection limits possible characterization of "pencil" beams, but is quite acceptable for "broad" (1 meter diameter) beams. For pencil beams, several diagnostic problems will be the stability of the boom tip in positioning the Faraday Cup and beam motion during the burst. The diverging and converging electrostatic lens system (Subsystem E2) of the electron accelerator has the capability of adjusting electron beam exit diameter from some as yet undetermined minimum value to approximately 1 meter in diameter. For experiments on interation between the electron beam and the ambient space plasmas, variation of beam diameter will be desirable.

The present selection of Faraday cup diameter at 10 centimeters establishes a lower limit on characterization ability of narrow beams (although very narrow beams may still be characterizable through the Gas Plume Release).

The Faraday cup characterization of an ion beam would have to be achieved by point-to-point motion of the probe with repeated bursts from the ion accelerator, since magnetic 2-D scanning of these high momentum particles is not included in the present AMPS accelerator system concept.

The Retarding Potential Analyzer determines particle acceleration energy in both electron and ion beams. Listed resolution of this instrument is $\Delta E/E = .01$. For growth versions of the Diagnostics package, either an increase in resolution could be carried out, or there could be substitution (or addition) or an electrostatic analyzer.

The Cold Probe provides a measure of exhaust beam plasma potential. By appropriate use of the probe and also by insertion of the probe into the ambient plasma, Orbiter charge build-up during electron beam release can be monitored. The probe can also determine the effectiveness of the neutralization of the ion accelerator beam.

The Level II Probe Group is mounted on a 2-meter Boom capable of stowage alongside the pallet in the Orbiter Bay. Insertion of the Probe Group into the beam is accomplished using the Remote Manipulator System. Defining the axis of the Electron beam at the beam exit plane as $X' = X' = Y' = Z' = 0$, the Probe Group movement should be within a volume defined by

$$0 \leq X' \leq 5 \text{ meters}$$

$$0 \leq Y' \leq 5 \text{ meters}$$

$$0 \leq Z' \leq 10 \text{ meters}$$

The Probe Group should also be capable of movement for insertion into the ambient space plasma. Cables and connectors from the 2-meter boom end to an Orbiter readout will not be specified here.

The Level III diagnostic group provides measures of dB/dt, $E(t)$, and $V(t)$. These measurements would be required in experiments on the interaction of the electron beam with the ambient space plasma (or, at

sufficient densities, of the plasma formed in the gas plume release-electron beam excitation). The instrument package here requires deployment, through the RMS or a dedicated boom system. The up-rating of the resolution of the Retarding Potential Analyzer (or the addition of the Electrostatic Analyzer) in the Level II group also provides a diagnostic instrument for Level III applications.

Diagnosis of the MPD arc plume and the High Voltage Plasma Gun plume will not be treated in this study.

10.0 SPACECRAFT CURRENT AND CHARGE NEUTRALIZATION

Section 8.8.2.1 has discussed aspects of spacecraft charge-up as a result of release of large currents of electrons from the electron accelerator. Discussion in this section will review possible methods for alleviation of this charge-up.

Four possible methods to achieve a current balance (zero net rate of charge release) on the spacecraft are (1) collection of a return current of ionospheric electrons on conducting portions of the Orbiter surface, (2) release of a current of ions equal to the current of released electrons in the accelerated beam, (3) collection of electrons from the ionosphere on a remote collecting "sail", connected by a conductor to the body of the Orbiter, and (4) creation of ion-electron pairs by electron beam passage through a gas plume, with collection of electrons from these pairs back to the Orbiter with the ion portion of the pair left behind in the ionosphere. Each of these methods has possible operational problems.

Method (1), collection of electrons by conducting portions of the Orbiter surface in contact with the ionosphere, may not be effective in view of the comparatively small area of Orbiter surface which is conducting, and because of plasma wake effects for bodies orbiting in the lower ionosphere. The release of large ion currents, Method 2, also poses problems. The energy required to generate and release these ions impacts on available energy for AMPS payload operation. Ampere levels of ion generation and release are required in the ion accelerator portions of the payload. This is, however, a major subsystem of the particle accelerators. Operations of similar systmes for ion expulsion alone is a costly requirement.

Method (3), collection of electrons by a remote conducting "sail" offers many other experiment possibilities. It requires, however, the release of a tethered object from the Orbiter which requires, in time, a complete satisfaction of all hazard aspects of the cable and sail relative to the Orbiter. It should be emphasized that AMPS requires frequent reorientation of the spacecraft to carry out its experiments. This reorientation could be severely hampered by the tether and collecting sail.

The final method, (4), of a gas plume release has several possible uses which have been discussed in Section 9, including beam diagnosis. The potential problem in the plume as a current balance mechanism is in the dynamics of the released, created, and collected charge. Energetic electrons, accelerated in the electron gun and released to space, move to distances in space very distant, in general, from the Orbiter. The ion-electron pair, formed by electron impact on the gas plume must allow its electrons to be collected by the Orbiter to set up a current balance. This leaves the ion portion of the ion-electron pair in the ionosphere but near the Orbiter while the electron "mate" is now distantly deposited. This large separation of charge should result in current flows in the ionosphere. It has also, however, resulted in an ionosphere electrically imbalanced to some degree, and this may, in turn, impact on the validity of certain experiments. There is no positive assurance, moreover,that the Orbiter can collect the electron portion of the ion-electron pair created in the gas plume without itself maintaining some state of charge-up since two positive charges, one in the Orbiter and the other in the gas plume, are in competition for the created electron. In spite of these possible problems, however, the gas plume release offers the simplest possible solution to charge-up, and since it has other potential applications, its inclusion in the accelerator payload is recommended.

11.0 GROWTH MODES AND INITIAL SYSTEM CONFIGURATION

Table 10 has listed growth modes for the AMPS accelerator system, and discussion in the various sections have treated developed mission effectiveness as it derives from system expansion. The principals of modularity for the elements of the accelerator system have also been described. This section will consider an initial accelerator system

version with total weight less than 1000 pounds, but which has elements at meaningful size power and energy levels and can be expanded into the system illustrated in Figure 9. This initial system would consist of a first stage power processor at 1.5 kilowatts, a capacitor storage bank rated at 67 kiloJoules storage and 50 kiloJoules energy transfer per burst capability, a 50 kilowatt second stage processor, an electron accelerator with control grid modulation of the output beam plus divergence, refocusing and deflection stages, a gas plume release, and Level II and III beam diagnostic groups. Table 17 summarizes these elements.

12. SUMMARY

Table 18 provides a summary of the areas examined in the AMPS Particle Accelerator Facility Study. The initial aim of the study was to develop a series of system design criteria. These criteria recognize constraints and limitations in the Orbiter flight and advance, for exploitation, the unique advantages in the Shuttle/Orbiter System. These constraints, limitations, and opportunities have been defined. The system design criteria also require the execution of a broad spectrum of mission objectives, and both monitoring and modification missions have been identified.

The requirements for both monitor and modification missions have been derived and common areas of performance in these missions have been identified. Mission effectiveness as a function of time has been postulated for both missions, and, by pursuit of both sets of mission goals, a continued high mission effectiveness will be realized. To obtain continued effectiveness requires facility growth and this has been recognized in the system design criteria.

A requirement for particle beam power in excess of allowable fuel cell power leads to a required energy storage and transfer stage. Both single tier and dual tier power processing configurations involving the energy storage unit were examined and a dual tier power processing arrangement was adopted using a midrange voltage energy storage unit.

The study then advanced a total particle and plasma accelerator facility listing elements and sub-elements, and estimating weights and volumes. This system design incorporates another of the system design

ELEMENT	WEIGHT (POUNDS)
First stage power processor (PPUI) (1.5 kilowatts)	30
Capacitor Bank, 67 kiloJoule storage, 50 kiloJoule per burst transfer	500
Capacitor Cabling, Diodes, Enclosures	100
Second Stage Power Processor (PPUII)	120
Electron Accelerator; Cathode, Cathode Heater, Grid Drive, Diverging Lens, Divergence Section, Converging Lens, Output Deflection Coils	125
Gas Plume Release	25
Level II Diagnostic Group	30
Level II Diagnostic Group	20
Controls, Wiring, Readouts	50
Total	1000

Table 17. Elements and Sub-Elements of an Initial Version of the AMPS Electron Accelerator.

criteria in its common usage of the major mass and volume elements of the payload for a variety of particle accelerators, and plasma guns as well as other possible high power payload elements on AMPS. This common usage allows for a broad range of mission objectives without costly retrofit or system reinitiation.

The energy storage unit of the particle accelerator system may utilize capacitors or batteries. The study evaluated performance of both systems, including hazards associated with the energy storage, and concluded that capacitor bank storage offers a better overall performance. The beam power-burst duration "corridor" allowed by the capacitor bank and the fuel cell encompasses a large number of monitor and modification mission experiments. Capacitor bank storage is also modular, satisfying a system design criteria for modular expansion capability from initial system configurations into the growth mode versions of these systems.

The initial and final stage power processors in the dual tier configuration were examined and found to match to the beam power-burst duration requirements of the combined mission mode. The power processor modularity also matches to capacitor bank modularity so that both systems permit expansion.

The study next examined electron beam system requirements for acceleration voltage, voltage modulation, beam current, current modulation, beam angular divergence, beam pitch angle and pitch angle modulation for both monitor and modification missions. These beam requirements have been summarized and open the possibility of a satisfaction of requirements in both missions by a single electron beam system. A proposed system has been described and the operation of that system and the operation of the Orbiter jointly examined for interactive effects: A series of electron beam performance parameters have been recommended.

The diagnosis of the electron beam has been treated at three levels whose elements have been described and for which estimates of weight and volume have been made. Time-saving diagnostic approaches in the determination of beam current density patterns have been derived. Orbiter charge-up mechanisms during electron beam release have been examined, and a series of methods for reduction or elimination of this charge-up have been proposed.

From these several areas of the system study, an initial electron beam system, including power processing stages, energy storage units, and beam diagnostic elements has been described. This initial system at an estimated 1000 pound weight satisfies the system design criteria for capability of expansion into the growth modes of the accelerator. The successful verification of the system unity by in flight operation, and the modular expansion capability would provide for continued system growth at minimum cost per growth.

In conclusion to this study, the particle accelerator system which has been derived provides an excellent opportunity for the pursuit of the classical problems of space physics as well as for the extension of the understanding of that space by new and exciting methods and capabilities. The capability for system expansion allows for an orderly, cost effective, growth through the decade of AMPS space explorations.

APPENDIX A1

DESIGN CONSIDERATIONS FOR A HIGH CURRENT HIGH POWER ELECTRON BEAM FOR THE PLASMA PHYSICS AND ENVIRONMENTAL PERTURBATION LABORATORY

J. M. Sellen, Jr., and N. L. Roy

APPENDICES

DESIGN CONSIDERATIONS FOR A HIGH CURRENT HIGH POWER ELECTRON BEAM FOR THE PLASMA PHYSICS AND ENVIRONMENTAL PERTURBATION LABORATORY

1.0 INTRODUCTION

A previous document[1] has outlined general design criteria and potential problem areas for the high power electron, proton, and plasma guns on PPEPL. This present discussion will focus attention on the electron gun of that array, and will outline a specific configurational approach for that accelerator. In this approach, a crucial parameter has been the level of ejected current. The design goal is 1 ampere of electron flow at a minimum acceleration energy of 10,000 volts. Of equal importance is the desired limitation on total angular spread of the ejected electrons. The design goal here will be a full width of 5° in electron angular divergence. If these design goals can be realized, the PPEPL electron accelerator will be approximately two orders of magnitude more intense in phase space density than previous electron release devices utilized in space experiments. These increases in ejected current and in directional specification of the electrons should provide for a broad range of vital new experimentation for electron beams in the space environment.

2.0 SPACE CHARGE CONSIDERATIONS

A 1 ampere beam of electrons at 10,000 volts acceleration potential and with a beam diameter of 2 centimeters will have an electron density, n_e, in electrons/cm^3 of

$$n_e = \frac{I_b}{e v_e A_b} = \frac{1}{1.6(6)\pi} (10)^{10} \frac{\text{electrons}}{\text{cm}^3} \qquad (1)$$

where I_b is beam current in amperes (=1), $e = 1.6 \times 10^{-19}$ coulombs, v_e is electron velocity ($=6 \times 10^9$ cm/sec), and A_b is beam area in square centimeters ($= \pi$). The space charge forces in this "unit perveance" beam are very large and beam divergence will occur as a result of the radial space charge field. For the listed electron current and voltage the aspect ratio of this beam is 0.74, using the notation of Ref. 2, and the final total divergence angle for an (assumed) initially parallel flow will be approximately 50°. (See Ref. 2.) Since many of the possible space applications

of the electron beam require angular specification almost an order of magnitude less than this 50° figure, the usefulness of such a beam would be questionable.

To diminish the space charge spreading the beam current could be diminished. However, it is possible that some experiments will demand ampere levels of electron release signal. An alternative approach is to use the space plasma electrons and ions as a neutralizing background for the beam electrons. Reference 1 has outlined considerations on electron mobility in the space plasma which make the "space plasma" nuetralization approach an appealing possibility. For this possibility to be realized, however, will certainly require, at the minimum, that beam electron density be less than space plasma electron density. Since $n_e = 3 \times 10^8$ electrons/cm^3 in the example of Eq. (1) and since space plasma electron density is, at the most, = 10^6 electrons/cm^3, some procedure will be required by which the beam electron density can be reduced by, at least, three orders of magnitude while maintaining the 1 ampere level of electron flow and while maintaining total angular divergence within, say 5°. Two possible approaches to this electron beam "dilution" will be considered here.

In the first approach the total beam is formed by the operation of a large number of sub-beams. For example, 10 sub-beams operating at 0.1 ampere per beam would make up the total 1 ampere of beam current. These sub-beams would be distributed over an area of $\simeq 10^4$ cm^2 and, after merging by separate expansion of the sub-beams, beam electron density in Eq. (1) would be approximately 10^5 electrons per cm^3. This beam density level would satisfy the criteria $n_{eb} < n_{esp}$ where "b" and "sp" denote beam and space plasma. Such an electron gun configuration is described in Ref. 3. However, it should be noted that electron densities in the sub-beams are initially at levels of almost 10^8 electrons per cm^3, even for a 10 beam array, and beam expansion forces will result in total angular spreading of $\sim 10°$ before beam merging and immersion in the space plasma can occur. There are, moreover, many operational aspects which may be expected to become more difficult as the number of sub-beams is increased. Diagnosis of the beam and the specification of its parameters will certainly become more difficult. Gun-to-gun variations may cause graininess in the

overall beam which results in further particle trajectory bending. Beam modulation may be expected to require more complicated electronic systems when separate modulation of many beams is required to produce overall beam variations. For these several reasons, an alternate beam approach was utilized.

In the second approach to beam dilution, a single electron gun is employed. The outlet beam for the gun is expanded in a drift section and is then refocused, using electrostatic lenses, so that the resulting beam emerges over a broad area but with only a narrowly diverging flow. In the example which will be treated here, the beam diameter at the gun exit is 2 cm and, following expansion and refocusing, is 50 cm. For this beam, $n_{eb} = 4 \times 10^5$ electrons per cm^3, which may be acceptably small compared to n_{esp} to allow propagation without any further beam divergence. The advantage of the single gun approach is in simplicity in beam control and beam specification. The added complexities are the required electron drift tube, and the refocusing electrostatic lens. The refocusing lens, however, would appear to be a very worthwhile addition to the overall beam system. Operated for focus conditions at infinity, it produces a narrowly divergent electron flow into the space plasma (hopefully within the total divergence angle of 5° given earlier as a desirable operating condition). Furthermore, by varying the focus condition of this lens an angular spreading modulation may be introduced into the total beam. This property opens up new possibilities for experiments with beams in the space environment.

3.0 OVERALL ELECTRON BEAM SYSTEM

Figure 1 illustrates in block diagram the elements of the overall beam system. Electrons are generated at the cathode of the gun and are modulated there by a gridded electrode. The gun acceleration on the current emerging past the modulation grid raises the electrons to 10,000 electron volts. The next element is the diverging electrostatic lens. This element may not be required, however, if an alternative approach is found to be feasible. In the alternative approach, the acceleration fields for the gun accelerator are shaped so as to produce an initially diverging conical beam with sufficient beam angular width to fill up the exit plane of the refocusing electrostatic lens. The refocusing lens returns the

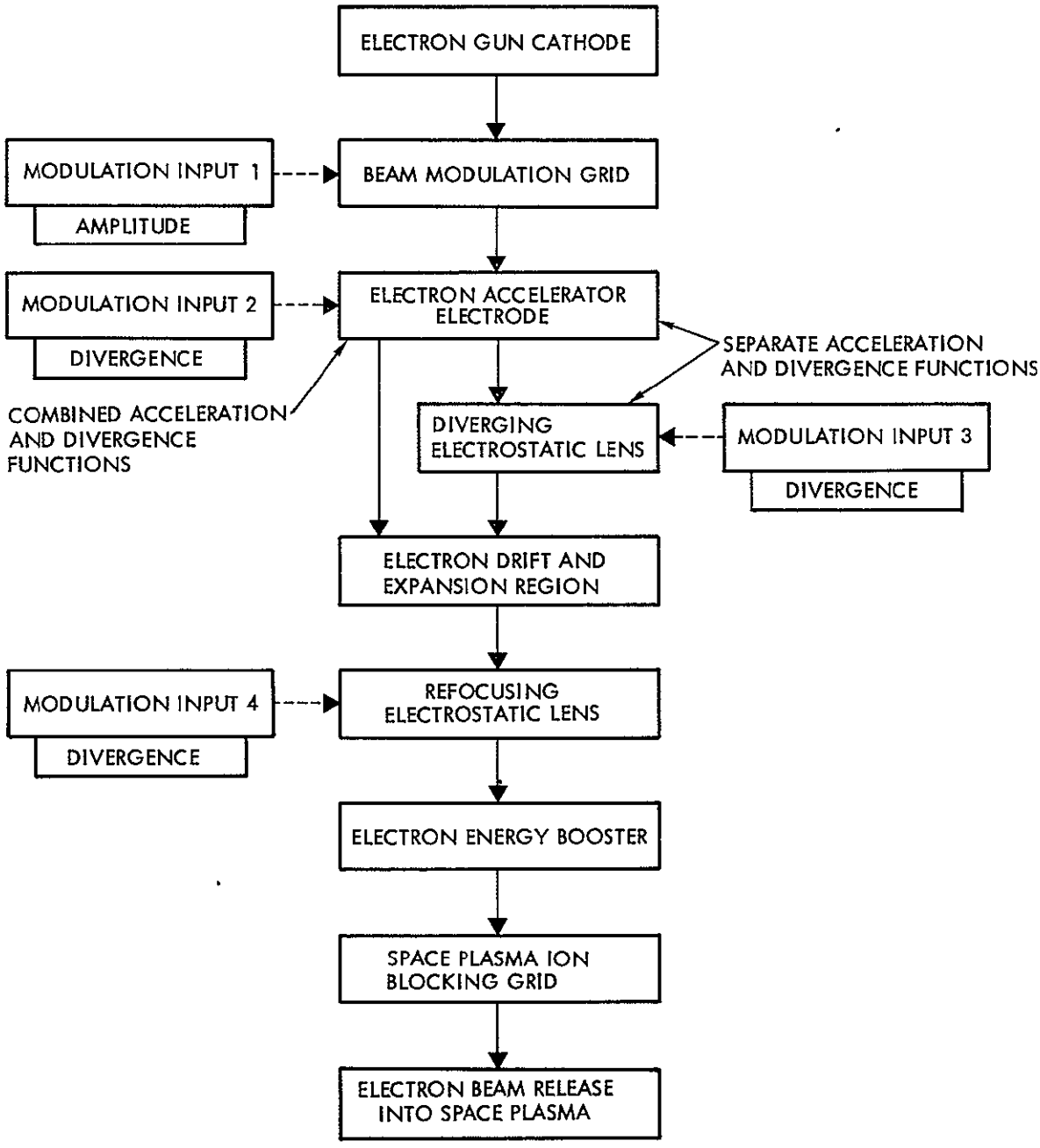

Figure A1-1. Block Diagram of Elements of Overall Electron Beam System.

flow to an axial parallel beam which enters the booster stage where post-acceleration occurs if electron energies in excess of 10,000 eV are desired. A final section of the electron beam system electrostatically blocks out space plasma ions which would damage the gun cathode if allowed to flow upstream.

Several modulation inputs are indicated on Figure 1. Modulation input is applied to the beam modulation grid and determines the amplitude of the accelerated current. If this beam enters the diverging electrostatic lens and electron drift regions, the varying intensity of space charge forces (due to variations in beam magnitude) would result in divergence variations and beam width variations at the output of the electron expansion region. If these variations lead to eventual beam changes outside of acceptable variance limits, then modulation of the lens actions in the diverging lens and in the refocusing lens may be required. If the electron acceleration and divergence functions are combined, a separate modulation of the gun electric fields near the exit may be required to counteract the amplitude coupled beam divergence modulations. Finally, through modulation introduced into the refocusing lens, the final beam angular width may be varied.

Two major criteria have been active in the selection of this present configuration. The first criteria is that a single source - high current - low density electron beam be capable of generation within a narrow final angular beam width. The second criteria is that the system should not exclude future possible growth modes.

One of the major growth modes for future systems is in electron beam energy. By placing the beam generation, modulation, and dilution functions prior to the final acceleration stage, the growth in electron energy through final booster setting is conveniently exercised. A second growth mode is in the forms and extent of beam current modulation. By utilizing beam modulation at the cathode, power requirements in modulation are at minimal values and growth in additional modes of beam modulation are easily attainable. Finally, a growth mode in the variation of beam angular width is present in the modulation action of the refocusing lens.

What is realized, then, in the overall sense is a high current (diluted density) electron flow with good angular collimation for a broad range of presently visualized space experiments, and a system capable of growth in several important beam parameters for additional possible ranges of space plasma experiments.

4.0 BEAM PROFILES IN THE ELECTRON EXPANSION REGION

The expansion region of the overall system is required to produce a diluted beam electron density. Since electron trajectory bending should not proceed beyond 20° to 30° of divergence angle of an electron relative to the beam axis, a certain axial length is required in this expansion. Figures 2 and 3 illustrate the beam radius as a function of axial distance for several conditions. In Figure 2, the beam radius is given for lens action on a very dilute beam with maximum bending of $\sim 5°$ by the lens. Also shown on Figure 2 is the beam radius for a 1 ampere of 10 keV electrons subject to the initial lens action and to space charge spreading. Large variations of beam width and beam divergence angle are obtained here between the $I_b = 0$ and $I_b = 1$ ampere case. These beam variations are not desirable when modulation of the electron flow level is to be utilized (simple ON and OFF modulation may be acceptable, provided that switching times are short compared to the periods of interest in the experiments). Note that if the refocusing lens is set to produce a parallel flow for the 1 ampere case, that the $I_b \to 0$ case would be strongly over-focused, and, if beam amplitude modulation were employed, comparatively large variations in beam angular width would result.

Figure 3 illustrates three cases. The first of these is a 1 ampere flow in expansion and with no initial lens action. A second curve is this same 1 ampere flow subject to both space charge and an initial defocusing action (15° maximum trajectory bending). Also shown is the beam profile for $I_b \to 0$ and a lens action of 15° maximum bending. As may be noted here, only modest variations occur between $I_b = 0$ and $I_b = 1$ ampere with the lens action present. Hence, the final output beam will exhibit little angular modulation as a result of beam amplitude modulation (and, even this minimized variation may be further minimized by appropriate signals on modulation inputs 2, 3, or 4 of Figure 1). What is required,

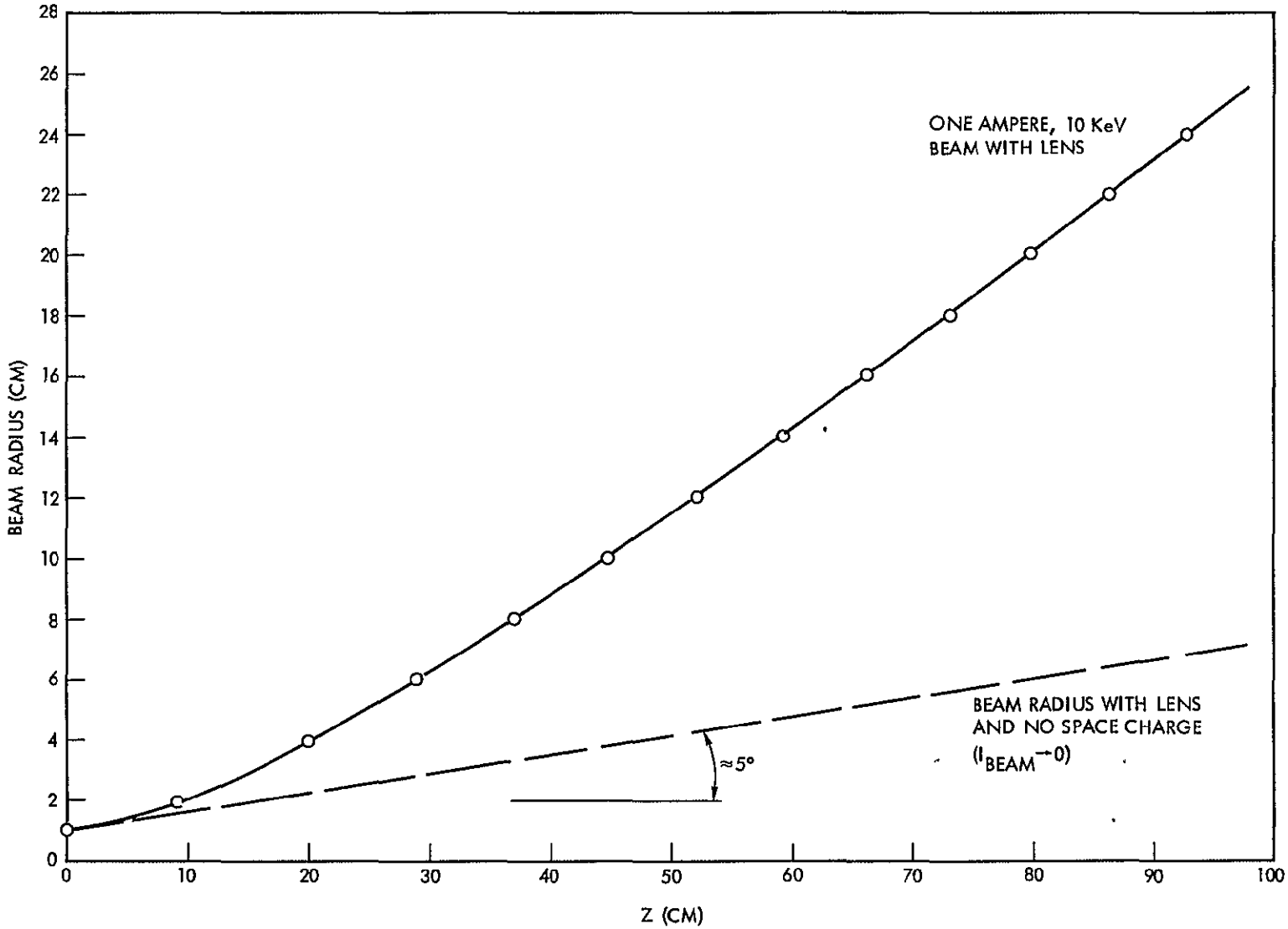

Figure A1-2. Outer Beam Radius as a Function of Axial Position with 5° Lens Action.

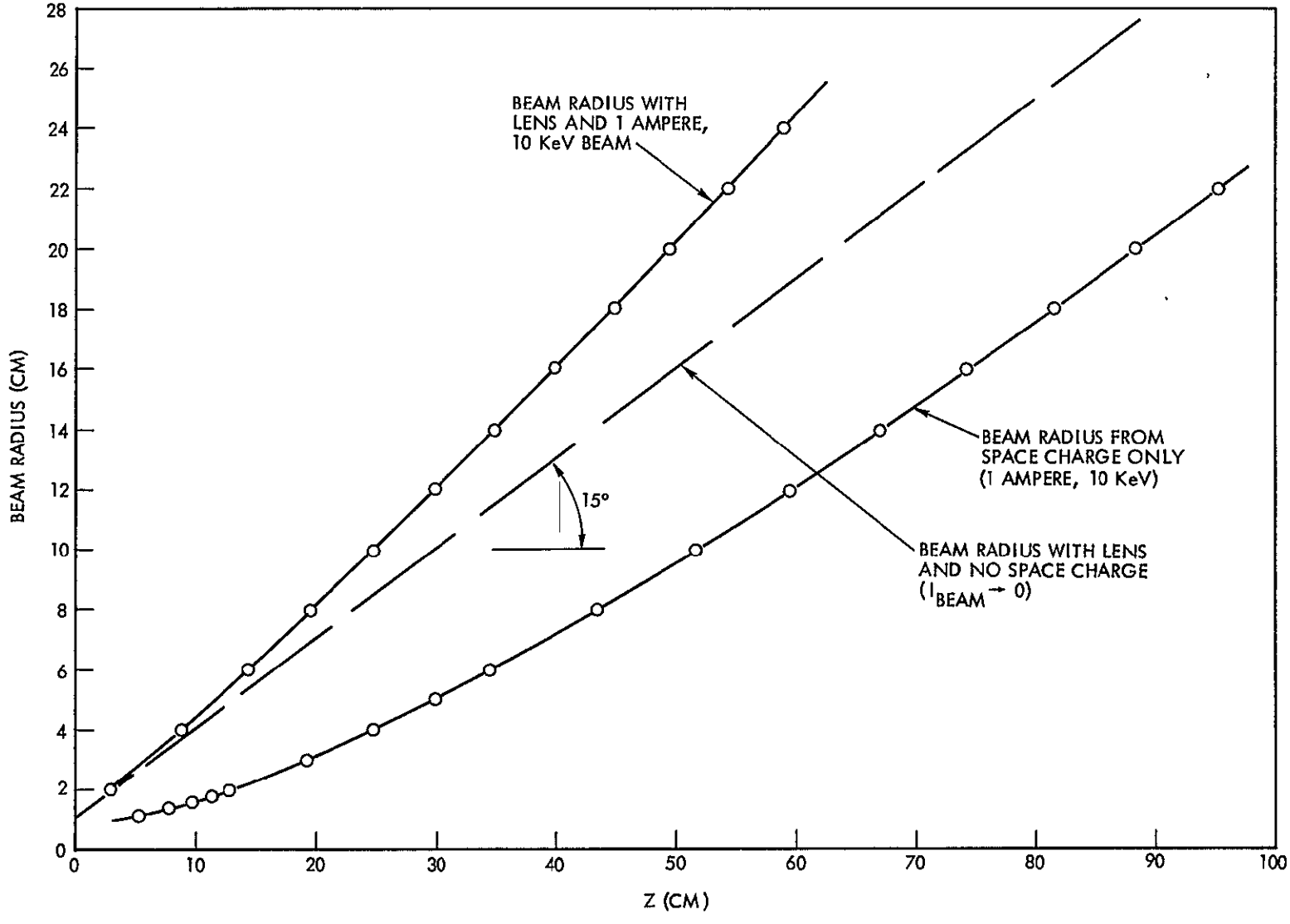

Figure A1-3. Outer Beam Radius as a Function of Axial Position with 15° Lens Action.

then, is sufficient electrostatic action to provide approximately 15° bending of the outer edge of the beam (with proportionate interior bending). This may be obtained through either the diverging lens or through deliberate production of a conically expanding beam through shaped accelerator electrodes. With these input conditions, sufficient beam dilution will be obtained in approximately 1 meter of axial drift.

A final note relates to total angular spread in the output beam. The total angular spread of particles entering the refocusing lens for the conditions of Figure 2 (1 ampere beam plus lens action) is ∿ 50°. To reduce this divergence by one order of magnitude in the refocusing action is required if 5° total width is to be realized in the exit flow. To achieve this optical quality in an electrostatic lens in the presence of space charge is, we believe, possible. However, a gridded electrostatic lens system will be required, we believe, for more accurate determination of the lens fields in the midst of the electron flow. Appropriate system testing and electrode shape reconfiguring will also be required, to ensure that all portions of the electron flow are refocused to infinity within the previously specified angular range.

5.0 SYSTEM CONFIGURATION AND POSSIBLE PROBELM AREAS

The required axial length for expansion, refocusing, and the electron boost stage may be estimated at ∿1 meter for each of these functions for a combined system length of between 2 and 3 meters. The diameter may be estimated to be somewhat less than 1 meter. While these dimensions are large, the required structures are not massive so that the principal system problem is one of size. Since the pallet in the PPEPL can accommodate lengths in the minor direction in excess of 4 meters, system size is not considered a problem area. It should be noted that beam direction from this system is determined by adjusting the PPEPL orientation. Minor variations in beam axis direction may be possible if an additional electrostatic lens is provided. To this point, the systems study has not included such final stage beam axis variations.

An earlier discussion[1] has treated possible problem areas in the operation of the PPEPL particle accelerators. That earlier treatment

remains valid. In addition, a specific problem must be considered for this proposed configuration. That problem relates to the required immersion of grids into the electron flow. A modulation grid is present to modulate current flow from the cathode. The acceptable power dissipation figure for this grid will establish permissible ON times and permissible ON current levels. A grid is immersed in the flow at the refocusing lens and at the output of the booster stage. Electrons striking these grids will emit soft X-rays. The magnitude and spatial distribution of these X-rays must be determined.

In the area of beam-plasma instabilities, both wave-particle interactions and total beam motion unstable modes must be investigated to determine if such intense parallel electron flows will propagate to distant points in the space environment. These studies and those related to beam interception on immersed grids are continuing.

6.0 SUMMARY

A high current high power electron beam has been configured so that exit beam density is small compared to space plasma electron density. The principal mechanism for continued propagation of these high current beams without disruption would be a neutralizing action by the space plasma sufficient to prevent space charge blow-up of the ejected beam. In this regard, the presence of the space plasma ion provides space charge neutralization for the beam electron, and the mobility of space plasma electrons is, hopefully, sufficiently fast to prevent unstable space charge wave growth in the accelerated beam (the hope here is to limit the growth rates for instabilities in the beam; clearly, space plasma electron thermal speed cannot follow beam-transported electron acoustic waves). The beam-in-plasma instabilities and appropriate wave particle interactions are currently under study.

The configuration of the electron beam calls for a single gun followed by an expansion stage and a refocusing stage. If lens action in the refocusing stage may be made to be sufficiently invariant over the total flow, the phase space density for the ejected electrons may reach some two orders of magnitude in excess of previously realized electron beams for space experimentation.

REFERENCES

1. "An Outline of Problem Areas for the PPEPL Accelerator Package," J. M. Sellen, Jr., October 2, 1972.

2. "Space Charge Measurements in Expanding Ion Beams," J. M. Sellen, Jr., and H. Shelton, presented at the ARS Semiannual Meeting and Astronautical Exposition, Los Angeles, California, May 9-12, 1960. ARS Preprint 1160-60.

3. "Electron Accelerator for Aerobee 350 Rocket - Description, Development, and Flight Performance," William G. Beggs, Final Report, Contract NAS5-9326, Ion Physics Corporation, Burlington, MA., 30 November 1970.

APPENDIX A2

POWER PROCESSING SYSTEM FOR ION AND ELECTRON PARTICLE EXPERIMENTS FOR SPACE SHUTTLE

J. J. Biess

POWER PROCESSING SYSTEM FOR ION AND ELECTRON PARTICLE EXPERIMENTS FOR SPACE SHUTTLE

1.0 INTRODUCTION

A preliminary study of the power processing system for particle experiments has been performed in shuttle applications. An attempt has been made to establish a base line power processor system configuration, to establish interface requirements, to estimate equipment characteristics and to identify a possible power processor technology problem area.

2.0 SYSTEM CONFIGURATION

Figure 1 represents the proposed power processor system configuration in support of the projected planned experiments.

28VDC power from the shuttle fuel cell is processed by a charger system that has a maximum power limit of 1.5KW in order to prevent any power surge transients from being reflected to the shuttle power system and to match the shuttle power system interface. The charger provides input/output ground isolation in order to eliminate any possible transients in the shuttle power system during the high energy pulsing of the experiments or possible arc-over of the energy storage system.

The energy storage system can be either high energy density capacitors or storage batteries. The charger can be designed to be compatible with either type of energy storage system. Preliminary analysis shows that the high energy density capacitors may be the lowest weight energy system that would be compatible with the expected experiment loads.

The 250 to 500VDC voltage of the energy storage systen is further processed by the high voltage DC to DC Converter System. The high voltage converter system can be commanded to provide the variable output voltage for the experiment and the necessary regulation and output ripple so that meaningful experiment results can be obtained. The high voltage DC to DC converter system has input/output ground isolation to prevent ground loop currents that can flow when there are shorts in the high voltage experiment.

All of the power processor technology is within the present state of the art and no extensive circuit development is required.

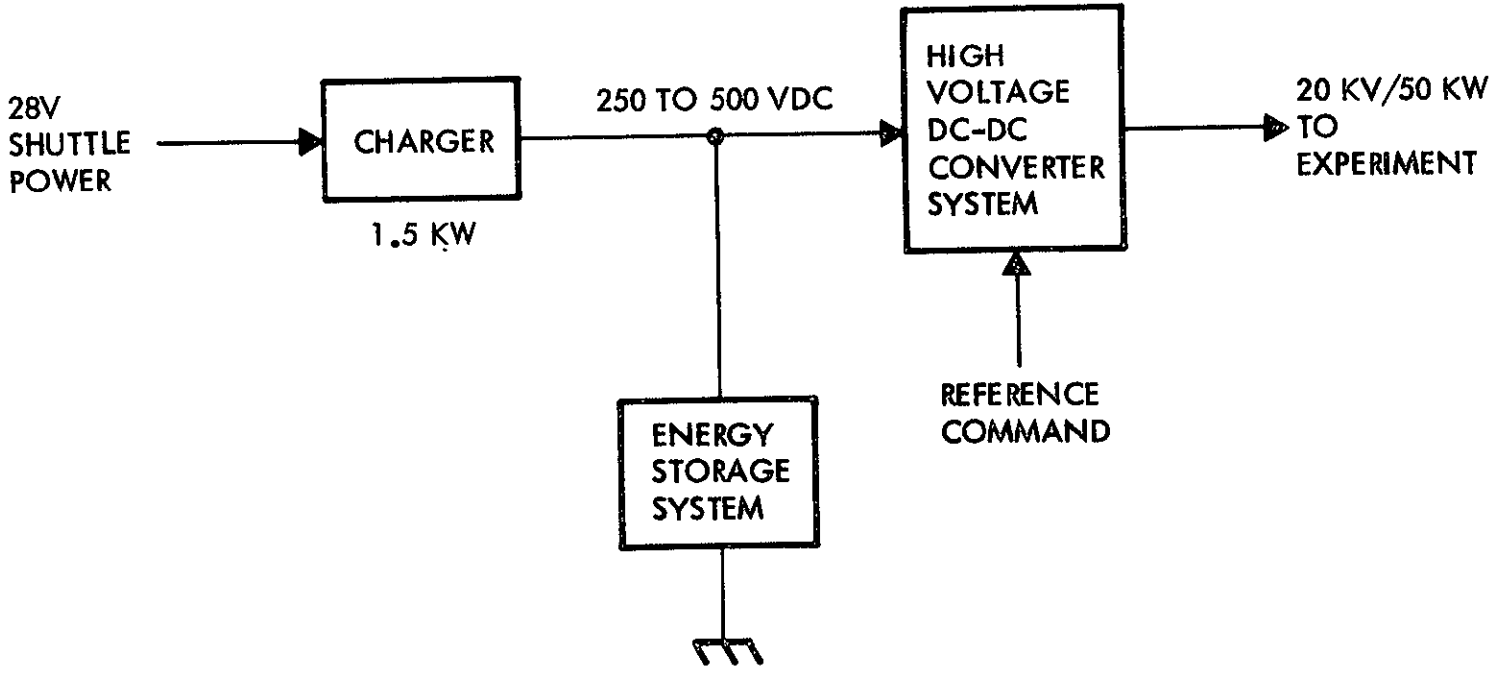

Figure A2-1. Particle Experiment Power Processing Block Diagram.

The power processor system will use the shuttle thermal control system to ensure minimum power processor weight.

3.0 CHARGER

The charger uses transistor power processing technology to provide the necessary current limiting and voltage regulation. With the 28VDC input, the power transistor used as a switch provides the maximum charger efficiency. Three parallel modules are used to obtain the 1.5KW power rating due to the power transistor power limitation and to ensure reliable semiconductor operation.

Preliminary estimates of the charger equipment characteristics when using the shuttle thermal control system are 12 KG weight and 85 percent efficiency. Tradeoffs can be made between weight, efficiency and thermal control systems to further optimize the system.

4.0 DC TO DC HIGH VOLTAGE CONVERTER

The DC to DC high voltage converter will use the LC series resonant inverter with thyristor or Silicon Controlled Rectifiers (SCR) as the switching power semiconductor. The 50KW power stage will use two parallel modules to obtain the power rating with the present state of-the-art components.

The LC series resonant inverter power stage has been under development for application in the primary ion propulsion power processing system. The series resonant is a current source power stage that provides the protection of the power components and power source during startup and ion engine internal arcs. Due to the nature of the series resonant inverter, sinewave current flows in all of the semiconductors and therefore allows high frequency operation without the attendant switching power losses and electromagnetic interference common to squarewave current operation.

The series resonant inverter is used as the basic AC inversion stage and as a means of matching the 250-500VDC input DC power to the output power and voltage requirements of the ion thruster. The basic series resonant converter circuit is shown in Figure 2. It consists of two SCR's, SCR1 and SCR2, two identical inductors each with an inductance L, two identical capacitors each with a capacitance C, an output transformer T, a diode bridge, and a current-averaging capacitor filter C1. When an

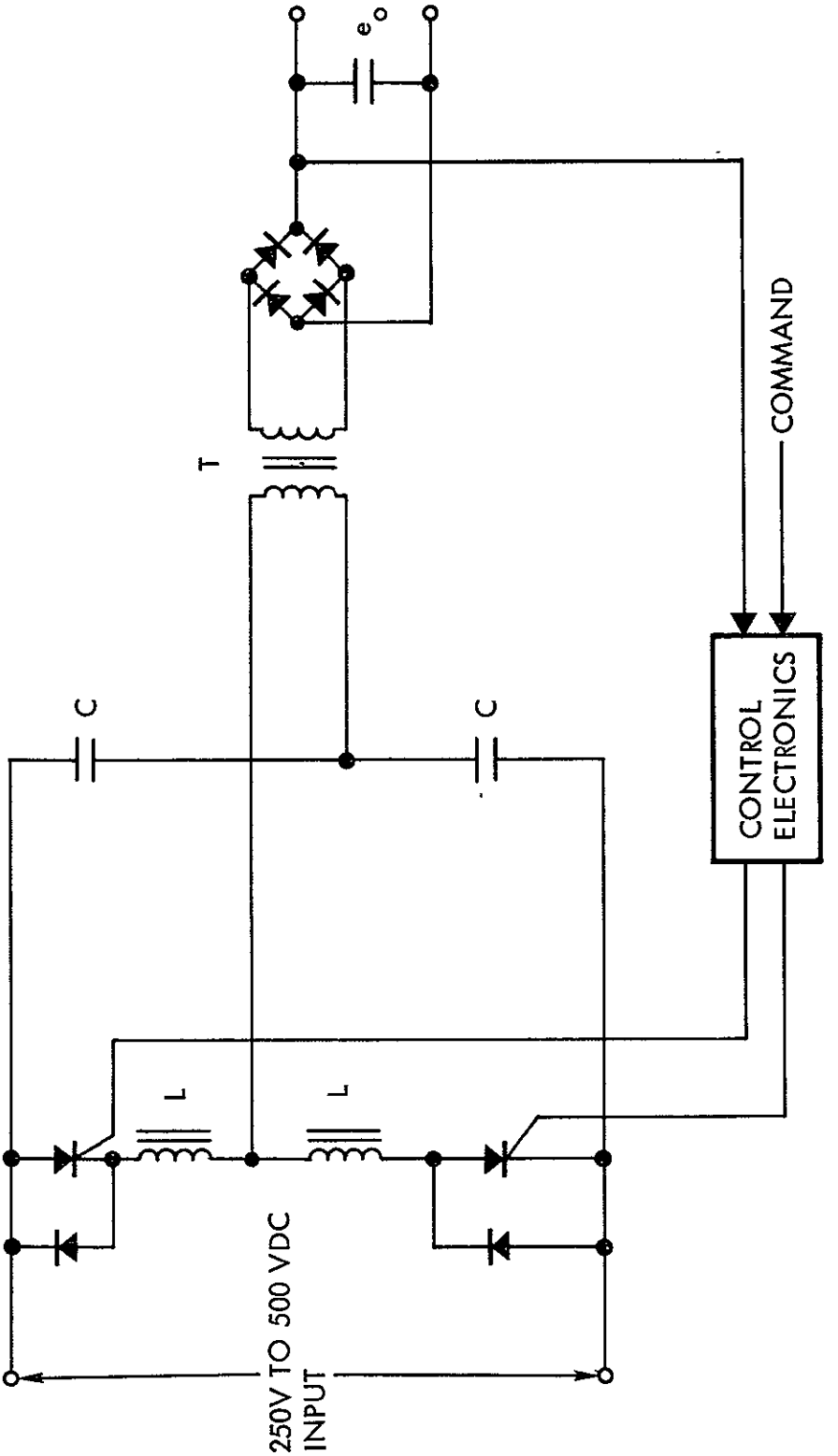

Figure A2-2. DC to DC High Voltage Converter.

SCR is turned on, an oscillatory current flows through the series combination of L, T and C. The sinusoidal current flow, occurring at a frequency determined by the L-C components, is zero when an SCR is initially turned on, builds up to a maximum determined by the circuit design, and then returns to zero. As the current passes through zero, the capacitor is charged to a voltage higher than the supply voltage and the inductor voltage drops to zero. The sum of the capacitor voltage and transformer voltage appears as a reverse voltage on the conducting SCR during its recovery to a blocking state. The inductive and capacitative circuit elements therefore provide a natural commutation circuit which is an integral part of the power circuit. No auxiliary transformer windings or capacitors are necessary as additional elements to generate commutating pulses to turn off the SCR's. This feature is unique to this type of converter.

The sinewave current ensures SCR operation below the maximum di/dt rating and minimizes the voltage-current product during the initial switching interval to mitigate the disadvantage of slow SCR switching. Along these lines it is interesting to note that in most parallel inverter transistor circuits used for this application, high switching losses and high stress occur since both high voltage and high current exist at the same time. The sinewave current amplitude is changed by the turns ratio of transformer T before it is rectified and filtered by capacitor C1, which provides a low ripple circuit-voltage output. The transformer turns ratio may be quite large in the case of ion thruster loads, in order to produce the high voltages required for loads such as the beam and accelerator supplies. The distributed capacitance of the windings of such transformers can be considerable. This is no problem in the design of series inverters since the reflected capacitance of the large filter capacitor C1 is much greater than the winding capacitance so that the latter may be neglected.

The control electronics can accept external commands and changes the operating condition of the LC series resonant inverter to provide the different possible DC output voltage required by the experiments.

The DC to DC high voltge converter can be operated continuous at the 1.5 KW level allowed by the charger or in pulse output power mode to 50 KW. Preliminary thermal analysis work is in progress and two different possible power processor configurations are under consideration:

CONFIGURATION	WEIGHT	EFFICIENCY AT 50 KW
I	55 KG	90%
II	35 KG	85%

At the present time, there has not been a selection of which would be the most promising system for the shuttle system.

In the pulse mode of operation, the thermal control system will impact the overall design.

5.0 THERMAL ANALYSIS

A preliminary thermal analysis has been performed to identify the thermal control characteristics and requirements for the power processing equipment.

The payload heat rejection of the shuttle is accomplished by a heat exchanger located in the Freon 21 loop of the active thermal control subsystem. A maximum of 21,500 BTU/hr of payload heat rejection can be provided during noncritical mission time using water as payload heat exchanger coolant with a flow of 550 lb/hr (.07 KG/sec) and payload coolant temperature of 70° to 90°F (57°C-66°C).

In the pulse power mode of operation, the heat generated by the power electronics must be stored in the thermal mass of the power electronics. The low flow rate of the active cooling system cannot become effective during the short on time of 20 seconds.

The specific heat of the power processing equipment is assumed to be 0.1. The Configuration I with a total weight of 55 KG will have a temperature rise of 5°C after 20 seconds based on its 90% efficiency and Configuration II with a total weight of 35 KG will have a temperature rise of 12°C after 20 seconds based on its 85% efficiency.

Configuration I can run continuously if it is the only heat load on the payload thermal control system.

Configuration II may have to be turned off after about 1 minute of operation due to the overload of the shuttle payload thermal control system in order to maintain adequate component operating temperatures.

APPENDIX A3

CONTAMINANT MAGNETIC FIELDS FROM AMPS PAYLOAD CURRENTS

J. M. Sellen, Jr.

CONTAMINANT MAGNETIC FIELDS FROM AMPS PAYLOAD CURRENTS

1.0 INTRODUCTION

This technical memorandum will examine contaminant magnetic field magnitudes for current flow in two "reference" configurations for an AMPS spacecraft. Impact of such contaminant fields on payload operation will be discussed, and factors which will distinguish actual payloads from the referenced Configurations will be noted. The magnitudes of contaminant fields in the reference configurations suggest a need for more accurate current flow specification, calculations of the fields resulting from these more complicated flow patterns, and, probably, corrective actions through particular designs in circuit placement, current flow scheduling (in time) and positioning.

2.0 MAGNETIC FIELD CALCULATIONS

Figure 1 illustrates a rectangular current loop in the x-y plane of an x-y-z space. Configuration A is 18 meters in length and 4.5 meters in width and would correspond, for example, to a conductor placed around the perimeter of the Orbiter payload bay. Configuration B is a square current loop of 4.5 meters on a side, and could represent, for example, a current flow from an Orbiter cockpit area to the forward bulkhead of a module and return, configured for maximum contaminant field generation. The point x=y=z=0 is chosen at the loop midpoint, for convenience.

Figure 2 illustrates the contaminant field generated in these two configurations for a 100 ampere flow around the loop. Along the z axis, only B_z is non-zero. For Configuration A, B_z at x=y=z=0 is 18,500γ (1 γ = 10^{-5} gauss), and has diminished to 900 γ at z = 10 meters. For Configuration B, B_z = 25,100γ at (0,0,0) and diminishes to 370γ at 10 meters. The increase in B_z at (0,0,0) for configuration B (compared to A) should be expected since the proximity to the origin of the y-directed current flows is more than sufficient compensation for the reduced extent of x-directed flow in the smaller loop. For large z, however, Configuration A generates a higher level of contaminant field than Configuration B.

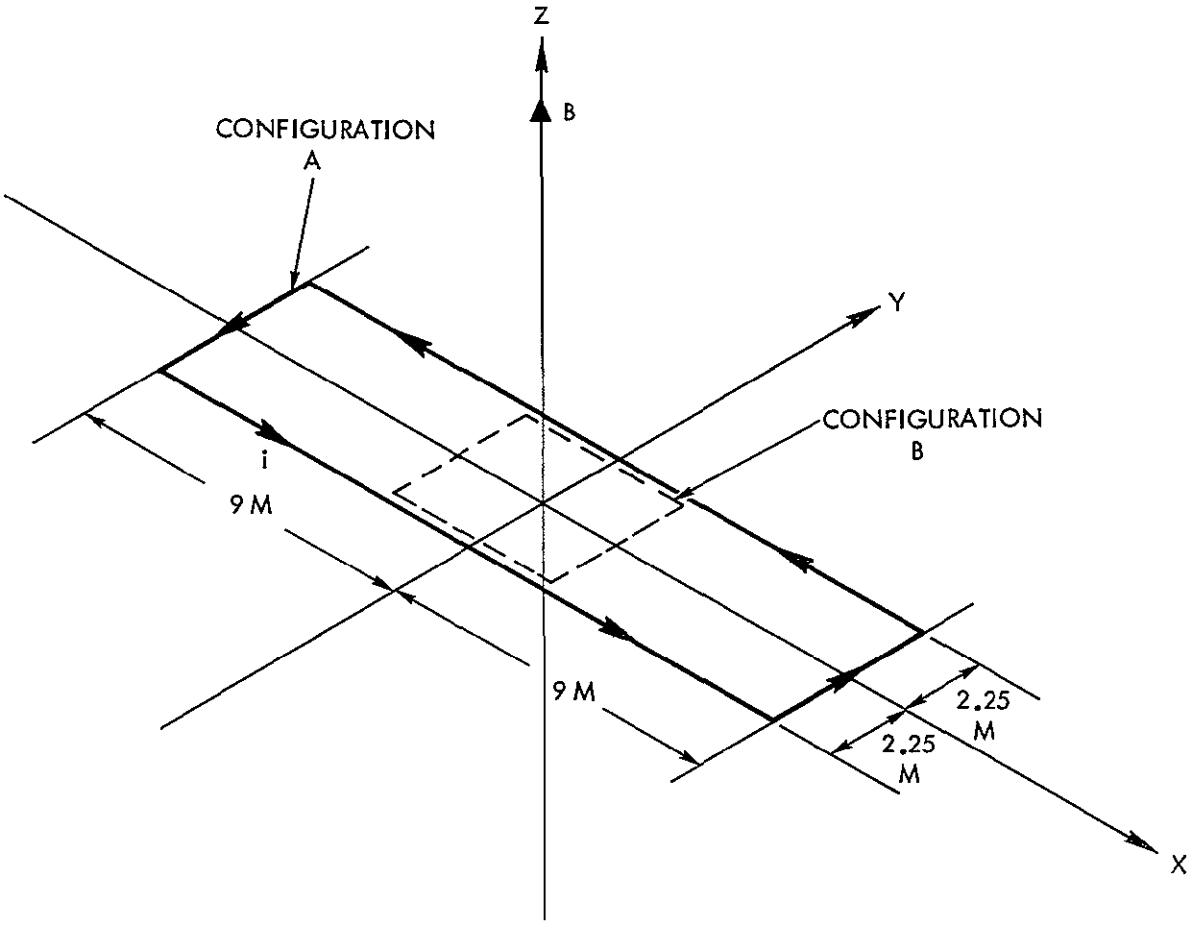

Figure A3-1. Current Flow Configuration and Axes.

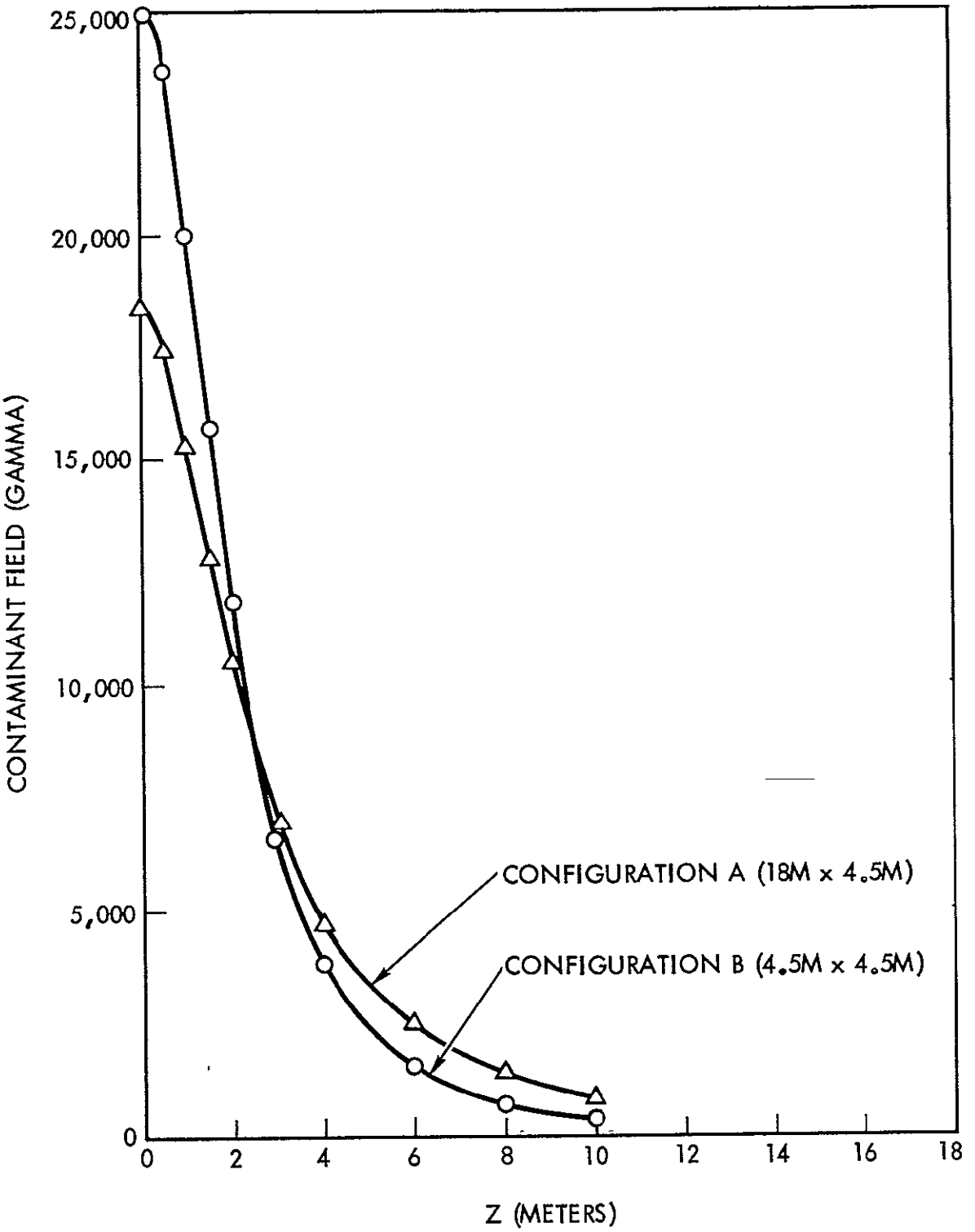

Figure A3-2. Contaminant Magnetic Field Along Axis for 100 Ampere Current Flow in Illustrated Geometry as a Function of Z Separation.

3.0 IMPACT OF CONTAMINANT FIELDS ON PAYLOAD OPERATION

The magnitude of contaminant B_z for z within a few meters of the origin, (0,0,0), and for either configuration, is comparable to or larger than the Earth's magnetic field. If electrons in an energetic electron beam were to be released from the origin, the $\vec{v}_e \times \vec{B}$ force on these particles would be roughly equal from the Earth's field and from the contaminant field for, at least, the first few meters of flight, and any intention for these electrons to respond to only the magnetic field of the Earth would not be realized. Configuration A perturbations, at the 100 ampere level of current circulation, are unacceptably large and some measures of reduction would be required (either by reducing current flow during electron beam operation or by rearrangement of current paths).

- Configuration B would also be too severe a perturbation to an electron beam if the beam were to be released along the z-axis at x=y=0. If, however, the electron beam were to be directed along the z-axis from a point near the rear of the Orbiter payload bay, and the 4.5 x 4.5 meter current loop were to be at the forward end of the bay, then contaminant field effects on electron motion would (probably) be at acceptably reduced levels. The presence of a high level contaminant field in the forward portion of the Orbiter bay would not be tolerable, on the other hand, if the B-field sensing magnetometer were to be located in this forward region. In presently on-going accelerator systems studies, the use of a magnetometer to detect the direction of the Earth's magnetic field has been proposed as a portion of electron accelerator operation. In this mode, magnetometer signal is fed to appropriate signal conditioning circuits which supply the drive currents to megnetic deflection coils at the electron accelerator output so that electrons emerge at a specified pitch angle with respect to $\vec{B}_e$, the Earth's field. This pitch angle specification method is attractive from the standpoint of reducing orientation requirements on the Orbiter. If, however, contaminant fields exist in the region of the magnetometer, the effects of this field would be present in the electron beam flow as an indirect, rather than direct, perturbation. The location of the magnetometer in the rear portion of the payload bay, on

the other hand, could introduce perturbations in the measurements of $\vec{B}_e$ (and on resultant electron beam motion) because of stray fields from the e-beam deflection coils. A solution to this problem is provided by, 1) location of the magnetometer in the forward part of the payload bay, and, 2) reducing contaminant fields in that region to an acceptable level.

4.0 CONTAMINANT FIELD REDUCTION

Contaminant field magnitudes of 10^3 to $10^4\gamma$ are clearly excessive and methods of reduction should be explored. In previous studies[1,2], a large area solar array was configured so that contaminant fields, within a few meters of the array remained within a range from 0.1 to 1γ. Total array current for this large area source was 100 amperes, demonstrating that γ-level magnetic cleanliness can be achieved over broad areas in the presence of large currents. Admittedly, a much more determined current flow pattern existed for this array than exists at present (or possibly even in the future) for the Shuttle and its payload. Nevertheless, substantial reductions of Orbiter contaminant field should be achievable by applying comparatively simple procedures.

A pre-requisite for field reduction is a more accurate specification of current magnitudes, initiating and terminating points and routing. Volume XIV (Payload Accommodations Handbook) does not provide exit points for power connectors, except for general statements of X-axis locations. In the absence of further information, a possible first step may be to insert assumed values for current exit points from the Orbiter to the payload bay.

Routing of currents inside the AMPS modules and on AMPS pallets also remains unspecified. Since the Particle Accelerator System employs two leads in current circulation, their placement to avoid contaminant field generation can (and should) remain as one of the system design criteria, and further consideration will not be given to stray fields from these elements on the pallet (Note: fringe fields from the e-beam magnetic deflection coils are a possible perturbation but will be treated separately). Principal attention, then, should be directed toward current flows in elements located within the modules.

The use of the Orbiter frmae to return current from elements in the modules introduces uncertainties in analysis. The B-field generation derives from current flow patterns in distributed conductors which is, in itself, sufficiently complicated. The multiple injection of currents (through simultaneous operation of several circuits) into the frame, and injection at more than a single point causes contaminant field generation which is not a super-position of the stray fields from individual injections because of current flow reorientation for self-consistent flow in a resistance matrix. In principle, a mapping of contaminant field would be not only three dimensional, but would also be a function of the specific circuit elements in use and the specific levels of power for operation of these elements.

While the exact levels of stray field may depend upon many parameters in some "operational matrix", a more simplified situation may be present in practice (and for somewhat relaxed standards of cleanliness). Contaminant fields for this practical situation probably arise from the major power users, and superposition, though not exact, may be sufficiently precise for present purposes (here interpreted as reducing contaminant fields to levels which are small compared to the Earth's field).

The factors noted above suggest a plan for contaminant field reduction:

1) Specification of current output points from the Orbiter into the payload bay.

2) Identification of principal power users in the modules, and element currents and locations.

3) Modeling of frame return paths for individual flows for elements determined above.

4) Iteration of location for high contaminant generation elements in Item 3) analysis.

5) Mock-up with current flow, of best analytical configuration in 4) with experimental determination of contaminant fields.

6) Carrier relocation in mock-up for remaining high contaminant level generators.

7) Placement of magnetometers and other sensitive elements in deliberately produced "safe zones" or in "opportunity" safe zones (discovered but not necessarily planned for).

The first four steps in the procedure above should be initiated sufficiently early to prevent conductor placement in inappropriate locations. At present both Orbiter and modules are not completely specified in inlet-outlet points. The contaminant reduction program should also derive weight and location requirements for additional current flow paths and should specify circuit placement in the module before such specifications introduce extra design and relocation.

Two other factors in contaminant field reduction which should be noted in this technical brief are the stray fields from "finalized" Orbiter wiring patterns, and AC contaminant fields. While module and pallet design can presumably be influenced, certain portions of the Orbiter are probably in firm design and these contaminant fields cannot be altered. The magnitudes and locations of such "fixed" perturbations should be determined. Under certain circumstances these contaminants may be eliminated by arranging for opposing contaminant fields from those circuits still flexible to design. Finally, and although no previous emphasis has been given to AC magnetic field contaminants, their reduction can follow the reduction of the steady state magnetic moments of the various circuits.

REFERENCES

1. "Contaminant Magnetic Fields From Large Area Solar Arrays", J. M. Sellen, Jr. and H. S. Ogawa, TRW 12738-6006-R000, 16 June 1969. Also Section IV A. Final Report, Study of Electric Propulsion Spacecraft Plasmas and Field Interactions, Robert K. Cole, H. S. Ogawa, and J. M. Sellen, Jr. TRW 12738-6016-RO-00, July 1, 1970.

2. "Backwire and Busbar Placement for Magnetic Cleanliness on Large Area Solar Arrays", J. M. Sellen, Jr., TRW 12738-6007-RO-00, 30 June 1969, also Section IVB. Final Report, noted above.

APPRNDIX A4

ENERGY STORAGE WITH FLYWHEELS

R. K. Cole

ENERGY STORAGE WITH FLYWHEELS

1.0 INTRODUCTION

Flywheels are presently being considered as efficient and compact energy storage devices for both stationary and mobile systems. Energy can be stored and extracted with high efficiency and power levels, and the available energy stored to mass ratio compares very favorably with batteries. Flywheels have a long useful life and may be cycled, charged and discharged, almost indefinitely. In addition, flywheels offer the possibility of combining energy and angular momentum storage for attitude control.

Recent developments[1] in high strength filamentary materials promise much greater energy storage per unit mass than the usual isotropic materials, such as steel. Magnetic suspension bearings have also been developed which can operate at higher angular speeds with lower power losses than conventional bearings. Recent designs of motor generators provide the possibility of efficient (greater than 90%)--low weight--high power energy extraction.

In this section, flywheels are evaluated in terms of the current technology of rotors, bearings, and generator motor systems. Several flywheel storage systems are discussed in terms of total energy stored, specific energy storage, power, angular momentum stored, and the effects of flywheel angular momentum on vehicle maneuvers.

2.0 MECHANICS OF FLYWHEELS

The rotational kinetic energy of a wheel of moment of inertia I rotating with angular speed ω is

$$E = \frac{1}{2} I\omega^2 \quad . \tag{A4-1}$$

$$I = \int r^2 \, dm \quad . \tag{A4-2}$$

The specific energy U may be written

$$U = \frac{E}{M} = QR^2\omega^2 \quad , \tag{A4-3}$$

where

Q is a shape factor.

R is the radius of the wheel.

The upper limit of the kinetic energy a given wheel can store depends on the maximum tensile strength of the material used.[1]

$$U_{max} = K \frac{\sigma}{\rho} \quad , \tag{A4-4}$$

where

σ is the maximum allowable stress.

ρ is the mass density.

K is a configuration factor.

The maximum angular speed is

$$\omega_{MAX} = \frac{Y}{R} \sqrt{\frac{\sigma}{\rho}} \quad , \tag{A4-5}$$

where

$$Y = \sqrt{\frac{K}{Q}}$$

For example, Q = 1/2 and K = 1/2 for a thin rim wheel. An ideal wheel is the tapered disc in which the radial and tangential stresses are equal.[2,3] This maximizes the specific energy for a homogeneous, isotropic wheel. One practical tapered disc design yields K = 0.925 and Q ≈ 0.115.[1]

A simple, yet good, approximation to the equal stress tapered disc for isotropic materials is a constant taper or triangular taper shape. The thickness of the wheel decreases uniformly with radius from the axis to the rim. This shape yields a simple analytical model. For a wheel of maximum thickness H at the axis and of radius R where H = 2αR, the mass and moment of inertia of a homogeneous wheel of density ρ are

$$M = \frac{2}{3} \pi \rho \alpha R^3 \quad , \tag{A4-6}$$

$$I = \frac{\pi \rho}{5} \alpha R^5 \quad . \tag{A4-7}$$

and

$$Q = 0.15 \tag{A4-8}$$

For our calculation, we will use K = 0.80, which yields Y = 2.31.

3.0 FLYWHEEL ENERGY SYSTEMS

Three constant taper flywheels are considered here: a large or maxi-wheel of 1000 kg mass; an intermediate wheel of 100 kg mass; and a small or mini-wheel of 10 kg mass. For each size rotor, two shape factors, $\alpha = 0.10$ and $\alpha = 0.20$, are considered. Wheels constructed of three common isotropic materials, aluminum, steel, and titanium alloy, and one of filamentary composite material, silica filament-epoxy composite (S-glass) are evaluated. Rotors machined of steel, titanium, and other common materials have been employed in many applications. Filamentary wheels are of recent development and have been constructed for special applications. Their use offers greater specific energy storage because of their higher tensile strength to density ratio which permits higher rotational speeds. Additional development is indicated for the construction and balancing of rotors made of these materials and the determination of the peak working stress consistent with long life. For this reason, the steel and titanium alloy rotors are considered more representative of present technology than the filamentary composites. The S-glass wheel is presented for comparison to illustrate the possibilities of these materials.

Table A4-1 summarizes the parameters used to calculate the maximum specific energy available in aluminum, titanium, steel, and S-glass rotors for the constant taper wheels using $K = 0.80$ and $Y = 2.31$.

Table A4-1
Parameters and Maximum Specific Energies of Rotor Materials

Material	Maximum Stress σ (N/m^2)	Density ρ (kg/m^3)	Maximum Rim Speed $R\omega_{MAX}$ (m/sec)	Specific Energy (rotor only) (M joules/kg)
Aluminum 7075	5.0×10^8	2.81×10^3	974	0.142
Ti-6Al-4V	9.0×10^8	4.43×10^3	1041	0.163
Maraging Steel 300 Grade	1.8×10^9	8.00×10^3	1095	0.180
S-Glass	2.3×10^9	2.11×10^3	2411	0.872

The values of Table 4A-1 were used to obtain the maximum energy and angular momentum stored in a 1000 kg, 100 kg, and a 10 kg constant taper wheel. The momenta of inertia, radii, and maximum angular speed together with the maximum energies and angular momenta for the three wheels are given in Tables A4-2, A4-3 and A4-4.

Table A4-2.

Physical Properties of 1000 Kg Rotor

MAXI-WHEEL M = 1000 kg.

A) $\alpha = 0.10$

Material	I ($kg\text{-}m^2$)	ω_{MAX} ($rad\text{-}sec^{-1}$)	R (m)	L_{MAX} (N-m-sec)	U_{MAX} (M-joule)
Aluminum 7075	427	818	1.19	3.49×10^5	143
Ti-6Al-4V	307	1030	1.01	3.16×10^5	163
Steel	216	1286	0.85	2.78×10^5	179
S-Glass	516	1840	1.31	9.49×10^5	873

B) $\alpha = 0.20$

Aluminum 7075	269	1025	0.95	2.76×10^5	141
Ti-6Al-4V	194	1301	0.80	2.52×10^5	164
Steel	136	1634	0.67	2.22×10^5	181
S-Glass	326	2318	1.04	7.56×10^5	876

Table A4-3

Physical Properties of 100 kg Rotor

MIDI-WHEEL M = 100 kg.

A) $\alpha = 0.10$

Material	I ($kg\text{-}m^2$)	ω_{MAX} ($rad\text{-}sec^{-1}$)	R (m)	L_{MAX} (N-m-sec)	U_{MAX} (M-joule)
Aluminum 7075	9.20	1771	0.55	1.63×10^4	14.4
Ti-6Al-4V	6.63	2215	0.47	1.47×10^4	16.3
Steel	4.65	2808	0.39	1.31×10^4	18.3
S-Glass	11.1	3952	0.61	4.39×10^4	86.7

B) $\alpha = 0.20$

Aluminum 7075	5.80	2214	0.44	1.28×10^4	14.2
Ti-6Al-4V	4.17	2814	0.37	1.17×10^4	16.5
Steel	2.93	3532	0.31	1.03×10^4	18.3
S-Glass	7.02	5023	0.48	3.53×10^4	88.6

Table A4-4

Physical Properties of 10 kg Rotor

MINI-WHEEL M = 10 kg.

A) $\alpha = 0.10$

Material	I ($kg\text{-}m^2$)	ω_{MAX} ($rad\text{-}sec^{-1}$)	R (m)	L_{MAX} (N-m-sec)	U_{MAX} (M-joule)
Aluminum 7075	0.20	3746	0.26	769	1.40
Ti-6Al-4V	0.14	4732	0.22	662	1.57
Steel	0.10	6083	0.18	608	1.85
S-Glass	0.24	8611	0.28	2067	8.90

B) $\alpha = 0.20$

Aluminum 7075	0.12	4870	0.20	584	1.42
Ti-6Al-4V	0.090	6124	0.17	551	1.69
Steel	0.063	7552	0.145	476	1.80
S-glass	0.15	10959	0.22	1644	9.01

The values of the stored energy presented in Tables A4-2, A4-3 and A4-4 should be considered to be absolute maxima, that is, at the stress limit of the material. We now assume that operation of a rotor at 60% of the maximum angular speed ω_{MAX} is consistent with long wheel life and safety. This safety factor is consistent with using a peak working stress in steel of $\sigma(\text{working}) = 0.80 \times 10^9$ N/m^2 compared to the material stress limit of $\sigma = 1.80 \times 10^9$ N/m^2. Thus,

$$\frac{\omega_{(peak)}}{\omega_{MAX}} = \sqrt{\frac{\sigma_{(peak)}}{\sigma_{(working)}}} = 0.67 \quad , \tag{A4-9}$$

and

$$\frac{U_{(peak)}}{U_{MAX}} = \sqrt{\frac{\sigma_{(peak)}}{\sigma_{(working)}}} = 0.44 \quad . \tag{A4-10}$$

probably quite conservative for titanium. The resulting peak energy storage values should be considered to be conservative values as far as rotor stress is concerned.

Besides rotor material strength considerations, the maximum working speed of bearings consistent with long bearing life and lubrication problems must be examined. The detailed study of flywheels by J. E. Notti, A. Cormock, III, and W. C. Schmill[4] conclude that only ball bearings and magnetic suspension bearings are suitable for high speed energy storage wheels. The magnetic bearing is a non-contact, high speed, low power loss bearing. Several have been designed and used. For purposes of this study, only the ball bearings are considered since the maximum speeds of the isotropic rotors are within the limits of available ball bearings. Development of high speed magnetic suspension bearings should be encouraged, especially in conjunction with anisotropic rotor studies.

Drag losses require the rotor be operated in vacuum. Proper lubrication of the bearings now becomes a concern for maintenance of adequate bearing life and reliability. Although the adequate lubrication of bearings operated above 12,000 RPM in vacuum may require additional development, we will assume that bearing speed is limited by the DN limit of

present designs. Using DN = 3 x 10^5 mm RPM and a one-half inch shaft for the larger flywheels, a maximum speed of 24,000 RPM (2513 radian/sec) is obtained. We will use this value as an upper limit of the operating speeds of the two heavier rotors and a maximum angular speed of 36,000 RPM for the 10 kg wheels. These upper limits on bearing speed, in fact, limit only the working peak speed of the 10 kg S-glass rotor.

A comparison of the specific energy of flywheel systems to other energy storage devices should include, in addition to the mass of the rotor, the masses of the bearings, gimbals, housing, and safety shield, motor-generator, and associated transformer and electronics. Because of the conservative safety factor, we can assume a minimum enclosure. Our estimates of the housing and bearing weights are 200 kg, 50 kg, and 8 kg, respectively, for the large, intermediate, and small flywheels.

The weight of the motor generator system depends critically on power requirements and windup time. Permanent magnet generators of 10 kW at 10,000 RPM and weighing about 50 kg are feasible. Such a unit could possibly operate at higher power levels for a short time. However, generators of significantly higher power will require some development, especially of the weight and size are to be reasonable. There are designs that exceed this power level, especially at higher speeds, but the availability of these units is not presently known. For example, an alternator recently developed by Dr. Richter at General Electric is reported to deliver 70 kW at 21,000 RPM and weighs about 55 kg. This design appears to offer great promise for high speed rotors. We will assign a motor-generator of 12 kW and weighing 60 kg to the large and intermediate mass rotors and a 6 kW unit weighing 25 kg to the smaller system. Our estimates of the total mass of each system is given in Table A4-5.

Table A4-5

Mass Breakdown of Flywheel Systems

Item	Maxi-Wheel	Midi-Wheel	Mini-Wheel
Rotor	1000 kg	100 kg	10 kg
Housing and Bearings	200 kg	50 kg	8 kg
Motor Generator	60 kg	60 kg	25 kg
Total Mass	1260 kg	210 kg	47 kg

In addition, if the flywheel system is permitted to run down to one-half of the peak angular speed, then only 3/4 of the peak stored energy is available. The results of this discussion are presented in Table VI in terms of peak energy stored, available energy, peak angular momentum, and specific peak energy.

Table A4-6

Energy and Angular Momentum Stored by Flywheel Systems

A) MAXI-WHEEL (1000 kg) Total mass of system = 1260 kg.

Material	$\omega_{PEAK} = 0.60\ \omega_{MAX}$ (radian/sec)	E_{Peak} (M-joule)	$E_{Available}$ 3/4 E Peak	L_{Peak} (N-M-sec)	$E_{Peak/Sys.\ Mass}$ (M joule/kg)
Aluminum	491	51	38	20.9×10^4	0.040
Ti-6Al-4V	618	59	44	19.0×10^4	0.047
Steel	772	64	48	16.7×10^4	0.051
S-Glass	1104	314	235	57.0×10^4	0.25

B) MIDI-WHEEL (100 kg) Total mass of system = 210 kg.

Aluminum	1063	5.2	3.9	0.98×10^4	0.025
Ti-6Al-4V	1329	5.9	4.4	0.88×10^4	0.028
Steel	1685	6.6	5.0	0.78×10^4	0.031
S-Glass	2371	31	23	2.63×10^4	0.15

C) MINI-WHEEL (10 kg) ~ Total mass of system = 47 kg.

Aluminum	2248	0.50	0.38	4.5×10^2	0.010
Ti-6Al-4V	2839	0.57	0.43	4.0×10^2	0.012
Steel	3650	0.67	0.50	3.65×10^2	0.014
S-Glass	3770*	1.7	1.3	9.0×10^2	0.036

* Limited to 36,000 RPM by bearings.

The 1000 kg rotor and 100 kg rotor flywheel systems compare quite favorably with lead acid batteries which have a specific energy storage of about 0.08 M joule/kg without their associated power conditioner. Operation of these wheels at $\omega_{peak} = 0.60\ \omega_{max}$ is quite conservative; however, and experience will probably demonstrate that a well-balanced rotor can safely spin with higher angular speeds without the penalty of a massive safety shield. A higher peak speed of $\omega_{peak} = 0.75\ \omega_{MAX}$ is probably realizable for some alloys, such as Ti-6Al-4V. This would increase both the peak energy stored and the available energy by more than 50%. The peak energy stored for $\omega_{peak} = 0.75\ \omega_{MAX}$ is presented for comparison in Table A4-7 for steel and titanium heavier wheels.

Table A4-7

A) MAXI-WHEEL (1000 kg rotor)

Material	E_{Peak} (1) $\omega_{peak} = .6\ \omega_{MAX}$ (M-joules)	E_{Peak} (2) $\omega_{peak} = .75\ \omega_{MAX}$ (M-joules)	E_{peak}^2/Sys. Mass (M-joules/kg)
Ti-6Al-4V	59	92	0.073
Steel	64	100	0.079

B) MIDI-WHEEL (100 kg rotor)

Ti-6Al-4V	5.9	9.2	0.044
Steel	6.6	10	0.049

Comparison of Energy Stored at 0.60 ω_{MAX} and 0.75 ω_{MAX}

The stored energy requirement of AMPS is more than 10 mJ of available energy. This is certainly available in the 1000 kg rotors operated conservatively at $\omega_{peak} = .60\ \omega_{MAX}$. A power requirement of 10^6 watts for one second is not attainable with present generators, although some of the advanced designs approach 70 kW. One method of increasing power capbility would be to employ three flywheel systems (or even six), one wheel oriented along each of the three perpendicular axes of the

shuttle. Attitude control could be accomplished, at least in part, by removing or adding energy to one or more wheels. Since each wheel would have an associated motor generator unit, about 36 kW could be obtained with 3 wheels using conventional generators and possibly over 100 kW with the advanced designs. The rotor mass required to store 10 mJ of usable energy (3/4 E peak) for titanium, steel, and S-glass is presented in Table A4-8. Adding about 150 kg for the bearings, housing, and motor generator yields the system mass. The total mass of three-isotropic rotor-flywheel systems storing 30 M-Joulesis between 900 and 1000 kg. An S-glass rotor system would weigh 500-600 kg.

TABLE A4-8

	$\omega_{peak} = 0.60\ \omega_{MAX}$		$\omega_{peak} = 0.75\ \omega_{MAX}$	
Material	Rotor Mass (kg)	Mass System (kg)	Rotor Mass (kg)	Mass System (kg)
Titanium	227	377	145	295
Steel	208	358	133	283
S-Glass	43	193	27	177

In summary, flywheel systems using present technology have usable energy storage capabilities comparable to lead acid batteries. A three-wheel unit using steel or titanium rotors and storing 30 megaJoules of usable energy would weigh 900 to 1000 kg. The development of composite high strength rotors and magnetic high speed bearings could reduce this by about a factor of two. However, the power capabilities of a wheel system are presently limited by the generator or alternator and an extensive development program appears necessary if the megawatt level is to be approached. Energy withdrawal also produces a torque on the rotor shaft. The gyroscopic effects of energy withdrawal and altitude change are discussed in the next section.

4.0 GYROSCOPIC EFFECTS

An energy change of the flywheel will produce a torque on the rotor axis;

$$\tau = \frac{1}{\omega}\left(\frac{dE}{dt}\right) = \frac{P}{\omega} \quad , \tag{A4-11}$$

and result in the transfer to the craft of the angular momentum lost or gained by the wheel. If we assume that the space shuttle can be represented as a solid cylinder 30 meters in length, 5 meters in diameter, and 10^5 kg mass, it will have two different moments of inertia. The moment of inertia I_1 is associated with rotation about the axis of symmetry of the cylinder, the x axis of Figure 1; the moment of inertia I_2 is associated with rotation about the y or z axis. The origin of the coordinate system is at the center of mass of the craft.

$$I_1 = 3 \times 10^5 \text{ kg m}^2 \quad . \tag{A4-12}$$

$$I_2 = 75 \times 10^5 \text{ kg m}^2 \quad . \tag{A4-13}$$

A flywheel whose axis of rotation is parallel to the x-axis of the craft (axes of symmetry) rotating clockwise as viewed from the tail of the ship, will have angular momentum L in the positive x-direction,

$$L = I_o\omega \quad , \tag{A4-14}$$

where I_o is the moment of inertia of the flywheel and ω is the wheel's angular speed. Power withdrawal from the wheel will give the craft an angular acceleration,

$$\alpha_1 = \frac{\tau}{I_1} = \frac{P}{\omega I_1} \quad , \tag{A4-15}$$

and changing the energy of the wheel ΔE will change its angular momentum by ΔL,

$$\Delta L = \frac{\Delta E}{\omega} \quad . \tag{A4-16}$$

This angular momentum is now acquired by the craft, resulting in a change of angular speed,

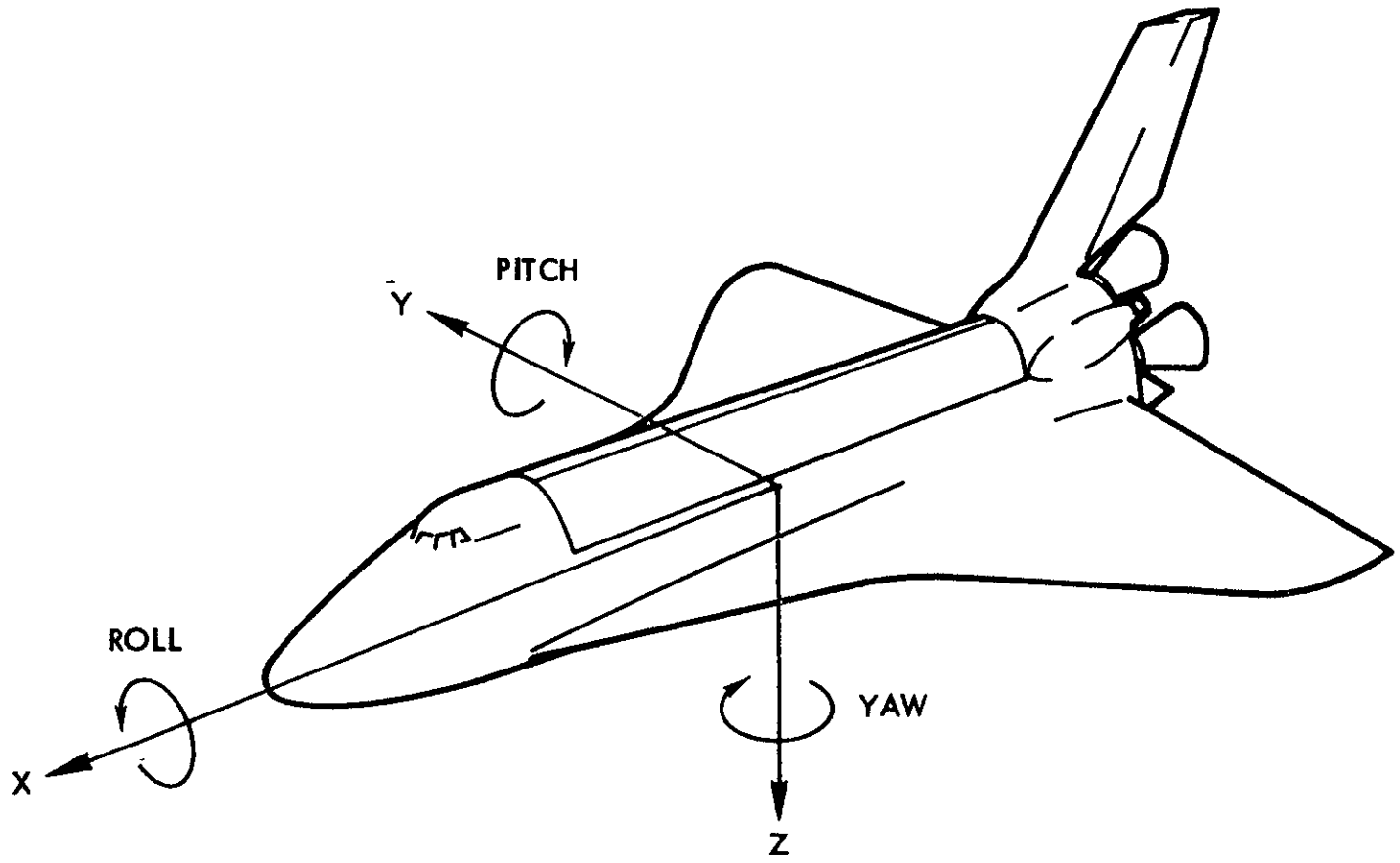

Figure A4-1. Shuttle Orbiter with Roll, Pitch, and Yaw Axes.

$$\Delta\omega_1 = \frac{\Delta L}{I_1} = \frac{\Delta E}{I_1 \omega} \quad . \tag{A4-17}$$

The orientation of the flywheel along either the y or z axes will yield the corresponding angular acceleration and changes in rotational speed about the appropriate axis,

$$\alpha_2 = \frac{P}{\omega I_2} \quad . \tag{A4-18}$$

$$\Delta\omega_2 = \frac{\Delta L}{I_2} \quad . \tag{A4-19}$$

The torque, angular acceleration, and angular speed given to the shuttle corresponding to power usage of 10^5 watts for one second ($\Delta E = 10^5$ joules and 10^6 watts for one second for flywheels oriented along the x and the y or z axis are presented in Table A4-9. An average angular speed of ω = 1000 radians/sec is assumed.

Table A4-9

	10^5 Watts for One Second			10^6 Watts for One Second		
Flywheel Orientation	Torque (N-m)	α (rad/sec^2)	$\Delta\omega$ (rad/sec)	Torque (N-m)	α (rad/sec^2)	$\Delta\omega$ (rad/sec)
x-axis	10^2	3.3×10^{-4}	3.3×10^{-4}	10^3	3.3×10^{-3}	3.3×10^{-3}
y- or z-axis	10^2	1.3×10^{-5}	1.3×10^{-5}	10^3	1.3×10^{-4}	1.3×10^{-4}

Effects on Shuttle of Energy Withdrawal from Flywheel

The resulting angular speeds are small due to the large moments of inertia of the shuttle and could be easily handled by the shuttle's attitude control system.

A catastrophic event such as a bearing seizure at full energy would result in the transfer of the angular momentum of the wheel to the vehicle. For the 1000 kg steel rotor of Table VI oriented along the x-axis, the resulting rotational speed would be .56 radians/sec or a complete revolution in 11 seconds. This would require immediate corrective action.

Changes in attitude of a vehicle equipped with a spinning flywheel attached to the vehicle will result in a torque on the craft equal to the rate of change of angular momentum of the wheel.

$$\tau = \frac{dL}{dt} = L\left(\frac{d\theta}{dt}\right) \quad , \tag{A4-20}$$

where $d\theta/dt$ is the angular rotation of the vehicle.

For a flywheel whose axis is oriented along the z-axis of Figure 1, a pitch movement, rotation about the y-axis, will result in a torque about the x-axis of the craft, producing a roll of the shuttle. If the nose of the vehicle is raised or lowered at the rate of $d\theta/dt = 0.10$ radians/sec, the torque resulting from the 1000 kg steel rotor of Table A4-6 would be

$$\tau_x = 1.67 \times 10^3 \text{ N-m} \tag{A4-21}$$

producing an angular acceleration about the x-axis,

$$\alpha_x = \frac{\tau_x}{I_1} = 5.6 \times 10^{-2} \text{ rad/sec}^2 \quad . \tag{A4-22}$$

Raising the nose 90° would result in a roll of 396°, or more than one complete revolution.

A roll maneuver of the same speed results in a torque about the y-axis or pitch and an angular acceleration of 0.0022 radians/sec^2. Thus, a 90° roll would pitch the vehicle about 15°.

A yaw movement, on the other hand, will produce no torque because the angular momentum of the flywheel is not affected.

Corresponding effects will be produced if the flywheel is oriented along the x-axis. A pitch results in a yaw movement; a yaw produces a pitch; and a roll has no affect.

As these figures show, a flywheel storing megajoules of energy may possess sufficient angular momentum to significantly influence the attitude control of the craft. The torques are transmitted by the bearings to the flywheel, so adequate allowance must be made for the most violent maneuver of the vehicle. This could be of special concern where magnetic suspension bearings are used.

REFERENCES

1. F. Beggs, Flywheel Energy Systems, SAND 74-0113, Sandia [redacted] Albuquerque, N.M.

2. M. Jakubowski, Flywheel Energy Buffer, 7th Intersociety Energy [redacted] version Engineering Conference 1972, Proceedings published by Ame[redacted] can Chemical Society, 1155 16th St., N. W. Washington, D. C.

3. G. L. Dugger, A. Brandt, J. F. George, L. L. Perini, D. W. Rabenhorst, T. R. Small, and R. O. Weiss, Heat-Engine-Mechanical-Energy-Storage Hybrid Propulsion Systems for Vehicles, P.B. 213417, The John Hopkins University, Applied Physics Laboratory, March 1972.

4. J. E. Notti, A. Cormock III, W. C. Schmill, Integrated Power/Attitude Control System (IPACS) Study, Vol. I SD73-SA-0101-1, Rockwell International Space Division.